UNIVERSITÀ DEGLI STUDI DI PALERMO

Dottorato di Ricerca in Medicina Sperimentale e Molecolare

Referente: Prof. Francesco Cappello
Dipartimento di Biomedicina Sperimentale e Neuroscienze Cliniche

EXPRESSION AND LOCALIZATION OF "CHAPEROKINE" HSP60 IN BRONCHIAL CULTURE MODELS MIMING COPD

Tesi di dottorato di:

Celeste Caruso Bavisotto

Tutor:

Chiar.mo Prof. Claudia Campanella

SSD: BIO/16

Co-Tutor:

Chiar.mo Prof. Mauro Carone

TRIENNIO 2013-2015

Ἤ τὰν ἢ ἐπὶ τᾶς

List of contents

List of Figures

List of Tables

List of Abbreviations

ADP: Adenosine diphosphate

ALIX: Apoptosis-linked gene 2-interacting protein X

ATP: Adenosine triphosphate

BEBM: Bronchial Epithelium Basal Medium

BEGM: Bronchial Epithelium Growth Medium

BM: Basal Membrane

BSA: Bovine serum albumin

COPD: Chronic Obstructive Pulmonary Disease

CS: Cigarette smoke

CSE: Cigarette smoke extract

CXCL8 or IL8: Interleukin 8

DAB: Diaminobenzidine

DMEM: Dulbecco’s modified Minimum Essential Medium

ECM: Extracellular matrix

EGF: Endothelial growth factor

EGFR: Epidermal growth factor receptor

EIA: Enzyme immuno-assay

EMT: Epithelium-Mesenchymal Transition

EMTU: Epithelial Mesenchymal Trophic Unit

Ep: Epithelium

ER: Endoplasmic Reticulum

ESCRT: Endosomal sorting complexes required for transport machinery

EVs: Extracellular Vesicles

FBS: Fetal bovine serum

FC: Fibro-Cartilage Layer

FCS: Fetal calf serum

FEV: Forced Expiratory Volume

FGF: Fibroblast growth factor

FITC: Fluorescein isothiocyanate

FVC: Forced Vital Capacity

G-CSF: Granulocyte colony-stimulating factor

GM-CSF: Granulocyte macrophage colony-stimulating factor

GM-CSF: Granulocyte-macrophage colony–stimulating factor

GOLD: Chronic Obstructive Lung Disease

HRP: Horseradish peroxidase

Hsps: Heat Shock Proteins

IC: Inhibiting concentration

ICC: Immunocytochemistry

IF: Immunofluorescence

IGF: Insulin-like growth factor

IHC: Immunohistochemistry

IL: Interleukin

ILVs: Intraluminal vesicles

MCP-1: Monocyte chemoattractant protein-1

MIP-1: Macrophage inflammatory protein 1

MMPs: Matrix metalloproteinases

MVBs: Multivesicular bodies

MVE: Multi Vescicular Endosomes

MW: Molecular Weight

NTA: Nanotracking particle analysis

PBMC: Peripheral blood mononuclear cells

PBS: Phosphate Buffered Saline

PCR: Polymerase chain reaction

PET: Polyethylene terephthalate

PGE_2: Prostaglandin E_2

RIPA: Radioimmunoprecipitation assay

SD: Standard deviation

SM: Sub Mucosa

TEER: Transepithelial electrical resistance

TEER: Trans-epithelial electrical resistance

TEM: Transmission Electron Microscopy

TGFβ: Transforming growth factor β

TLR: Toll-like receptors

TNFα: Tumour necrosis factor α

TRITC: Tetramethylrhodamine

TSNAs: Tobacco specific nitrosamines

WB: Western blotting

Acknowledgements

I wish to express my sincere appreciation and gratitude to all of you who have helped me accomplish this thesis.

I would especially like to thank my supervisor, Prof. Claudia Campanella, for giving me the opportunity to work on this project, for her trust in my ideas, and for being inspiring and enthusiastic. I am thankful for her confidence in my abilities and teaching me to carry it through, even entrusting tasks of great importance.

My heartfelt, special thanks go to Prof. Cappello for encouraging my research and for allowing me to grow as a research scientist.

I am also very thankful to Prof Bucchieri for his support and priceless suggestions.

Special thanks to Antonella Marino for being a friend and inspiring me in my work and studies.

Thanks to Rosario Barone and Filippo Macaluso for their continuous, strong support and help.

Thanks to Prof. Antonio Marcilla for the internship opportunity in his laboratory.

Thanks to Dragana Nikolic and Filippa Lo Cascio which have patiently corrected my writing and Emanuele Mocciaro for his friendship.

I would also like to thank my husband Lucio for finding the strength in me even when he was away. And my parents which were always supporting and encouraging me.

Lastly, I would like to thank those who deliberately wanted to hinder me, because again I learned something.

Introduction

1. Respiratory system.

The respiratory system is essential for respiration, blood oxygenation and carbon dioxide removal [1].

This system consists of two functional elements: a system of ducts and cavities, *conducting zone*, that allows air to reach the sites of gas exchange, and a second element is the *respiratory portion* where gas exchanges occur. The conduction system includes the nasal cavity, paranasal sinuses, pharynx, larynx, bronchi and bronchioles.

Structurally, the respiratory system can be divided into *upper respiratory system* and *lower respiratory system* (Fig.1).

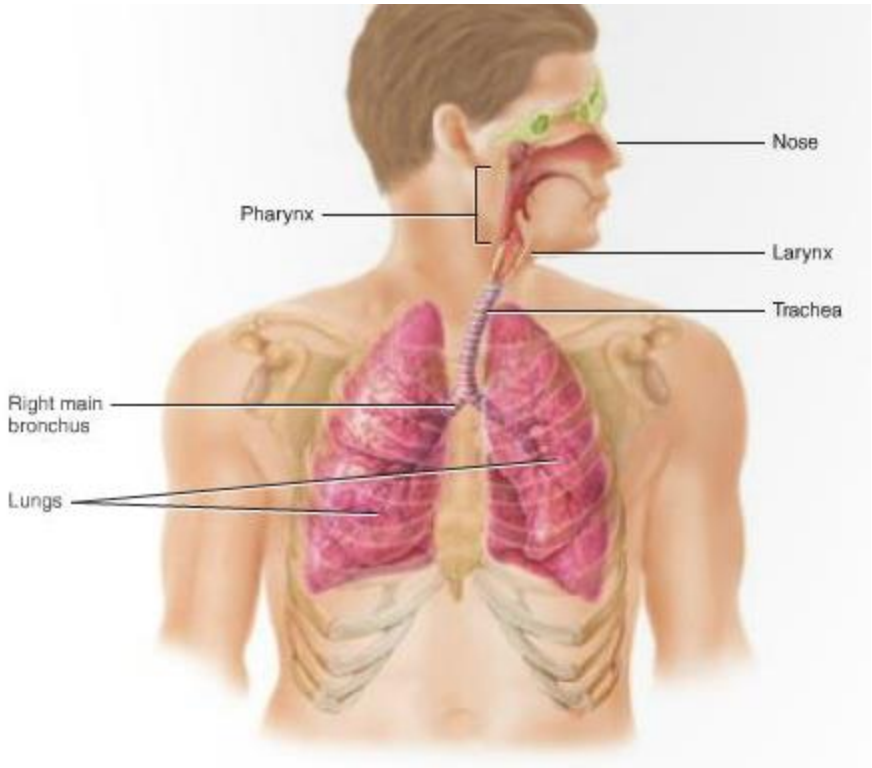

Figure 1.

Schematic representation of the organization of respiratory system.

1.1 Upper respiratory system.

The upper airways consist the nose, nasal cavity, paranasal sinuses, nasopharynx and pharynx, that filter, heat and humidify the air inhaled through the nostrils. These cavities are coated with a respiratory epithelium, a pseudostratified ciliated columnar epithelium, comprised of two cell types, *mucus goblet cells*, which secrete mucus which traps the particulate material and *main cells*, equipped with cilia that move the thin layer of mucus.

1.2 Lower respiratory system.

The next segment is the lower airways, that includes the larynx, trachea, bronchi and lung. The *trachea* (or windpipe) is a tubular passageway for air that branches repeatedly to form approximately 14 generations of conduits. The trachea begins at the level of the sixth cervical vertebra and ends in the mediastinum at the level of the fifth thoracic vertebra, where trachea bifurcates into the right and left primary bronchus, which carry the air into the lungs. The mucosa of trachea consists of an epithelial layer of pseudostratified ciliated columnar epithelium and an underlying layer of lamina propria that contains elastic and reticular fibres. The epithelium consists of ciliated columnar cells, goblet cells, that reach the luminal surface, and basal cells.

At superior border of the fifth thoracic vertebra, the trachea divides into a *right and left primary bronchus*, which goes, respectively, into a right and left lung.

In each lung, the primary bronchi (named also extra-pulmonary bronchi) branch into bronchi with a smaller diameter, *secondary (lobar) bronchi*, which form the bronchial tree. The secondary bronchi divide to form 9-10 *tertiary (segmental) bronchi* in each lung (intra-pulmonary bronchi). Each bronchus branches repeatedly in smaller bronchi named sub-segmental bronchi that branch into *bronchioles*. Bronchioles, in turn, branch repeatedly, and the smallest ones branch into even smaller tubes called *terminal bronchioles*.

These bronchioles contain *Clara cells*, columnar, non-ciliated cells interspersed among the epithelial cells. These cells are source of Clara cell secretory protein (CCSP) and release surfactant apoproteins, proteases, antimicrobial peptides, several cytokines and chemokines, and mucins to the extracellular fluid lining the airspaces [2].

As the branching in the bronchial tree proceeds, several morphological changes occur. The mucosa epithelium goes from pseudostratified ciliated columnar in the main bronchi, lobar and segmental bronchi to ciliated simple columnar epithelium with some goblet cells in larger bronchioles, to mostly ciliate simple cuboidal epithelium without goblet cells in smaller bronchioles, to mostly non-ciliated simple cuboidal epithelium in terminal bronchioles (Fig. 2).

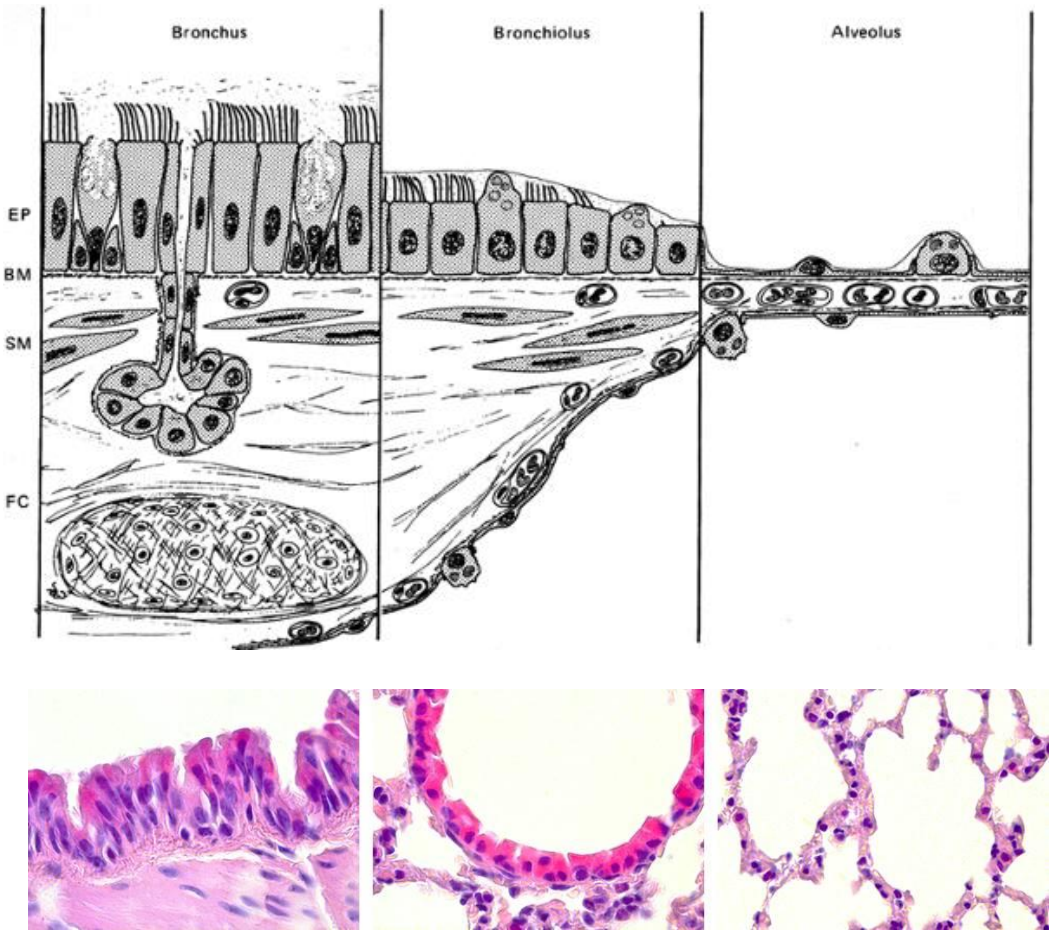

Figure 2.

The transition of the organization of ultrastructure of respiratory epithelium (from D. Kaminsky, Netter Collection of Medical Illustrations: Respiratory System [3]). Figure

showing the appearance of pseudostratified columnar, cuboidal and squamous epithelial tissues from bronchi to bronchioles and alveoli, respectively (Ep: Epithelium; BM: Basal Membrane; SM: Sub Mucosa: FC: Fibro-Cartilage Layer). In the lower panel, shown is haematoxylin and eosin staining of the histological section of the respiratory epithelium in bronchi, terminal bronchioles and alveoli. Magnification 1000X.

1.3 Respiratory units.

Terminal bronchioles subdivide into microscopic branches called *respiratory bronchioles* that in turn subdivide into several *alveolar ducts*, which consist of simple squamous epithelium. Around the alveolar ducts are numerous *alveoli*, consisting of simple squamous epithelium and supported by the *alveolar sac*, an elastic basal membrane. The cells that constitute the alveoli are *Type I alveolar cells*, squamous cells, and *Type II alveolar cells*, or septal cells which are cuboidal epithelial cells and secrete alveolar fluid. Moreover, associated with the alveolar wall are *alveolar macrophages* (*dust cells*). These cells of the alveolar wall, with the epithelial basement membrane, capillary basement membrane and endothelial cells form the respiratory units, where the gases exchange take place.

1.4 Microscopic anatomy of the lower airways.

Even though the cells composition of the airways is different from upper to lower airways, the basic structure of the airway mucosa is well preserved: its cross section consists of five layers: epithelium, basement membrane, sub-epithelial layer, submucosa and adventitia [4].

1.4.1 Tracheal and Bronchial Airways.

The epithelium from trachea through the small bronchi is pseudostratified and columnar. Cell types present are:

Ciliated epithelial cells, the most present and readily identifiable cells in the conducting airway wall. These structural cells have about 200 cilia

each that beat (about 1000 times/minute) in the liquid phase on epithelial surface, playing an essential role in clearance. These cells are more abundant in the lower portion of trachea.

Goblet cells, are more present in the large airway and become progressively rarer in smaller bronchi and all but absent in bronchioles. These cells secrete mucus.

Serous cells, represent 3% of respiratory epithelium cells and present microvillus and apical compartments containing liquid secretory serous.

Clara cells, are the other secretory cells, with rounded surface and short apical microvillus. These cells are confined to peripheral airways where secrete surfactant with the aim of lung defence [5].

Epithelium is pseudostratified and columnar. Epithelial cells interact and interconnect with one another through adhering junctions, tight junction and gap junction, to preserve the epithelial barrier function.

The basement membrane is acellular and composed by extracellular matrix. Airway epithelial cells are attached to the basement membrane through proteins including type IV collagen, fibronectin, entactin, laminin and proteoglycans. This matrix has been exposed to constant remodelling, with formation and degradation of extracellular matrix proteins, due to the matrix metalloproteinases (MMPs).

In the underlying layer is present a sub-epithelium with an extensive vascular and capillary network.

The submucosa present smooth muscle, glands and lymphoid tissue [6].

2. Chronic Obstructive Pulmonary Disease (COPD).

2.1 Aetiopathogenesis.

Chronic obstructive pulmonary disease (COPD) is an inflammatory disease of the airways, characterised by a progressive and not fully reversible limitation of expiratory airflow during forced expiration.

COPD predominantly affects small airways (conducting airways with diameter <2 mm). This is due by an increase in resistance in the small

conducting airways and by an emphysematous destruction of lung elastic tissue.

According to The Global Initiative for Chronic Obstructive Lung Disease (GOLD), symptoms consist of a cough, sputum production, or dyspnea and airflow limitation, confirmed by spirometry. Moreover, staging ranges from *Stage I*, *Mild COPD* (FEV_1 Forced Expiratory Volume /FVC Forced Vital Capacity < 70%), to *stage III*, *Severe COPD* (FEV_1 < 30% predicted) [7].

COPD is a multi-faceted disease and there are two main forms of COPD: *chronic bronchitis*, which involves a long-term cough with mucus, and *emphysema*, which involves the destruction of the lungs over time. Most people with COPD have a combination of both conditions.

COPD is a major cause of death worldwide, with a prevalence estimated in 2006 at 10% of the general population and up to 50% in heavy smokers [8] and further increases in its prevalence and mortality are expected in the coming decades [9]. In COPD can be contemporary present a mixture of several airway disease: chronic bronchitis, emphysema, asthma and pulmonary hypertension and the relative contributions of which vary from person to person.

This is accompanied by an abnormal inflammatory response against inhaled particles and gases in the lung, that establish increased mucus production and accumulation in the lumen of small airways; reduced mucociliary clearance, and increased permeability of the airspace epithelial barrier associated with early cell death.

COPD is mainly associated with cigarette smoke (CS) exposure, indeed smoke is traditionally considered a well-known cause of airway and oral tissue damage, as well one of the five leading risk factors for mortality in the world [10]. Exposure to pollutant and to biomass fuels is also increasingly considered a cause of COPD worldwide. Actually, only smoking cessation is the unique intervention capable of reducing the decline in lung function in patients affected by COPD.

CS induces chronic airway inflammation, through activation of both, structural and inflammatory cells within the lung and also peripheral inflammatory cell infiltration [11]. Several studies have been reporting that smokers have from two to threefold increase in the rate of decline in lung function compared with non-smokers. However, although CS stimulates abnormal and persistent inflammation reaction, this occurs only in a minority of smokers; COPD development could therefore depend on individual susceptibility [12].

2.2 Inflammation in COPD.

The inflammatory reaction is principally localised in the small airways, where exposure to air pollution activates an inflammatory cascade resulting in the production of a number of potent cytokines and chemokines which play a critical role in the induction of chronic inflammation and subsequent tissue destruction. In COPD pathogenesis are involved many cells types: both innate and adaptive immune responses mediators, including airway and alveolar epithelial cells, endothelial cells, and fibroblasts. Even epithelial cells take part in this contest, producing inflammatory mediators, including tumour necrosis factor (TNF) α, interleukin (IL)-1 β, IL-6, granulocyte-macrophage colony–stimulating factor (GM-CSF), and CXCL8 (IL-8) and transforming growth factor (TGF) β. Macrophages, neutrophils, eosinophils, dendritic cells and T lymphocytes contribute to determining increasing inflammation, oxidative stress, cell death, impaired cell repair, protease/anti-protease imbalance, and destruction of the extracellular matrix [13].

3. EMTU (Epithelial-Mesenchymal Trophic Unit).

In the small airways there are many cell type that contribute to performing the numerous function of the respiratory system. These functions, in addition to air exchange and filter, include differentiation during lung growth, repair of damaged tissue, and regulation of the inflammatory

response. Evans and co-worker [14] have demonstrated that in the airway wall a thin layer of fibroblasts makes contact with epithelial basal lamina. This area is close to the epithelial/environmental interface and consists of the epithelial cells and the subtending fibroblasts along with their associated nerves and extracellular matrix. This epithelial-mesenchymal trophic unit (EMTU) establish a means of cellular communication between matrix and cells and between the cells themselves. Gap junctions are present and connect one cell to the next; the tight junctions (zonula occludens) prevent the passage of material across the cellular layer through intercellular spaces, forming a continuous belt (zonula). This arrangement ensures that substances can only pass through the layer of cells by diffusion or transport through their apical membrane.

Tight junctions may achieve a direct signalling in this structure in which the function of epithelium might be coordinated by members of this unit, so as to organise components of the inflammatory as well as the repair and remodelling processes.

Therefore, EMTU consists of opposing layers of epithelial and mesenchymal cells, with extracellular matrix and nerve fibres, in which fibroblasts are clearly involved in the airway remodelling and wound repair, when EMTU undergoes several stimuli and external noxious. For example, in asthma, sub-epithelial myofibroblasts have been shown to be increased in response to allergen [15]. CS reduces cross-linking between fibroblast inhibiting the release of TGF-β, fibronectin, and PGE_2 (Prostaglandin E_2) [16] and inducing apoptosis through oxidative stress [17] (Fig. 3).

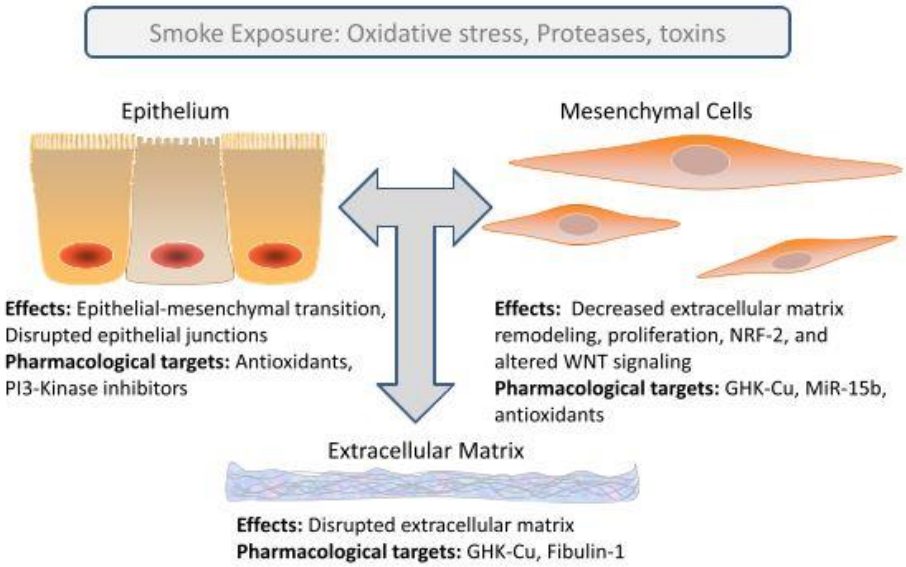

Figure 3.

Epithelial-mesenchymal transition in EMTU which is subject to stressors. (From Oluwaseun et al 2014 [18]).

Indeed, in COPD, where smoke is the main risk factor, the airway epithelium undergoes squamous, goblet cell metaplasia [19] and mesenchymal cells respond properly to epithelial cells injury.

Exacerbation of COPD is correlated with airway remodelling because this consists in airway wall thickening by fibrosis and/or emphysema. Many studies speculate on the involvement of growth factors and matrix metalloproteinases (MMPs). High levels of Prostaglandin E2 and MMP-2 correlate with the severity of airflow limitation in stable COPD [20] and genetic factors, such as MMPs haplotypes play a role in the disease severity [21].

3.1 EMTU remodelling in COPD.

As a result of the accumulation of inflammatory mucous in the lumen and infiltration of the wall by innate and adaptive inflammatory immune cells, in advanced stages of COPD the repair and remodelling processes occur. The fibroblasts of the EMTU, are involved in the increase of small airway

wall thickness. Indeed, fibroblasts are an important source of growth factors, extracellular matrix proteins and metalloproteases that remodel the interstitial space of the airway and alveolar tissue. The volatile compounds of CS are able to decrease the normal ability of the mesenchymal cell to respond properly to epithelial stimuli. Establishing, in this way, a failed lung repair [17].

In COPD patients, the risk of lung cancer is increased by 4-5 fold, implying that similar mechanisms may be involved in the pathogenesis of COPD and lung cancer [22], in which epithelial cells lose their cell polarity and cell-cell adhesion, and gain migratory and invasive properties to become mesenchymal-like cells.

The relationship between EMTU remodelling in severe COPD and Epithelium-Mesenchymal Transition (EMT) was previously demonstrated: increased expression of EMT markers and reduced expression of epithelial junction molecules in the airways of smokers, and in particularly with COPD were shown [23,24]. It has been proposed a common genetic susceptibility to COPD and lung cancer, such as a polymorphism that are expressed in airway epithelium. Also several molecular pathways are shared by chronic inflammation in COPD and tumorigenesis: the transcription factor STAT3, which is activated in COPD lung, is also expressed in lung adenocarcinomas [25]; the involvement of NF-kB, implicated in tumor growth; TGF-β and MMP may promote the EMT transition; finally the reduction of expression of antioxidant mediators, that increase the oxidative stress [26].

4. In vitro models of COPD.

There are different models to mimic COPD pathogenesis, both *in vivo* and *in vitro*.

Regarding *in vivo* models, the most common approaches in animal studies consist in the inhalation of noxious stimuli, (i.e., whole-body cigarette exposure system [27]) or the tracheal instillation of tissue-degrading enzymes to induce emphysema-like lesions and gene-targeting [28]. Among

laboratory animals, mice represent the most favored to study COPD, particularly concerning the immune system, because they permit to manipulate gene expression; otherwise, at least 6 months of smoke exposure are required to produce structural and physiological changes consistent with emphysema [29]. Moreover, it is difficult to assess lung function and there are many differences, both anatomical and functional, between the murine and the human respiratory tract [30] [31]. Furthermore, concerning the animal models to test drugs, many of these fail to show efficacy and safety when advanced from animal studies to human clinical trials.

In order to verify the responses to main environmental stimuli, involved in COPD progression, cell culture methods are widely used. Primary cells, obtained *ex vivo* and immortalized cell lines, both from carcinoma and/or transformed cell, can be used with the advantage of understanding the cellular and molecular process of disease, as well as, a high level of data reproducibility.

Cell cultures provide appropriate standard model systems, but they grow in monolayer and in an artificial environment; therefore, they are not able to reproduce the cell and tissue physiology accurately. In contrast, three-dimensional (3D) cell cultures produce a growth environment that mimics the native tissue as closely as possible, allowing an improvement in viability, morphology, proliferation, differentiation, response to stimuli and cell-cell communication. 3D cell cultures provide more accurate cell polarization and establish the cell–cell and cell–ECM (extracellular matrix) interactions that are not completely modelled in 2D culture.

In 3D co-cultures of epithelial and mesenchymal cells in collagen gel, Zhang and colleagues have developed achieve an EMTU system, which reproduce the small airway organization in which epithelial cells are an important regulator of airway remodelling after cell damage exposition; indeed 3D cultures reproduce tissue- and organ-level pathophysiology *in vitro* [32].

Given these consideration, the choice of material for the scaffold, the source of cells, and the actual methods of culture, which vary considerably according to the tissue of study, assume great importance. Moreover, 3D cells have greater stability and longer lifespans to allow more appropriate long-term studies [33]. Indeed, 3D culture techniques provide an organotypic culture that allow the real-time study of mammalian tissues.

4.1 Bronchial epithelial 3D Outgrowth cultures.

Conducting airways of the lung are composed by a highly specialized epithelium with varies structures and functions. Normal bronchial epithelium contains ciliated epithelial cells, secreting cells, and basal cells that can proliferate and differentiate into each of the three major cell types [34].

The 3D outgrowth model allows cells to re-establish mutual contacts and specific microenvironments that permit them to express a tissue-like phenotype. Indeed, in this culture model, in which are reproduced airways, cells form a pseudostratified layer in the air-liquid interface and can be used to study properties of the human airways, as well as to mimic heterotypic cellular interactions.

Furthermore, The 3D culture system shows improvements in several fields in order to study the basic biological mechanisms like: cell number monitoring, viability, morphology, proliferation, differentiation, response to stimuli, cell-cell communication, migration and invasion of tumor cells into surrounding tissues, angiogenesis stimulation and immune system evasion, drug metabolism, gene expression and protein synthesis, general cell function and *in vivo* relevance [35].

Moreover, this 3D organotypic model represents a breakthrough in studies of biological mechanism and particularly, in this case, is an important tool to evaluate the airway epithelial defence mechanisms, to study effects of toxins, cancer progression, and in addition, can be used to test new drugs and study their effects on ‘‘normal’’ or ‘‘preneoplastic’’ epithelia [36].

4.2 Cigarette smoke extract (CSE).

COPD was initially recognized in 1821. COPD develops most commonly in people with a history of cigarette smoking and/or prolonged exposure to air pollutants. Indeed the cigarette smoking has been firmly established as the most important risk factor for the development of COPD. But the influence of others risk factors was still not clarified. The reason because some people develop COPD over others is under study.

There are many works that use different approaches to mimic the stimuli that cause COPD. The *in vitro* methods directly assesses the cellular response exposing cells to smoke [37], oxidants [38], fine particles [39] and proteolytic enzymes [40].

The most common exposure model for the study of the development of COPD is the generation of cigarette smoke extract (CSE). The most abundant component of smoke is nicotine, but a wide kind of different compounds derive from the combustion of tobacco. CSE is a concentrated complex of thousands of chemicals that consist of a particulate (polycyclic aromatic hydrocarbons and tobacco-specific nitrosamines, TSNAs) and a gas phase (formaldehyde, acrolein, and hydrogen cyanid). It has been established that the particulate phase is associated with cancer and, instead, the gas phase with COPD [41].

The CSE is normally obtained, using a smoking machine, by the bubbling of CS in the medium; which is directly or diluted added to bronchial or lung cell cultures. The advantage of this method is that it captures the both particulate and gas phases; but remains not completely unknown the exact quantity of gas and chemicals present in the suspension. Although the smoke is constituted by many chemicals and additives, of which several are volatile, CSE is the most useful model in order to study the mechanism by which smoke induces direct lung damages. Indeed, CSE consists of several components that are able to pass through the mucus layer to reach epithelial cells, where induces DNA damages, cellular senescence, the increase of release of growth factors and cytokines,

production of metalloproteases and mucin secretion, reduction of cilia beat frequency and proliferation [42].

The exposure to smoke directly impairs the lung, inducing oxidative stress, due to the action of toxic substances which are able to induce, for example, a glutathione depletion [43]. Moreover, CSE causes inflammatory events because of the release of pro-inflammatory mediators and then the recruitment of cells of immune system, which enhance the inflammatory response. Indeed, the chronic inflammation in COPD is due to the repeated and progressive activation of immune cells. Several data support the hypothesis that exposure to CSE cause inflammatory airway events, considering that it has been shown that CSE may promote inflammatory cytokine and chemokine production in airway epithelium both *in vitro* [44–46] and *in vivo* [47] models.

5. Heat Shock Proteins.

The Heat Shock Proteins (Hsps) are evolutionarily conserved proteins, present in the cells of all organisms, eukaryotes and prokaryotes, whose expression can be induced by different types of environmental stressors, such as disease states, hypoxia, ischemia, hyperoxia, exposure to toxic and carcinogenic factors [48]. Many Hsps are part of the cellular chaperoning system, actually the primary function of Hsps appears to serve as molecular chaperones, indeed, they are essential for the control of protein homeostasis and the maintenance of correct and functional conformation of proteins and of nascent polypeptides, preventing their aggregation and misfolding [49]. The Hsps have also been assigned other functions, not necessarily related to homeostasis of proteins, such as the regulation of gene expression and DNA replication [50], cell differentiation [51], signal transduction [52] and inflammatory response [53], the process of carcinogenesis [54], senescence [55] and cell apoptosis [56].

Traditionally, HSPs are regarded as intracellular proteins, with localization in the cytoplasm, mitochondria, endoplasmic reticulum, peroxisomes and in the nucleus. However, their presence has been demonstrated in several

sites in the extracellular environment, indeed, can be released from cells in a variety of circumstances and interact with adjacent cells or in some cases enter the bloodstream and are present in fluids such as blood, lymph and cerebrospinal fluids [57].

The Hsps are generally grouped into classes, based on their peptide sequence homology, structure, or in the molecular weight. Therefore, it is possible to distinguish: Hsps with high molecular weight (with a mass greater than or equal to 100 kD), Hsp90 (with mass between the 81 and 99 kD), Hsp70 (with a molecular weight between 65 and 80 kD), Hsp60 (between 55 and 64 kDa), Hsp40 (between 35 and 54 kD) and small Hsps (having a mass less than or equal to 34 kD). Each of these families includes various isoforms (Table 1) [58].

Name	***HUGO Name*** [59]	***Old Name***	***Mass (kDa)***	***Main functions***
Super-heavy	DNAJC28	Sacsin	≥200	Prevents protein aggregation, helps protein folding.
Heavy	HSPH	High MW; Hsp100	100-199	Prevents protein aggregation, helps protein folding.
Hsp90	HSPC	HSP86, HSP89A,HSP90A, HSP90N, HSPC1, HSPCA, LAP2, FLJ31884	81–99	Protein folding, cytoprotection; intracellular signalling (e.g., steroid receptor); cell-cycle control.
Hsp70	HSPA	Chaperones, DnaK	65–80	Prevents protein aggregation, protein folding, cytoprotection and anti-apoptotic function.
Hsp60	HSPD1	Chaperonins (groups I and II), Cpn60 and	55–64 35–54	Prevention of protein aggregation, protein

		CCT		folding, cytoprotection, macrophage activator possibly through Toll-like receptor.
Hsp40	DNAJA	DnaJ	35-54	Protein folding and refolding together with Hsp70/Hsc70.
Small Hsp	HSPE1	sHsp, alpha-crystallins, Hsp10	≤34	Protein folding together with Hsp60; modulation of immune system.
Other		Proteases, isomerases, AAA+ proteins (e.g., paraplegin or SPG7, spastin or SPG4); α-hemoglobin-stabilizing protein	Various	

Table 1.

Subpopulations of Hsp chaperones (modified from Macario and colleagues, 2010 [55])

5.1 Chaperonopathies and Hsps in lung diseases.

When a malfunctioning of chaperones occurs, due to structural damage or gene dysregulation, a condition known as *Chaperonopathia* persist.

The chaperonopathies are pathological conditions associated with the impairment of one or more molecular chaperones and are classified etiologically as genetic or acquired, as by defect, excess or mistake. In chaperonopathies due to a genetic mutation or a post translational modifications, the chaperone is altered or abolished in its functions. On the other hand, in chaperonopathies by defect, excess or mistake, the alteration is in the quantity of the chaperone and in its level and type of its function (Table 2) [55].

Types of chaperonopathies	***Causes***	***Condition***
Genetic	Gene mutation, Hereditary, Congenital	Motor neuropathies, ataxias, Bardet-Bield and Williams syndromes; cardiomyopathies; endoplasmic reticulum pathologies [55,60]
Acquired	By defect and By excess	Aging due to pathological post-translational modifications, such as oxidation, phosphorylation, acetylation, or glycation [55,60]
	By mistake or collaborationism	Autoimmune and inflammatory disease, cancer [55,61]

Table 2.

Types of chaperonopathies and main features

Mammalian cells produce endogenous stress proteins following a stimulus harmful and these can be also secreted outside or released from dying cells. Generally, Hsps have a protective role intracellularly but have potentially adverse effects when secreted outside cells (Table 3). Hsps are constitutively produced and released from cells and the levels are higher in response to trauma. When Hsps are secreted they can bind to the surface of adjacent cells, through receptors such as Toll-like receptors (TLRs) 2 and 4, CD40, CD91, starting the signal transduction cascade [62–64]. Indeed, Hsps have a powerful effect on the immune response. Regarding the extracellular role of some Hsps, because they are key factors in activation of immune system, a dysfunction of these proteins may lead to an inflammation condition and may play a central role in the pathogenesis of inflammatory diseases.

Stress protein	***Protein function***	
	Intracellular	*Extracellular*
Hsp27	Antideath	Anti-inflammatory
Hsp60	Chaperonin	Pro-inflammatory
Hsp70	Antideath	Immunoregulatory, proinflammatory, neuronal survival
Hsp90	Cell regulation	Pro-immune, pro-metastatic
Hsp110	Co-chaperone	Pro-immune
Grp78	ER (Endoplasmic Reticulum) chaperone	Anti-inflammatory
Grp94	ER chaperone	Immunoregulatory
Grp170	ER chaperone	Pro-immune

Table 3.

Intracellular and extracellular properties of Hsps. Modified from Calderwood and colleagues, 2007 [57].

Actually, the involvement of Hsps in inflammatory disorders, such as lung disease, has been documented [65]. In inflammatory lung diseases, the innate immunity is the first line of defence of the immune system, providing initial protection against various pathogens and infections. In this context, a large number of works have demonstrated that Hsps, such as Hsp60, Hsp70, Hsp90 and gp96, are involved in the activation and regulation of the immune signaling pathways. Hsps were seen to be implicated in antigen direct presentation and cross-presentation leading to CD8+ T cell activation, being a part of the endogenous pathway of antigen presentation through the MHC (major histocompatibility complex) class I molecules [66]. Moreover, Hsps induce the maturation of dendritic cells by up-regulation of MHC class I and MHC class II [67] and are observed to have cytokine effects mediated by TLR (Toll-like receptors) [68] and protein kinases cascade activation [62].

The leukocyte migration into alveolar space and the production of inflammatory mediators by epithelial cells play a critical role in pulmonary inflammation resulting in lung injury. In COPD, some Hsps were seen to

be related or overexpressed, such as HspB5, Hsp70 and Hsp27, which appear to be predominantly in extracellular space and may activate the Toll-like receptors and provoke inflammation [69–72]. This could be due to the necessity to keep the proteostasis and the cellular homeostasis to counteract the oxidative stress, both in COPD smokers and non-smokers; conversely, Hsps may have not a cytoprotective properties when secreted outside from cells, such as Hsp60 [65].

5.2 Hsp60.

The Hsp60 is a ubiquitous and highly conserved protein presents both in eukaryotes and prokaryotes, including pathogens [73]. The human Hsp60 is a mitochondrial chaperone phylogenetically related to the bacterial protein GroEL [74]. This chaperonin is constituted by wide double-loop complex and each of these loops is composed of 7 subunits of about 57 kDa, that contains three domains: an apical domain, which represents the binding site for polypeptides, an equatorial domain, which contains the binding site of ATP/ADP and an intermediate domain, which acts as a connector of the other domains (Fig. 4) [75,76].

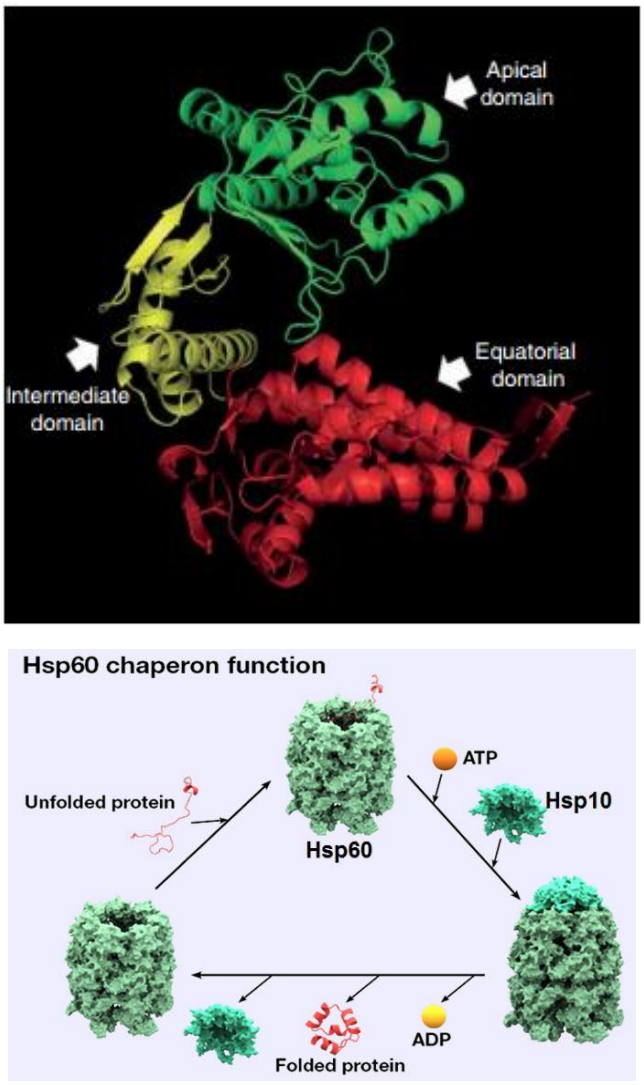

Figure 4.

Hsp60 monomer structure showing its three structural domains: apical in green, intermediate in yellow and equatorial in red. (from Cappello and colleagues, 2014 [76]). Hsp60 works in cooperation with Hsp10, its co-chaperonin, to assist protein folding of unfolded mitochondrial proteins by an ATP-dependent mechanism.

Hsp60 is classically considered an intracellular chaperone and works, during the folding process, with Hsp10, its co-chaperone, and covers many essential roles in cells; being responsible for the protection of cells against all stressors is essential for cell survival [77]. The typical localization of Hsp60 is the matrix of mitochondria, but numerous studies have shown its presence in extra-mitochondrial sites, such as the cytosol and plasma

membrane. Furthermore, this chaperon is present in the extracellular environment and bloodstream, where is able to interact with immune system cells and to stimulate cells at distant sites in the body. For this reason, Hsp60 was identified as a *chaperokine*. Indeed, Hsp60 may induce maturation of human monocyte-derived dendritic cells and T cell polarization and may trigger the monocyte and macrophage cells to synthetize pro-inflammatory cytokines, such as TNF-α, IL-12 and IL-15 [78,79].

It has been proposed that the immunological characteristics of Hsp60 are due to the high degree of homology with prokaryotic Hsp60, as a failure of the mechanism of self-, not self-discrimination, inducing autoimmunity [74]; determining the maintenance of inflammation in autoimmune [80] and chronic inflammatory disease [65].

The Hsp60 secretion is an active mechanism that, among others, involves the exosomes pathways [81].

6. Exosomes.

Cell communication is imperative to live [82]. Therefore, in order to maintain cellular homeostasis or to respond to pathogens in the extracellular milieu, cells often exchange information through direct cell-cell contact or by secretion of soluble factors. Abundant evidence has shown a newly identified mechanism of intercellular interaction through lipid vesicles, such as exosomes, in which phospholipid-enclosed vesicles are released into the extracellular environment that can bind the specific receptor to the target cells, and these vesicles are, frequently, internalized by recipient cells [83].

As described by Pan in 1983, it was initially thought that exosomes could be a mechanism for shedding the cytoplasm in maturing sheep reticulocytes [84]. Several recent studies provide further support to show that exosomes are extracellular small particles of 30-100 nm in diameter, which have an endosomal origin and are secreted by all cell types. Exosomes are also present in many body fluids such as blood, urine, cerebrospinal

fluid, breast milk, saliva, bronchoalveolar lavage fluid, ascitic fluid and amniotic fluid [85]. Exosomes are released into the extracellular space after the merging of late endosomes with the cell membrane. Previously, early endosomes become part of multivesicular bodies (MVBs), which undergo a maturing process that provides a gradual change in protein composition of the vesicles (intraluminal vesicles, ILVs). During this maturation process, the vesicles accumulated in the MVBs, can have three potential outcomes: 1) they may merge with the lysosomes, causing protein content degradation (e.g., in the case of receptors); 2) they may constitute a temporary storage compartment; 3) they may blend with the plasma membrane, releasing exosomes. Therefore, exosomes correspond to the intraluminal vesicles of MVBs. MVBs merge with the plasma membrane, resulting in exocytosis of the vesicles contained in MVBs; as such, vesicles maintain the same topological orientation as the plasma membrane [82,86].

The endosomal sorting complexes required for transport machinery (ESCRT) are involved in exosome biogenesis and in their loading. Different evidence sources support the idea that ESCRT could assist in the sorting of ubiquitinated cargo proteins at the endosome membranes. The ESCRT-associated protein ALIX (apoptosis-linked gene 2-interacting protein X) can regulate this function [87].

Exosomes exhibit specific cell-type dependent content. Numerous studies are conducted to find the whole content of exosomes for the purpose of understanding them function and to exploit them as drug delivery, for instance.

Generally, it seems plausible that the exosomes standard composition depend on parental cells condition, and contains lipids, nucleic acids, such as DNA, non-coding RNA, rRNA (Ribosomal RNA) and miRNAs (microRNAs) and proteins.

It has been reported that the lipid composition is specifically sorted out in emerging exosomes and is enriched of cholesterol, phosphatidylcholine, sphingolipid ceramide and sphingomyelin that probably provide to stabilize

the bilayer membrane integrity in the extracellular milieu [88] and, in particular, sphingolipid ceramide play a key role in the budding of exosomes [89].

The presence of mRNA [90] and miRNA [91] in exosomes vesicles indicate the activity in expression regulation in both recipient and donor cells, proof of horizontal transfer of genetic information. This has been showed frequently in immune system cell to aim to allow immunological function [92].

Concerning the proteins composition, in exosomes are found different classes of these, strictly involved in vesicles trafficking, such as cell surface receptor or specific content of endocytic pathway (GTPases; annexins; flotillin, endosomal sorting complex required for transport, ESCRT, such as Alix; tumor susceptibility gene 101, TSG101; integrin and a number of tetraspanins such as CD9, CD53, CD63, CD81 and CD82, depending on the origin cell). On the other hand, are present important proteins to long distance communication, such as cytokine [93], hormones [94], growth factors, transcriptional factors [95] and heat shock proteins [96,97] (Fig. 5).

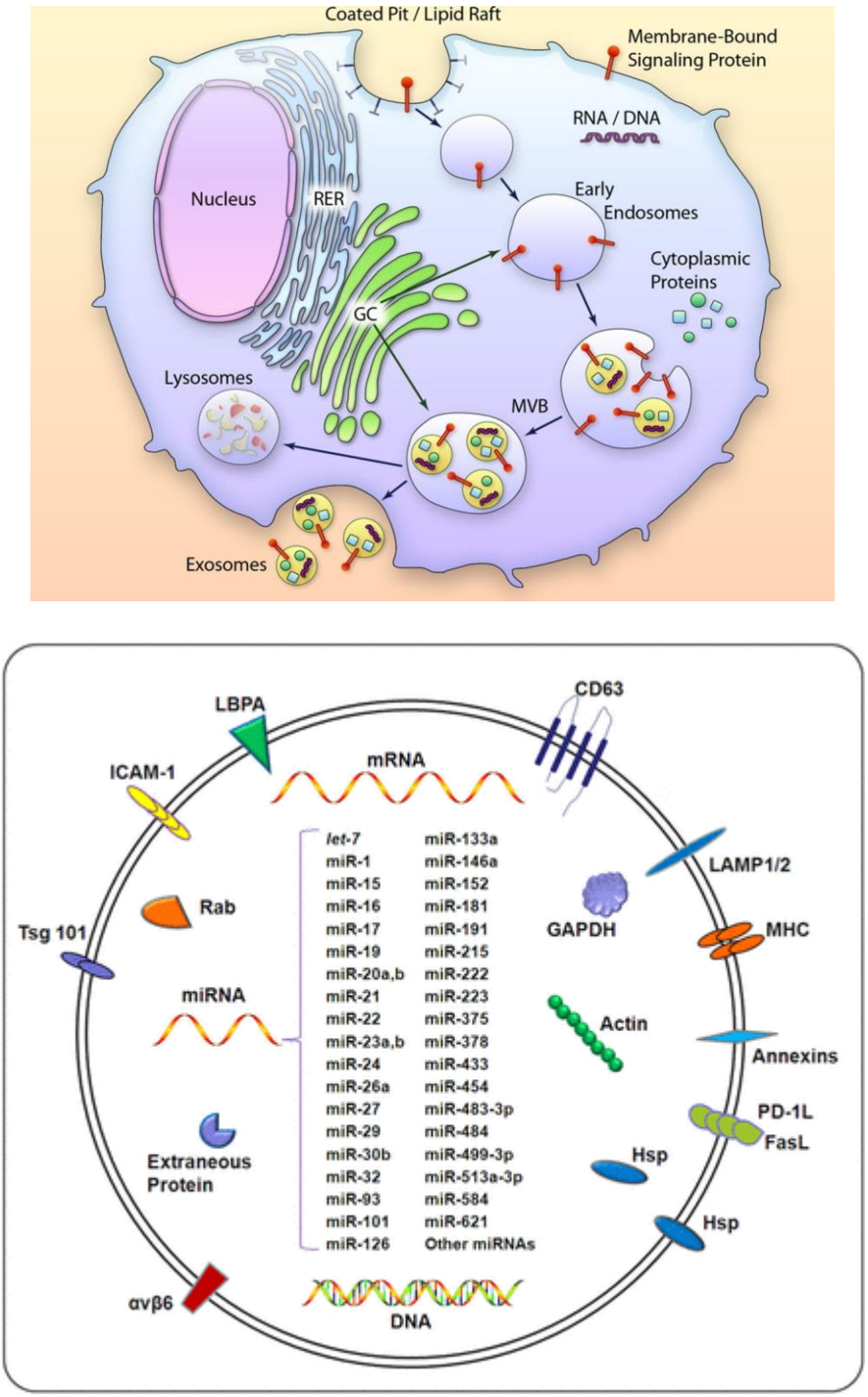

Figure 5.

Biogenesis and content of exosomes comprising mRNA, DNA, microRNAs, proteins (ie, enzymes, growth factors, and cytokines), and transmembrane proteins of different kinds, including tetraspanins, annexin, and intracellular cell adhesion molecule (from [98]).

Depending on the source cell and the content, many different functions have been attributed to exosomes. They are involved in cell-to-cell information transfer [99], immune response [100], inflammation [101], coagulation [102], stem cell activation [103] and programmed cell death [104]. Exosomes can participate in cellular responses against stress [105]. It has been shown that exposing B-cell lines to heat stress results in a marked increase of Hsps expression by exosomes and in an increase in the quantity of exosomes produced [105]. Recent studies have validated this hypothesis by demonstrating that specific members of the Hsp family, such as Hsp60, Hsp70 and Hsp90, can be secreted by cancerous cells via exosome pathway [81,96,106] (Fig. 6). Exosomal Hsps may have opposing roles, that is, immunosuppressing or immunostimulating effects. These different effects depend on the interaction between exosomal Hsps and cells or immune system components.

Given that exosomes can mediate the transfer of specific molecules, they may play a role in intercellular transmission in disease pathogenesis, including tumour development, viral infections and neurological diseases [107–110].

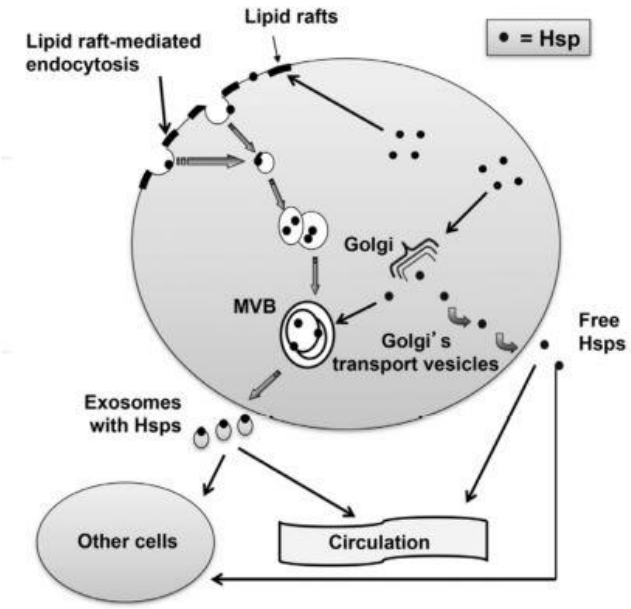

Figure 6.

Exosomal Hsps and mechanism of release from Campanella and colleagues, 2014 [111].

Aim

As discussed in the introduction of this thesis, COPD is one of the leading causes of mortality and morbidity in the world and is rapidly increasing among the world population. The main risk factor for the disease is cigarette smoke (CS), which is linked to approximately 90% of COPD cases. CS acts as an inflammatory mediator inducing pulmonary inflammation by damaging the respiratory epithelial barrier. In the smoker’s lung, these mediators, together with infections, accentuate a milieu of chronic inflammation on patients with stable COPD, characterized by the presence of immune cells [65].

Among the molecules involved in lung diseases, it has been already demonstrated [65] that several Hsps, such as Hsp60, have “cytokine-like” functions in different bronchial pathologies, such as COPD and lung cancer. In this context, our hypothesis is that Hsp60 could be released from the stressed bronchial mucosa into the bloodstream and may act as a cytokine, determining the activation of the immune cells and subsequently, influencing the exacerbation of inflammatory response.

The main aims of this thesis were to find a further correlation between the chronic inflammation in COPD and Hsp60, to clarify which pathways are involved in Hsp60 export from bronchial epithelial cells and to investigate whether the extracellular Hsp60 might effectively cause activation of PBMC (peripheral blood mononuclear cells).

In order to test our hypothesis, we assessed three different models that mimic COPD and the experimental design was developed as follow:

1. Assessment of Hsp60 and its co-chaperone Hsp10 levels and localization *in vivo* (bronchial specimens obtained from smokers and non-smokers).

2. Development of an *in vitro* monolayer model to reproduce the oxidative stress induced by CSE and subsequent evaluation of Hsp60 levels and localization.

3. Optimization of a three-dimensional *ex vivo* model to understand the mechanisms of the pro-inflammatory effects after CSE exposure. In this perspective, we investigated whether CS can modulate the expression of Hsp60 and trigger the release of this “chaperokine” as well as the release of other inflammatory cytokines. Furthermore, we investigated the effects of extracellular Hsp60 on monocyte-cytokines production.

Materials and Methods

1. Experiments *in vivo.*

Method	Antigen	Type and source	Clone	Supplier	Catalogue Number	Dilution
IHC, ICC, WB; IF	Hsp60	Mouse monoclonal	LK-1	Sigma-Aldrich, St. Louis, MO, USA	H4149	1:400 (IHC, ICC, IF) 1:2000 (WB)
IHC, ICC	Hsp10	Rabbit polyclonal	Cpn10	StressGen Biotechnologies, Victoria BC, Canada,	SPA-110	1:300
WB	B-actin	Mouse monoclonal HRP-conjugated	C4	Santa Cruz Biotechnology, Dallas, TX	sc-47778	1:3000
WB	Alix	Mouse monoclonal	AIP1	Pharmingen (BD Biosciences, San Diego, CA	611620	1:500
WB	Hsp70	Mouse monoclonal	3A3	Santa Cruz Biotechnology, Dallas, TX	sc-32239	
IF	EGFR	Mouse monoclonal	0.N.26 8	Santa Cruz Biotechnology, Dallas, TX	sc-71034	1:500
iF	α-actinin	Mouse monoclonal	EA-53	Sigma-Aldrich, Milan	A7811	1:300
IF	TJP1	Rabbit polyclonal	ZO1	Sigma-Aldrich, Milan	HPA00163 6	1:200

Table 4.

Primary antibodies used for immunohistochemistry (IHC), immunocytochemistry (ICC), western blotting (WB), and immunofluorescent (IF).

1.1 Immunohistochemistry (IHC)

Samples for immunohistochemistry were obtained from 19 subjects with normal lung function, among whom nine were current smokers (age= 64±8; M:F=8:1) and 10 non-smokers (age= 65±9; M:F= 9:1).

A standardized procedure [112] was followed for fiberoptic bronchoscopy and collection of bronchial biopsies. Using local anesthesia with lidocaine (4%) to the upper airways and larynx, a fiberoptic bronchoscope (Olympus BF10 Key-Med, Southend, UK) was passed through the nasal passages into the trachea and four bronchial biopsy specimens were taken from segmental and sub segmental airways.

For histological analysis, the samples were embedded in Tissue Tek II OCT (Miles Scientific, Naperville, IL) and 6 mm thick cryostat sections were cut and processed for immunohistochemical analysis.

The sections were rehydrated, at room temperature, by three sequential washing in PBS (Phosphate Buffered Saline pH 7.4), for five minutes each. Subsequently, the sections were immersed for 10 minutes in Sodium Citrate Buffer (pH 6) at room temperature for antigen exposing. After three washing with PBS for 5 minutes, the sections were treated for 5 minutes with Peroxidase Quenching Solution (reagent A of Histostain®-Plus 3rd Gen IHC Detection Kit, Invitrogen) to inhibit any endogenous peroxidase activity. After that, another washing was carried out in PBS for 5 minutes and then the sections were treated with a blocking protein (reagent B of Histostain®-Plus 3rd Gen IHC Detection Kit, Invitrogen) for 10 minutes in order to block non-specific antigenic sites. Subsequently, the sections were incubated overnight with a primary antibody against human Hsp10 (Rabbit Anti-Cpn10 Polyclonal Antibody, StressGen Biotechnologies, Victoria BC, Canada, Cat. No. SPA-110, dilution 1:300), human Hsp60 (mouse anti-Hsp60 monoclonal antibody, Sigma, St. Louis, MO, catalogue no. H4149, dilution 1:400). After one washing with PBS for 5 minutes, the sections were incubated with a universal biotinylated secondary antibody (Biotinylated Secondary Antibody reagent C Histostain®-Plus 3rd Gen IHC Detection Kit, Invitrogen) for 10 minutes.

After another washing with PBS for 5 minutes, the sections were incubated with streptavidin-peroxidase complex (Streptavidin-Peroxidase Conjugate reagent D Histostain®-Plus 3rd Gen IHC Detection Kit, Invitrogen) for 10 minutes. Following a further washing in PBS for 5 minutes, the slides were incubated in the dark for 5 minutes using the DAB chromogen (diaminobenzidine) (DAB chromogen reagents E1 and E2 Histostain®-Plus 3rd Gen IHC Detection Kit, Invitrogen). Nuclear counterstaining was obtained using hematoxylin (DAKO, Cat. No. S2020). Finally, the slides were prepared for observation with coverslips with an aqueous mounting solution. The observation of the sections was performed with an optical microscope (Leica DM 5000 B) connected to a digital camera (Leica DC 300F).

Ten fields were examined in each slide and cell counting was performed at the same magnification.

2. Experiments *in vitro*.

2.1 Cells cultures.

In this study immortalized normal bronchial epithelial cell line (16-HBE) and human mucoepidermoid bronchial carcinoma cell line (NCI-H292) were used.

16-HBE is a cell line that retains the differentiated morphology and function of normal airway epithelial cells [113]. 16-HBE cells were cultured in Dulbecco-modified Eagle’s medium (DMEM) with 10% heat-inactivated fetal calf serum (FCS) and supplemented with 2 mM glutamine, 50 U/ml penicillin, and 50 mg/ml streptomycin.

NCI-H292, derived from a cervical node metastasis of a pulmonary mucoepidermoid carcinoma, were maintained in Roswell Park Memorial Institute (RPMI) 1640 Medium with 10% FCS and in the same way as 16-HBE, supplemented with glutamine, penicillin and streptomycin.

Cell cultures were grown as monolayers attached to the culture flask and cultured at 37°C, 5% CO_2 in a humidified incubator. Passage number of cells used in this study ranged from 12 to 35.

2.2 Cigarette smoke extract (CSE).

Kentucky 1R4F research cigarettes (University of Kentucky, Lexington, KY) were used in this study.

CSE was prepared by modification of the methods of Carp and Janoff [114]. The smoke from two cigarettes without filter was gurgled, for 60-70 sec, through 40 ml of serum-free DMEM or RPMI, for monolayer cell culture, or BEBM, for 3D outgrowth culture. A Buchner flask connected to a system acting as a vacuum-driven apparatus was used. Then, the resulting suspension was adjusted to pH 7.4 with concentrated NaOH and filtered through a 0.22 µm pore filter Syringe filter (Whatman, Fisher scientific), to remove bacteria and large particles, and was defined as 100% CSE. It was used immediately to treat cell cultures at different percentages and for different incubation times.

2.3 Cell viability Assay (MTT).

Preliminary analyses were performed to identify the best time point as well as the best CSE concentration.

In order to study whether exposure to cigarettes smoking was or not associated with cytotoxicity, cell viability was assessed by reduction of the tetrazolium salt 3-(4,5-dimethylthiazol-2-yl)-2,5-diphenyl tetrazolium bromide (MTT) to its insoluble formazan, which has a purple dye by mitochondrial enzymes associated with metabolic activity, indicating living cells [115]. Briefly, cells were seeded in 96-well plates (6,000 cells/well) and were allowed to adhere overnight, then were treated with CSE (0-100%) for 24, 48 and 72 hours. 20 µL of fresh MTT solution (5 mg/mL) was dissolved in PBS and was added to the cells that were cultured for 5h at 37ºC. After that, the medium was removed and 200 µL of DMSO solution

was added to dissolve formazan crystals. Therefore, absorbance was measured at 550 nm by a plate reader and the viability was set as 100% in non-treated cells.

2.4 Total RNA Extraction and Retro Transcription PCR.

RNA from both treated and untreated cells, was obtained, as previously described by Rappa and colleagues [116], by the use of TRI Reagent© (Catalog Number T9424, Sigma-Aldrich, Saint Lois, MO), which is a mixture of guanidine thiocyanate and phenol that allow to isolate simultaneously RNA, DNA, and protein.

Cells were seeding with density of 6 x 10^6 cells/25 cm^2 and after treatment were detached and centrifuged at 300 x g, 4°C. Each cell pellet was homogenized in 1 ml of TRI Reagent© and subsequently centrifuged at 12000 x g for 10 minutes at 4°C to remove the insoluble material. Then, 0.2 ml of chloroform was added to the samples. After 15 minutes, the mixtures were centrifuged at 12000 x g for 15 minutes at 4°C, to separate the RNA phase from proteins and DNA, and RNA phase was transferred to a fresh tube and then 0.5 ml of isopropanol was added. After 10 minutes, the samples were centrifuged at 12000 x g for 10 minutes at 4°C. The supernatant was removed and the RNA pellet was added to 1 ml of 75% ethanol and then shaken. The mixture was centrifuged at 7500 x g for 5 minutes at 4°C. Finally, we dissolute the air-dried RNA in 50µl of RNase/DNase-free H_2O by repeated pipetting with a micropipette at 55–60 °C for 10–15 minutes.

The concentration of the RNA extract was determined using Thermo Scientific NanoDrop ND-2000 1-position Spectrophotometer (Thermo Scientific Massachusetts, USA).

cDNA was synthesized, as described by Campanella and colleagues [117], using ImProm–II Reverse Transcriptase (Catalog Number A3800, Promega Corporation, Madison, WI, USA). To obtain 200 ng of cDNA, twenty microliters of mixed solution with RNA template, 0.5 µg Oligo(dT) primers, 6mM MgCl2, reaction buffer 5X, 1 µL dNTP (0.5 mM mixture of

dATP, dCTP, dGTP, and dTTP), 20U RNase inhibitor, 1 µL ImProm-II reverse transcriptase, and nuclease-free distilled water was incubated at 25℃ for 5 minutes and then at 42℃ for 90 minutes. To inactivate reverse-transcriptase, the mixture was incubated at 70℃ for 15 minutes. Thereafter, cDNA was amplified using GoTaq® Flexi DNA Polymerase (Catalog Number M8291, Promega Corporation, Madison, WI, USA), using 1.25U GoTaq Polymerase. Semi-quantitative PCR was performed by adding primers specific for human Hsp60 and β-actin, the latter was analyzed as a housekeeping gene internal control (Table 6). Reactions were carried out for 2 minutes of preheating at 95℃ and 35 repeated cycles of reactions at 95℃ for 1 minute, 60℃ for 1 minute, and 72℃ for 3 minutes. A final incubation was done at 72℃ for 5 minutes, and the reaction was stopped at 4℃. The PCR product was visualized on 1.5% agarose gel with the SYBR stain (SYBR SafeTM DNA gel stain, 10,000X concentrated in DMSO- Invitrogen, Carlsbad, CA).

Experiments were performed in triplicate. Quantitative measurements of bands were performed using the NIH Image J 1.40 analysis program (National Institutes of Health, Bethesda, MD) [116]

2.5 Immunomorphological analyses: immunocytochemistry and immunofluorescence.

Cells were routinely photographed before and after treatment to observe any morphological changes occurring in the cells.

2.5.1 Immunocytochemistry (ICC).

Analysis was performed on 16-HBE cells cultured on chamber slides and treated with 0, 5 and 10% of CSE for 24 hours. After culturing, cells were fixed with ice-cold methanol for 30 minutes, and, after rinse with PBS (three times for 5 minutes), permeabilized with 0.1% (v/v) Triton X-100 and 0.1% sodium citrate in PBS for 5 minutes. Fixed cells were treated with Histostain®-Plus 3rd Gen IHC Detection Kit (Invitrogen), following manufacturer’s instructions, in the same way as immunohistochemistry (see above) .

After incubation with blocking reagent for 10 minutes, cells were incubated with primary antibodies overnight at 4°C (anti-HSP60, LK1 clone, Sigma-Aldrich; anti Hsp10 clone D8, Santa Cruz Biotechnology). Finally, cells were incubated with universal biotinylated secondary antibody and then with streptavidin-peroxidase complex for 10 minutes. Following a further washing with PBS for 5 minutes, the slides were incubated in the dark for 5 minutes in the DAB chromogen. Haematoxylin was used for counterstaining. The positive reaction was observed using a light microscope (Leica DM5000B, Leica Microsystems, Heidelberg, Germany). Experiments were performed in triplicate.

2.5.2 Double immunofluorescence (IF) in monolayer cell cultures.

To assess the subcellular localization of the chaperonin Hsp60 and its possible co-localization with the EGF-Receptor (a plasma membrane marker), a double immunofluorescence was carried out.

The immunofluorescence was performed as previously described by Marino Gammazza and colleagues [118]. Briefly, 16-HBE cells were seated in 8-well microscope chamber slide at the density of ten thousand cells/well, cultured for 24 hours and then treated with CSE (0, 2.5, 5 and 10%) for 24 hours. Cells were fixed with ice cold methanol for 30 minutes, washed three times with PBS pH 7.4 and then were incubated with

unmasking solution (tri-sodium citrate 10mM, 0.05% Tween 20, pH 6) for 10 minutes at RT (room temperature, 24°C). After rinsing twice with PBS, the cells were blocked with 3% (w/v) bovine serum albumin (BSA, Sigma Aldrich) for 30 minutes at RT and incubated with the first primary antibodies anti-EGF-R (clone 0.N.268, from Santa Cruz Biotechnology, Dallas, TX) diluted 1:500, overnight at 4°C. The day after, the cells were incubated with the second primary antibody anti-HSP60 (clone LK1, monoclonal antibody from Sigma-Aldrich, St. Louis, MO), diluted 1:500, overnight in a humidified chamber at 4°C. Once again, cells were incubated with fluorescent secondary mouse IgG antibody TRITC conjugated (from Sigma-Aldrich), diluted 1:250, for 1h at RT. Therefore, we used FITC conjugated rabbit IgG secondary antibody (from Sigma-Aldrich), diluted 1:250, for 1h at RT in a moist chamber. The nuclei were counterstained with Hoechst 33342 (Sigma-Aldrich) for 15 minutes at RT. Finally, the slides were covered with drops of PBS and mounted with coverslips, using a drop of Vectashield (Vector, Burlingame, CA). Imaging was immediately performed with an upright fluorescent microscope Leica DM5000. The cell positivity of both markers (“Merge”) was assessed through the ImageJ Free software (NIH).

2.6 Western blotting Analysis.

The 16-HBE and H292 cells were cultured in T25 flask and treated once cells reach 70-80% confluence. On the basis of the results obtained by MTT assay, cells were treated for 4, 8, 16 and 24 hours with different CSE concentration (0, 2.5, 5, 10%). Cells were mechanically detached from flask and centrifuged at 222 x g for 5 minutes. The pellet was washed two times with PBS and then cells were lysed using radioimmunoprecipitation assay (RIPA) buffer, containing 50mM Tris/HCl,150mM NaCl,1% NP-40, 1mM EGTA and supplemented with Protease Inhibitor Cocktail (Sigma-Aldrich, USA) (1mM AEBSF, 1µM Aprotinin, 50µM Bestatin, 15µM E-64, 20µM Leupeptin, 10µM Pepstatin A). The entire procedure was carried out on ice to prevent protein degradation. Cell lysates were then homogenized

by pipetting up and down several time on ice for 1 hour. To obtain only the whole protein suspension, lysates were centrifuged at 16,000 x g for 20 minutes. The supernatant was collected and stored in new tubes at -20°C [115].

Total proteins concentration was determined using Bradford assay, which allow to measure protein concentration by comparing the absorbance value with a known value based on a calibration curve of bovine serum albumin (BSA). Finally, the absorbance at 550 nm was read. This preparation is referred to as “total-cell lysate”.

A standard western blotting procedure was followed to separate protein using a 12% polyacrylamide gel (SDS-PAGE); in which equal amounts of protein (20 µg) were added to 4X Laemmli buffer and heated for 5 min at 95 °C. Therefore samples were loaded in each well and transferred onto a nitrocellulose membrane (BioRad, Milan, Italy). The membranes were stained with Ponceau S to verify the quality of transfer and loading similarity. After blocking with 5% albumin bovine serum (Sigma Aldrich), membranes, with the spotted proteins, were analyzed to measure the protein levels, probing with specific primary antibodies for 12 hours followed by incubation with horseradish peroxidase-conjugated secondary antibody if necessary. The final detection was performed using the enhanced chemiluminescence (ECL) detection system, Western Blotting Detection Reagent (Amersham Biosciences, GE Healthcare Life Science, Milan, Italy), according to the manufacturer’s instructions. Membranes were then exposed to X-ray film from few second to 5 min and the film was analyzed.

Densitometric analysis of the bands was evaluated and quantified using the NIH Image J 1.40 analysis program (National Institutes of Health, Bethesda, MD).

Each experiment was performed at least three times.

2.7 Exosomes isolation from culture supernatant.

Prior to each experiments, confluent cell monolayers were incubated in medium with serum exosomes–free (to avoid possible contaminations by bovine exosomes from the FBS) for 24 hours.

The 16 HBE and H292 cells were grown under the conditions described above (see the section 2.1). Once the reached 70% to 80% of confluence they were treated with different concentration of CSE (0 and 10%) for 24 hours. Eighty ml of conditioned medium from 80×10^6 were collected and then centrifuged (800 × g for 10 minutes at 4 °C) to eliminate cells and debris. The cell- and debris-free medium was collected on ice and centrifuged at 13,000 × g for 20 minutes at 4 °C to span down and eliminate small cellular debris and mitochondrial contaminants.

To obtain exosomes from the 3D outgrowth culture supernatant, conditioned medium was collected every two days. It was filtered with 0.22 µm pore filter in order to eliminate dead cells and large debris while small membranes were kept for further purification by ultracentrifugation. The media has been analysed in a group of seven days, and then results were compared between different groups.

The supernatant was collected and exosomes were separated by centrifugation at 110,000 × g for 2 hours at 4 °C using a Sorvall WX100 Ultra Series ultracentrifuge (Thermo Scientific, Milan, Italy). The exosome pellet was collected, washed once with PBS and then resuspended in 100 µl of PBS containing proteases inhibitors. Besides, the pellet was also resuspendend in RIPA buffer, supplemented with proteases inhibitors, in order to obtain protein specimens from exosome suspension. Proteins in exosomal preparations were quantified by the Quant-iT™ protein assay kit (Invitrogen Molecular Probes, Italy), using the Qubit fluorimeter according to the manufacturer's instructions (the kit is accurate for protein concentrations ranging from 12.5 µg/ml to 5 mg/ml).

2.7.1 Exosomes assessment: NanoSight Technology.

The Nanosight (NS 300, Amesebury, UK) system, was used in this work under the guidance of a technicians and it has allowed to assessing the size profile of extracellular vesicles in ultra-centrifuged pellets. This platform is based on nanoparticle tracking analysis (NTA), a method that lead to visualization and analysis of each single nanoparticle suspended in liquid in real-time, by direct observation of diffusion. NTA connects the rate of Brownian motion to particle size, and the vesicles are visualized by light scattering using a light microscope.

The conditioned media from 16-HBE and H292 cells, both treated and untreated with CSE, were collected and processed as described above (see the section 2.7). The resultant pellets were pooled between the same conditions, washed with PBS and stored at -80°C until use.

The samples were diluted and a finely focused laser beam was introduced to each sample. The particles contained in the sample were visualized by virtue of the light scattered by the particles when they were illuminated by light laser. Particles scattering from laser beam were captured using a scientific digital camera and the motion of each particle was tracked from frame to frame, recording video frames of 60 seconds. This rate of particle movement is related to a sphere equivalent hydrodynamic radius as calculated through the Stokes-Einstein equation.

2.7.2 Exosomes assessment: Transmission Electron Microscopy (TEM).

The purified exosome-like vesicles were resuspended in PBS and fixed with Karnovsky’s fixative (2.5% paraformaldehyde, 0.5% glutaraldehyde in 0.1M PBS pH 7.2) and then embedded in 2% low-gelling agarose (type VII; Sigma). The agarose-embedded samples were post-fixed in 1% OsO_4 for 2 hours, dehydrated in a graded ethanol series, passed through propylene oxide and infiltrated with epoxy resin (Epon812, Electron Microscopy Science, Hatfield, PA, USA) in propylene oxide (1:3, 1:2, and 1:1 for 30 minutes with agitation at room temperature, respectively), and

finally embedded in Epon812 with DMP30. Samples embedded in resin were polymerized at 60°C for 48 hours [119].

Ultrathin sections (60 nm) were cut with an ultra-microtome (Ultracut E, Reichert-Jung, Depew, NY, USA) and were finally stained with 2% uranyl acetate prior to viewing by transmission EM (TEM) using a Jeol JEM1010 microscope at 60 kV. Images were acquired with a digital camera MegaView III with Olympus Image Analysis Software (Secciòn de Microscopìa Electrònica, SCSIE, University of Valencia).

2.7.3 Exosomes assessment: Alix and Hsp70 detection.

The presence of exosomes was confirmed by detection of exosomal marker, such as Alix and Hsp70, using Western Blotting as described above.

3. Experiments *ex vivo.*

3.1 Biopsy specimens.

We obtained bronchial biopsies from 9 subjects (Table 5).

Status	Smoker	No smoker
Number	4	5
Male gender (%)	67%	33%
Mean age (range)	71±10	48±17

Table 5.

Characteristics of subjects studied by bronchial biopsy analysis.

3.1.1 Fiberoptic bronchoscopy, collection and processing of bronchial biopsies.

Subjects were at the bronchoscopy suite at 8.30 AM after having fasted from midnight and were pre-treated with atropine (0.6 mg IV) and midazolam (5–10 mg IV). Oxygen (3 l/minutes) was administered via nasal prongs throughout the procedure and oxygen saturation was monitored by

a digital oximeter. (Olympus BF10 Key-Med, Southend, UK) which was passed through the nasal passages into the trachea. Further lidocaine (2%) was sprayed into the lower airways, and four bronchial biopsy specimens were taken from segmental and sub-segmental airways of the right lower and upper lobes using size 19 cupped forceps

3.2 Bronchial Three-dimensional (3D) Outgrowth Model.

The three-dimensional culturing of bronchial biopsy cells was used to closely mimic the *in vivo* bronchial microenvironment, unlike the traditional two-dimensional monolayer culture.

To achieve the bronchial out-growth cultures, the necessary equipment are Tranwells with 0.4 µm pore size, Trasparent PET track-etched membrane (Falcon, 353095); 24 well plates (Falcon, 353504); BD Matrigel™ Basement Membrane Matrix (BD, 356234) and BEGM/DMEM mix medium (containing BPE, Bovine Pituitary Extract, 2.0 ml; Hydrocortisone, 0.5 ml; hEGF, 0.5 ml; Epinephrine, 0.5 ml; Transferrin, 0.5 ml; Insulin, 0.5 ml; Retinoic Acid, 0.5 ml; Triiodothyronine, 0.5 ml; GA, Gentamycin/Amphotericin, 0.5 ml).

Biopsies, few minutes after taking, were washed three times with PBS and cut into 0.5 mm^3 pieces using a sterile scalpel. Each piece was placed in the middle of transwell and embedded in 60 µl of BD Matrigel™. The Matrigel is a solubilized basement membrane preparation extracted from the Engelbreth-Holm-Swarm (EHS) mouse sarcoma, including laminin (a major component), collagen IV, heparan sulfate proteoglycans and also contains TGF-beta, EGF, IGF, FGF and tissue plasminogen activator. Matrigel provide specialized microenvironments that mimic native tissues and enable cells to grow and differentiate into specific cell types. The Transwells were placed in 24 well culture plates and these were then kept at 37°C for 5 minutes to facilitate Matrigel^{TM} jellification. 330 µl of growth medium mix was added to each well. This medium was constituted of BEGM/DMEM (1:1) (Bronchial Epithelium Growth Medium/ Dulbecco’s modified Minimum Essential Medium) with 10% fetal bovine serum (FBS).

The outgrowths were cultured at 37°C in 5% CO_2 atmosphere and the medium has been changed every 48 hours.

Bronchial out-growths were routinely observed by inverted phase contrast light microscopy (LEICA DM-IRB, Leica Microsystems Srl, Milan, Italy), and photographed to record the growth.

3.3 Treatments.

The conditioned medium to treat bronchial 3D outgrowth was obtained similarly to the CSE used for monolayer cultures. The smoke from one commercial cigarette, filters removed, was bubbles through 25 ml of BEBM (Bronchial Epithelium Basal Medium) medium serum-free (see the section 2.2). The filtered and pH adjusted CSE, called 100% was mix to BEGM in order to achieve the concentration range of CSE from 10 to 30%. This suspension was applied to the bronchial 3D outgrowth for different times (Fig. 7).

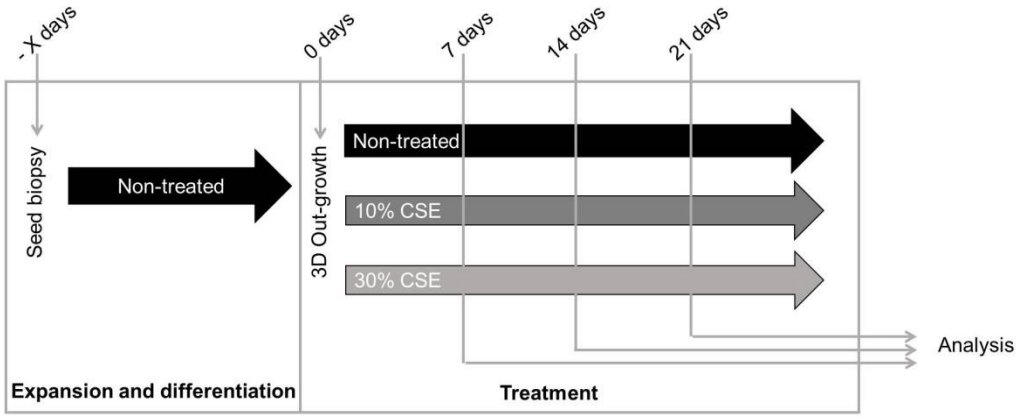

Figure 7.

Schematic overview of 3D outgrowth seeding and treatments (adapted from Schamberger at al 2015 [120]).

3.4 Teer measurement.

Transepithelial electrical resistance (TEER) was measured on 10th day to ensure the formation and integrity of tight junctions between cells in the

epithelium using an EVOM meter (World Precision Instruments, FL). Before measurement, the apical layer of the cultures was washed with PBS and then 15 µl of PBS was added to the apical and basolateral side in order to equilibrate the cultures (the incubation time was 15 minutes). Measurements were performed three times per well and a mean resistance value was calculated. Then, values were corrected for the blank resistance (membrane with no cells) and the surface area.

3.5 Determination of DNA damage: Tunel assay.

The presence of apoptotic cells, after CSE treatment, was detected through the study of DNA fragmentation using TUNEL assay, that preferentially labels DNA strand breaks, generated during apoptosis. The Fluorescein In situ cell death detection kit (Roche Applied Science, Indianapolis, IN) was used.

Both 3D outgrowths treated with 30% CSE for 7 days and untreated 3D outgrowths were washed with PBS twice and fixed with ice-cold methanol (30%, 10 minutes; 70%, 10 minutes and 100%, 10 minutes) at 4°C inside their plastic supports. After the cultures were fixed, outgrowths were left to dry in a laminar flow cabinet for 30 minutes and then removed from plastic supports. At this point outgrowths were embedded in Tissue Tek II OCT and 8 mm thick cryostat sections were cut and processed for Tunel analysis.

The sections were rehydrated accordingly with PBS and incubated with proteinase K, to avoid false-positive results, at 24°C for 30 minutes, then at 24°C for 8 minutes with a permeabilization solution (0.1% Triton X-100, 0.1% sodium citrate). Indeed, the slides were incubated in the Tunel reaction mixture, including Label solution and enzyme solution, in humidified atmosphere for 60 minutes at 37°C in the dark. Positive controls, using DNase I recombinant (20 U/ml) and negative controls (without terminal transferase) were included in each experiment. Therefore the sections were mounted using the Vectashield Antifade mounting medium (Vector) and examined under CSLM (Confocal Laser Scanning

Microscopy), Leica Confocal Microscopy (TCS SP8, Leica Microsystems, Milan, Italy). TUNEL-positive cells were enumerated by counting the labelled cells in eight randomly selected microscopic fields obtained from each specimen at 40× magnification. Therefore, the percentage of TUNEL-positive cells was calculated and averaged.

3.6 Study of Hsp60 levels in 3D bronchial outgrowths treated with CSE.

To assess the Hsp60 levels in bronchial outgrowths after treatment with different concentration of CSE for various times, the expression and proteins levels of this chaperon were evaluated.

3.6.1 RNA Isolation, Retro Transcriptional (RT PCR) and Real Time PCR (qPCR).

The bronchial outgrowths were stimulated by CSE (0, 10 and 30%) for 10 days and another group with CSE (10 and 30%) for 10 days and, than smoke-stimulated medium was removed and replaced with fresh medium for 10 days, in order to obtain a recovery. After that, the cells were removed from plastic supports and total cellular RNA was extracted using TRI Reagent®. PET membrane was taken out from resulting mixture and RT PCR was performed following the procedure described above (see the section 2.4).

The qPCR technique was performed for outgrowths treated by CSE for 21 days, using 20 ng of RNA. RNA was retro-transcribed using the ImProm-II Reverse Transcriptase Kit (Promega Corporation) in order to obtain cDNA, which was amplified using the GoTaq qPCR Master Mix (Promega Corporation, USA). The reaction mix was prepared with cDNA template, upstream and downstream PCR primers and GoTaq® qPCR Master Mix, 2X. The cycling program was carried out with the Rotor Gene Q, Qiagen (Qiagen, Milan, Italy), using the following steps: Hot-Start Activation, 1 cycle at 95°C for 2 minutes; denaturation, 40 cycles at 95°C for 15 seconds; annealing/extension at 60°C for 60 seconds; dissociation, 1

cycle at 60–95°C. The mRNA levels were normalised to the levels obtained for hypoxanthine phosphoribosyltransferase 1 (HPRT1) and for beta-glucuronidase (GUSB). Changes in the transcript level were calculated using the 2-ΔΔCt method [121]. The cDNA was amplified using the primers indicated in Table 6.

Primer	Forward	Reverse
Homo HSPD1 var1	5’-GAGTAGAGGCGGAGGGAG-3’	5’-AGTGAGATGAGGAGCCAGTA-3’
Homo GAPDH	5’-TCCCTCCAAAATCAAGTG-3’	5’-GGCAGAGATGATGACCC-3’
Homo GUSB	5’-CGAGTATGGAGCAGAAACGA-3’	5’-TTTATTCCCCAGCATCCTCG-3’
Homo HPRT1	5’-GAGTCCTATTGACATCGCCA-3’	5’-CGCCCAAAGGGAACTGATAG-3’
Homo β-actin	5’-CAC CTT CAC CGT TCC AGT TT-3’	5’-AGG TAC TCC GTG TGG ATC GG-3’

Table 6.

Forward and reverse primers used for the polymerase chain reaction.

3.6.2 Protein isolation and Western Blotting analysis.

The Hsp60 levels in 3D bronchial outgrowths were analyzed at different time points of CSE treatment: 2, 7 and 21 days. Samples were removed from their plastic supports and 500 µl of RIPA buffer was used to lyse cells. PET membrane was take out from resulting suspension and lysis method and western blotting were performed as described above (see the section 2.5).

3.7 Bronchial 3D outgrowths characterization by immunofluorescence and morphological assessment of CSE effect.

Immunofluorescence analysis was carried out to evaluate the distribution of epithelial markers and Hsp60.

3D cultures were grown up to reach the appropriate growth and then washed with PBS and fixed with ice-cold methanol (30%, 10 minutes; 70%, 10 minutes and 100%, 10 minutes) at 4°C. The fixed outgrowths were left to dry in a laminar flow cabinet for 30 minutes and then they were removed from plastic supports. At this point outgrowths were embedded in Tissue Tek II OCT and 8 mm thick cryostat sections were cut and processed for immunofluorescence analysis.

The specimens were washed with PBS, pH 7.4, and then were incubated with the unmasking solution (10mM trisodium citrate, 0.05% Tween 20) for 10 minutes at 23 °C. Therefore, the sections were incubated with the blocking solution (3% bovine serum albumin in PBS) for 30 minutes at 23 °C and with the pertinent primary antibody overnight at 4 °C. Subsequently, the sections were incubated with the second primary antibody overnight at 4 °C (anti-α-Actinin antibody, diluted 1:300; anti-TJP1 antibody, diluted 1:200; anti Hsp60 antibody; all purchased from Sigma-Aldrich, Milan, Italy). After washing twice with PBS, all slides were incubated with fluorescent secondary antibodies (rabbit IgG antibody conjugated with Texas Red, Gene Tex Inc, dilution 1:200; FITC-conjugated donkey anti-goat secondary antibody, Gene Tex Inc., dilution1:200) for 1hour each at 23°C. The nuclei were counterstained with Hoechst (Sigma-Aldrich, Inc, Milan, Italy) for 15 minutes at 23 °C. Finally, all slides were mounted by cover slips using a drop of Vectashield (Vector). Images were captured using inverted laser scanning fluorescence confocal microscope (Leica Confocal Microscope, TCS SP8; Leica Microsystems) equipped with acquisition and analyses software. FITC and TRITC filters were used.

3.7.1 Detection of Hsp60 in conditioned medium: ELISA.

Elisa was performed using a commercial Hsp60 (human) enzyme immuno-assay (EIA) kit (ADI EKS 600 ELISA kit from Enzo Life Sciences, Inc., Farmingdale, NY, USA). It is quantitative sandwich immunoassay, in which a mouse monoclonal antibody is pre-coated on the wells of plate. Hsp60, present in the sample, was captured by the immobilized antibody and detected by an Hsp60 specific, goat polyclonal antibody.

In addition, we performed a quantitative comparison of Hsp60 levels in conditioned medium of 3D bronchial outgrowth treated with CSE (30%) for 0, 7, 14 and 21 days. The assay was performed also to test Hsp60 levels in plasma collected from patients with mild/ severe COPD (age 68±14 years) and from healthy (age 60±10 years) volunteers as controls.

Whole blood sample from each subject were collected in EDTA-treated tubes. After a centrifugation at 2,000×g for 30 minutes, plasma was collected, aliquoted, and stored at −20 °C until use. The Hsp60 standard was diluted in sample diluent to generate a standard curve with six points, ranging from 3.125 to 100 ng/ml, and sample diluent alone was used as 0 (zero) standard.

First, 100 µl of prepared standards and undiluted plasma was added in duplicate to wells of the immunoassay plate precoated with mouse monoclonal antibody specific for Hsp60 and incubated at 23 °C for 1 h. The primary and the secondary antibodies were diluted according to the manufacturer's instructions. Therefore, 100 µl of diluted anti-Hsp60 goat polyclonal antibody was added to each well and incubated at 23 °C for 1 h. After washing, 100 µl of diluted horse radish peroxidase-conjugate anti-goat IgG was added to the plate and incubated at 23 °C for 30 minutes followed by 100 µl of 3,3′,5,5′- tetramethylbenzidine substrate for 15 minutes in the dark. Finally, 100 µl of Stop Solution was added, and absorbance was measured at 450 nm in a microplate photometric reader (Microplate reader, Euroclone, Milan, Italy). Sample concentration was calculated by interpolating the sample concentrations in the standard curve. The sensitivity of the human Hsp60, EIA kit was determined to be

3.125 ng/ml. Human Hsp60 EIA kit is specific for Hsp60 and the Hsp60 ELISA has been certified for the detection of human Hsp60.

3.7.2 Detection of cytokines in conditioned medium: Multiplex cytokine determination assay.

To evaluate the bioactive molecules release, such as cytokine, from outgrowths treated by the smoke extract, a cytokine profile assay was performed. Bio-Plex Pro™ Assay, human cytokine multiplex kit was purchased from Bio-Rad Laboratories (Bio-Rad, CA, USA) and was used following the manufacturer’s instructions.

The 3D bronchial outgrowths were treated by CSE (30%) for 0, 7, 14 and 21 days and culture supernatants were retrieved every two days and grouped in 7, 14 and 21 days treatment groups. Media were conserved a -80°C until use.

The supernatants were analysed simultaneously for 17 cytokines, including IL-1b, IL-2, IL-4, IL-5, IL-6, IL-7, IL-8, IL-10, IL-12p70, Il-13, IL-17, TNF-α, lFN-γ, TNF-β, MCP-1, MIP-1, G-CSF and GM-CSF with a Bio-Plex machine, which employed a bead-based sandwich immunoassay.

Plates were incubated with diluted beads (1X) and washed two times. Cytokine standards, controls and unknown samples were added (50 µl total volumes) to 96 well plates in duplicates and incubated with detection antibody-immobilised micro beads. Indeed, for the detection of multiple cytokines, a monoclonal antibody specific for each cytokine was coupled to a particular set of beads and Streptavidin-Phycoerythrin reagent (SA-PE, 1X), with known internal fluorescence, was used. The assay was analysed by the Bio-Plex manager software (version 4.0) and a standard curve was used to relate and calculate the concentration of each cytokine. The sensitivity of this method was less than 10 pg/ml and the assay could accurately detect cytokines in the range of 1-32,000 pg/ml.

4. Assessment of circulating levels of Hsp60 in COPD patients and exosomes-PBMC co-cultures.

4.1 Assessment of circulating levels of Hsp60 in COPD patients: ELISA.

3 ml of Ficoll-Paque media (Ficoll® Paque Plus GE Healthcare, Milan, Italy) were added to the anticoagulant-treated blood samples from COPD patients and healthy control volunteers (Table 7) and centrifuged at 300 x g, for 30 minutes at 23°C. The upper layer containing plasma was drawn off, while the mononuclear cell layer was transferred to a sterile centrifuge tubes for later use.

The plasma samples were diluted to perform ELISA using a commercial Hsp60 (human) enzyme immuno-assay (EIA) kit, as described above (see the section 3.7.1); to evaluate the levels of the circulating Hsp60 in COPD patients compared with normal controls.

Status	COPD	Healthy control
Number	5	7
Mean age (range)	68±14	60±10

Table 7.

Characteristics of subjects studied for Assessment of circulating levels of Hsp60.

4.2 Establishing of exosomes-(PBMC) peripheral blood mononuclear cells co-cultures.

PBMCs were cultured in RPMI 1640 with 10% heat-inactivated fetal calf serum (FCS) and supplemented with 2 mM glutamine, 50 U/ml penicillin, and 50 mg/ streptomycin; with a density of 2 x 10^6 cells.

Cell were treated for 24 hours with exosomes isolated from conditioned medium of outgrowths (0 and 30% of CSE at 21 days of treatment). The amount of exosomes used for the treatment was the volume corresponding to 50 µg of proteins (as described by Jong-Kuen and colleagues, 2013 [122]). Cells were also treated with 10 µg/ml of

recombinant Hsp60 (V13-31176, Vinci-Biochem srl, Firenze, Italy). To control for possible lipopolysaccharide contamination, antibiotics were used.

Therefore, the supernatants were collected and centrifuged at 300 x g in order to remove cells. The level of cytokines released was tested through Bio-Plex machine, as described above (see the section 3.7.2).

Results

1. *In vivo* analysis of Hsp10 and Hsp60 levels and cellular localization.

Firstly, the levels of Hsp10 and Hsp60 in epithelium and lamina propria of bronchial mucosa of non-smoking and smoking subjects with normal lung function were quantified, by immunohistochemistry. The aim was to evaluate the localization of these proteins and to determine whether an increase association with smoking was present. Neither Hsp10 nor Hsp60 levels showed significant quantitative changes in epithelium or in lamina propria of the bronchial mucosa of smokers compared with non-smokers (Figure 8 A). Both molecules showed a cytoplasmic positivity, often with a granular pattern resembling a mitochondrial positivity (figure 8 B). Hsp10 was positive in both groups of subjects, smokers and non-smokers, and in both epithelial and lamina propria cells, while Hsp60 positivity was clearly in the cytosol.

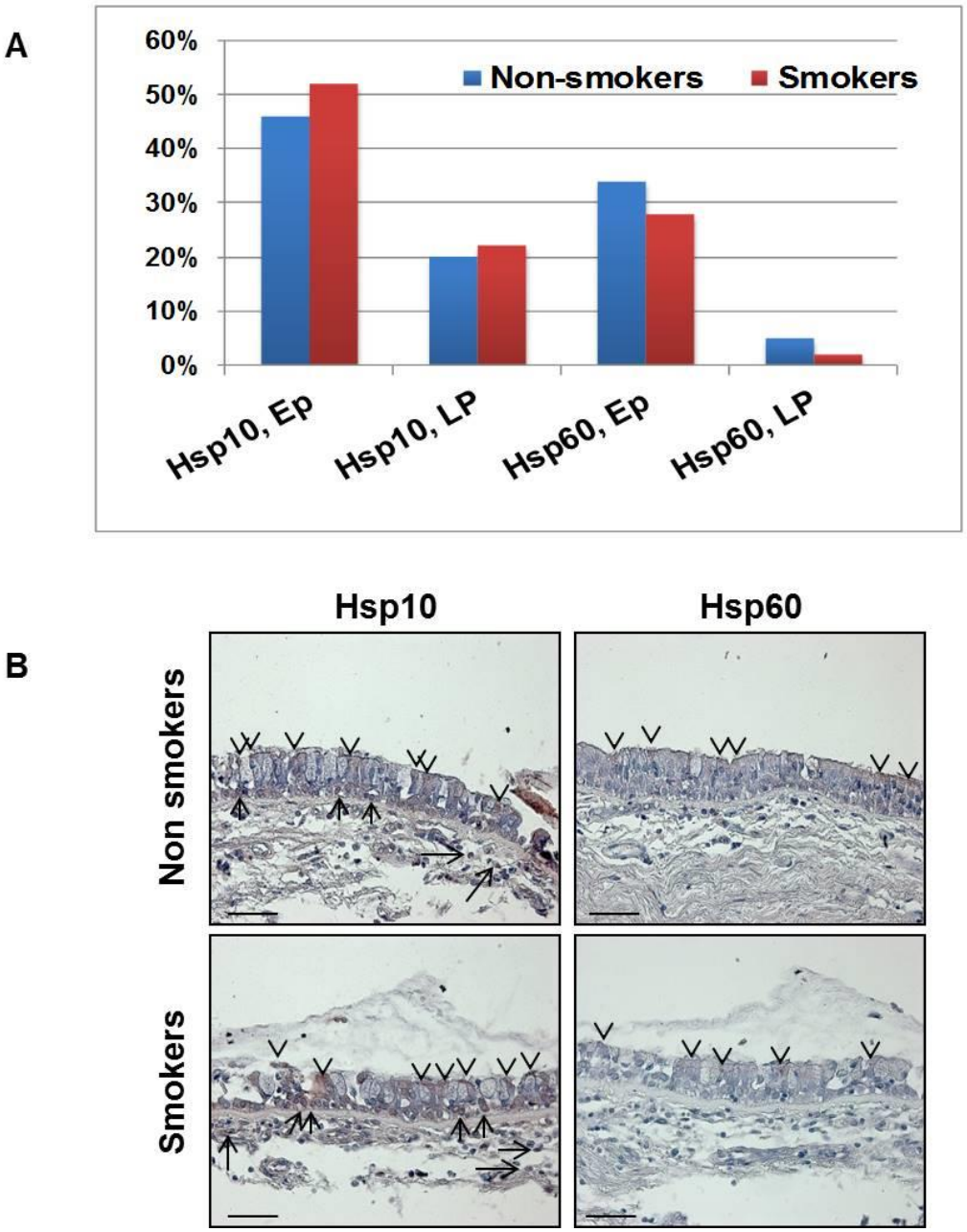

Figure 8.

Immunohistochemical detection of Hsp10 and Hsp60 in human bronchial mucosa. **(A)** The levels of Hsp10 in epithelium (Ep) and in lamina propria (LP) were similar in non-smokers compared with smokers. Hsp60 was detected only in epithelial cells and its levels were also similar in non-smokers and smokers. Statistical analyses showed that all of the variations were not significant with p-values ranging between p=0.1 and 0.4. **(B)** Representative immunohistochemical images. Hsp10 is present in epithelium and lamina propria cells of non-smokers and smokers, whereas Hsp60 is present only in epithelial cells. Arrowheads, epithelial positivity; arrows, lamina propria positivity. Scale bars, 50 µm.

2. Monolayer *in vitro* model. Reproducing smoke-induced oxidative stress and evaluation of Hsp60 levels and localization.

2.1 16 HBE cells exposure to CSE and cell viability evaluation.

To assess the cytotoxic effect of CSE on 16 HBE cells, cell viability was measured by MTT assay. Cells were treated with increasing concentrations (within the range of 0-100%) of CSE for 24 and 48 hours. The suspension had a dose- and time-dependent cytotoxic effect (Figure 9 A, A1 and B1). After 24 hours of treatment, CSE reduced cell viability by 70% with 25% of CSE (Figure R. 2A and R. 2A1). The effect was even more pronounced after 48 hours of treatment with 25% CSE when 80% of cells were dead with 25% of CSE (Figure 9 B). These effects were statistically significant when compared to untreated cells (p-value less than 0.05). The doses which caused the death of 50% of the cells (IC_{50}) were estimated to be 15% and 10% after 24 and 48 hours of CSE treatment, respectively. Using this method the viability of the cells that remain attached, regardless of the detached cells, were taken into account. Floating cells dead or were dying and this process was proportional to the CSE doses, indeed it did not invalidate MTT results.

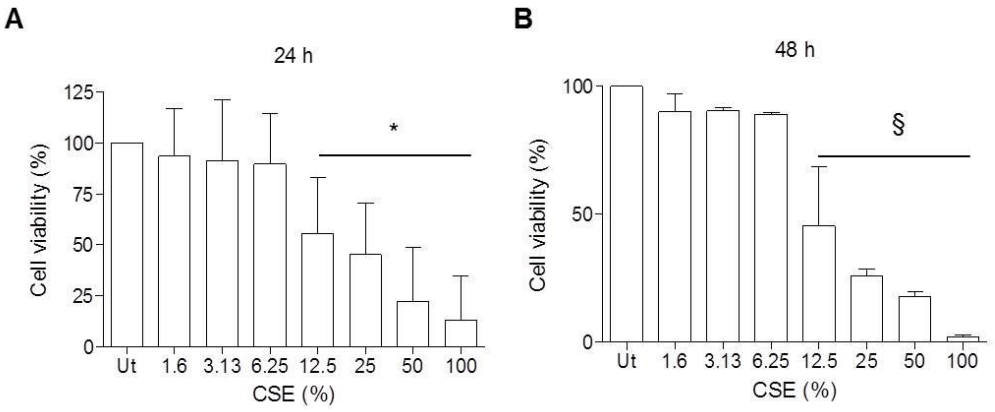

Figure 9.

16 HBE cells ($8x10^3$/well) were treated with increasing CSE doses for 24 **(A)** and 48 **(B)** hours, and then cell viability was assessed using the MTT test and expressed as the

percentage of the viable cells compared with untreated. A dose-dependent decrease of 16-HBE cell viability was observed. The IC_{50} values after 24 and 48 hours were 15 and 10%, respectively. Values represent the means of three independent experiments ± S.D. (*different from control p-value<0.001 and § different from control p-value<0.05).

2.2 Analysis of Hsp60 and Hsp10 mRNAs expression. RT-PCR.

The study of Hsp60 was the main objective of this study as Hsp60 is an important chaperonin involved in the protection of cells from oxidative stress. For that reason, in this work, we studied the level of this protein as well as of Hsp10, which is its co-chaperone.

At transcriptional level, the quantification of Hsp60 mRNA levels in 16 HBE cells by RT-PCR revealed that CSE treatment (10, 5 and 2.5%) did not have any significant effect on Hsp60 expression (Figure 10 A and B, upper panel). Likewise, we did not find any significant differences in Hsp10 mRNA levels between treated and non-treated cells (Figure 10 A and B, lower panel).

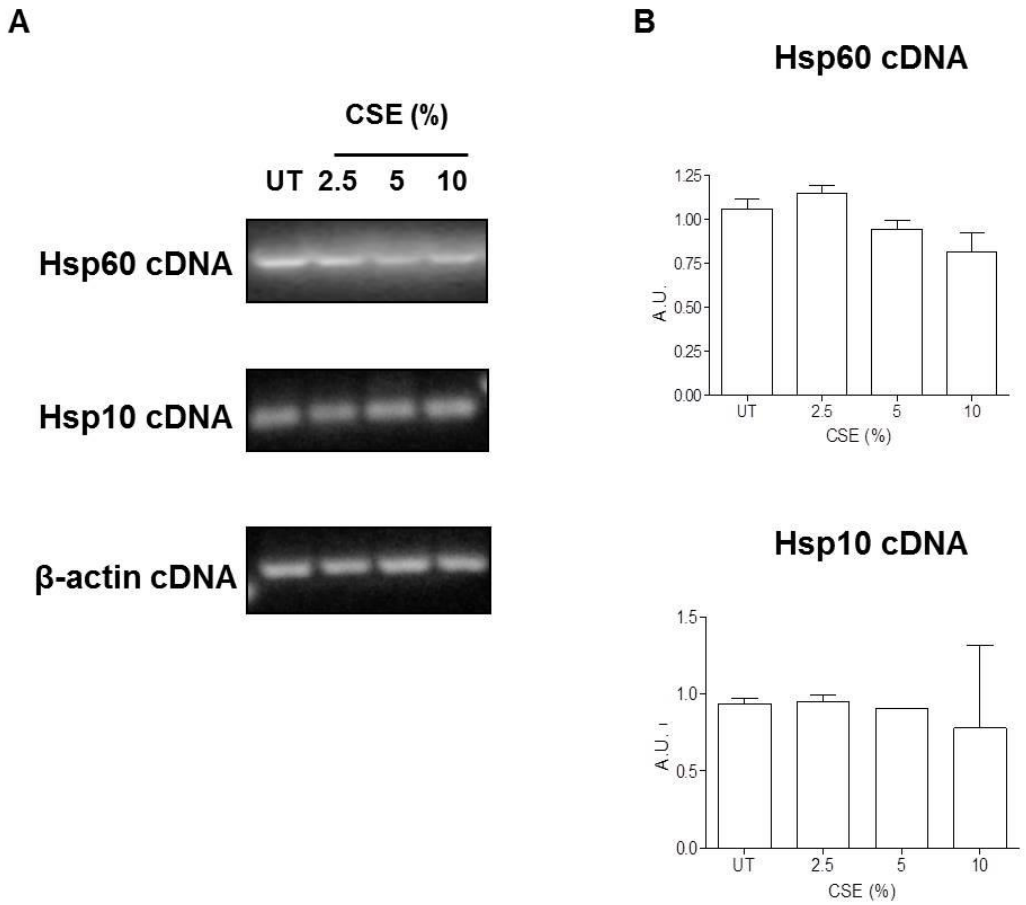

Figure 10.

(A) RT-PCR analysis of mRNA Hsp60 and Hsp10 levels and **(B)** respective densitometry of corresponding bands. Hsp60 mRNA was not significantly different after treatment with 10% CSE when compared with the untreated cells, and also the Hsp10 mRNA did not change significantly. Values represent the mean of three independent experiments ± S.D.

2.3 Hsp60 protein analysis: Immunocytochemistry (ICC).

In accordance with the RT-PCR data, neither Hsp60 nor Hsp10 expression were changed when cells were tested in all conditions (0, 2.5, 5 and 10% of CSE) and Hsp60 and Hsp10 levels were assessed by immunocytochemistry. Hsp60 positivity was localized in cytosol and mitochondria (Fig. 12 A), while Hsp10 was present normally in cytosol (Fig. 12 B).

For further *in vitro* studies we decided to be focused on Hsp60, because Hsp10 was object of another thesis from our department [112], were the

localization and changes of Hsp10 in lung cells in response to CS was studied.

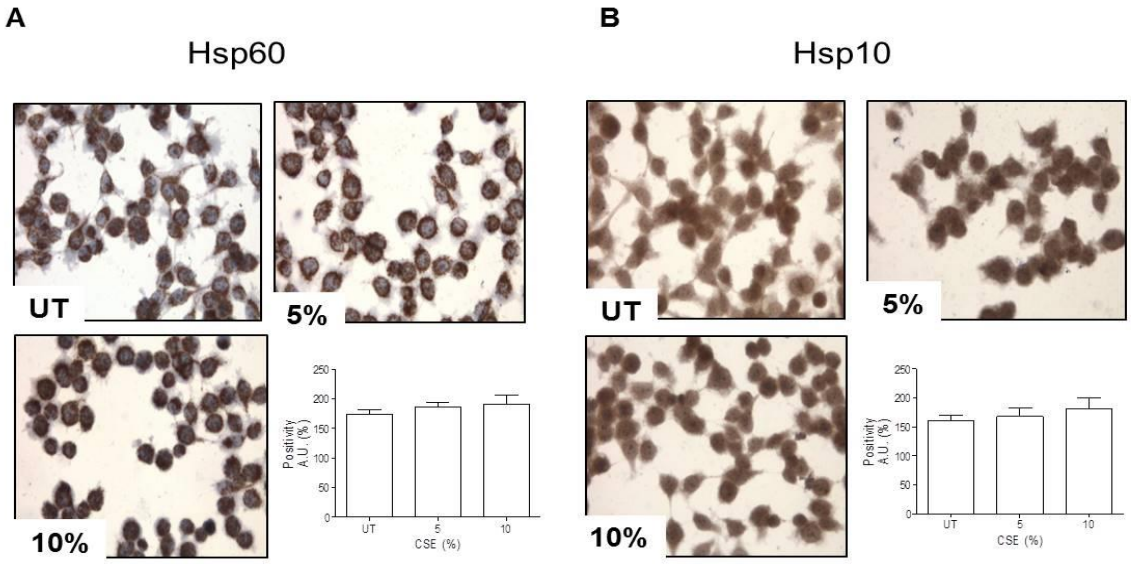

Figure 11.

Immunocytochemical analisys of Hsp60 **(A)** and Hsp10 **(B)** expression, after 24 hours of the CSE treatment (representative images of three experiments are presented here). Not significant changes were observed in both Hsp60 and Hsp10 expression. Magnification 40X.

2.4 Hsp60 protein analysis: Western Blotting (WB).

To determine whether CSE treatment (the same percentage of CSE to treat cells for different time points, as described above) induces changes in Hsp60 protein levels in 16 HBE cells, the western blotting analysis was performed. Western blotting analyses were performed at different times, after 4, 8, 16, 24 and 48 hours of the treatment in order to study if possible immediate or tardive variations of this protein exist (Fig. 11 A). The results do not show significant changes in the levels of Hsp60 in 16-HBE after treatment with 2.5, 5 and 10% of CSE compared to untreated (UT) cells (Fig. 11 B).

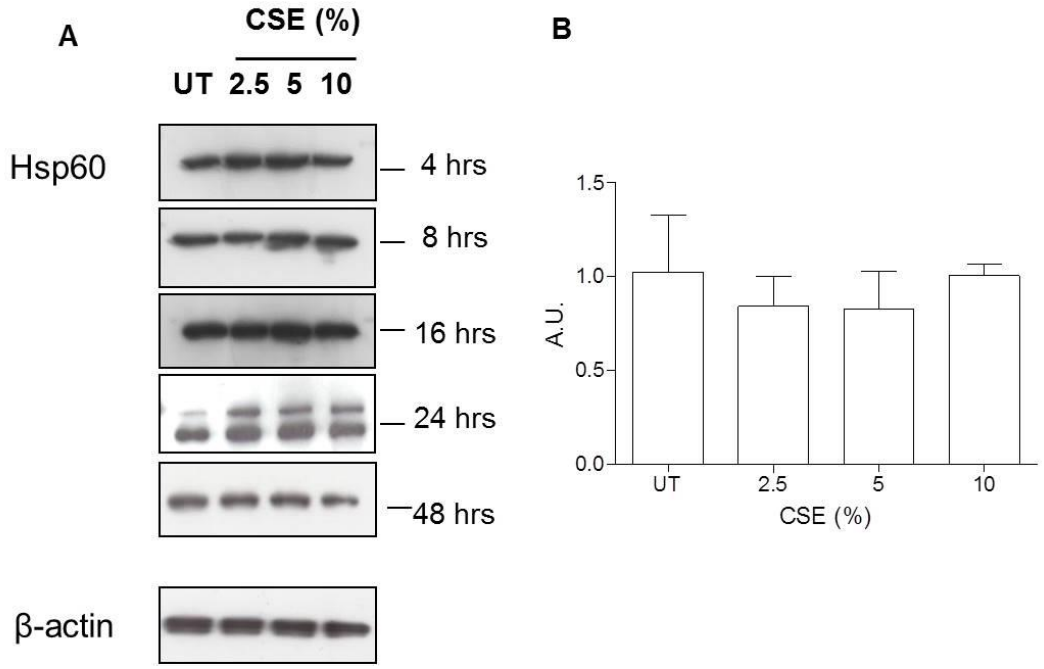

Figure 12.

(A) Western blotting of Hsp60 after 4, 8, 16, 24 and 48 hours of CSE treatment in 16 HBE cells; **(B)** representative densitometry of protein bands (24 hours). Arbitrary units (A.U.) of band intensities were normalized to those of the control in each series of experiments. Hsp60 protein levels did not change significantly after treatment when compared to the untreated cells.

2.5 Hsp60 cell distribution assessment: Immunofluorescence analysis (IF).

Double immunofluorescence tests were performed to assess the co-localization of Hsp60 and EGFR (a plasma membrane marker) in 16 HBE cells treated with smoke extract, considering the hypothesis that Hsp60 may be secreted by the cells following oxidative stress. The representative data (10% of CSE) shows only a single staining, indicating that Hsp60 was not present in the membrane (Fig. 13 A, B, C and D).

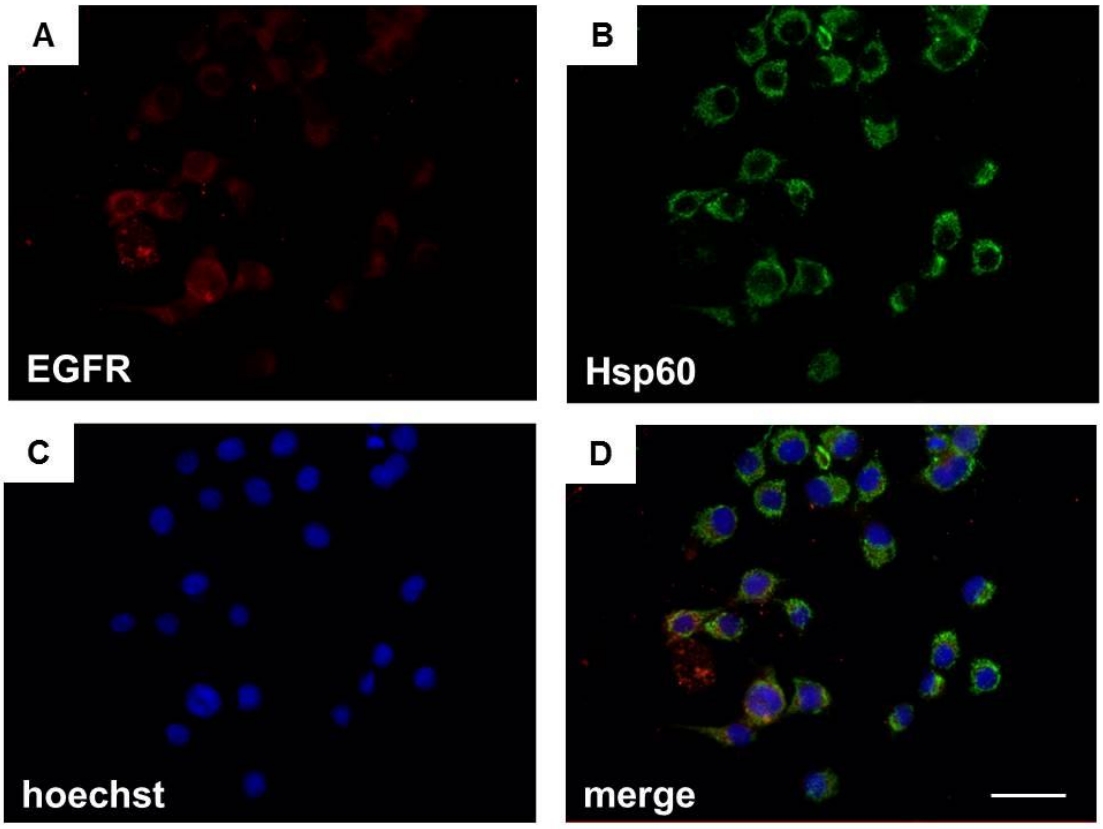

Figure 13.

Double immunofluorescence analysis of Hsp60 cellular distribution and EGF-R in CSE-treated 16 HBE cells showed Hsp60 positivity both in mitochondria and cytosol. **(A), (B), (C)** and **(D)** representative image of 16 HBE cells treated with 2.5% CSE. **(A)** EGF-R was detected by TRICT conjugated antibody, **(B)** Hsp60 by a FITC conjugated antibody and **(C)** nuclei were stained by Hoechst 33342 and fluorescent cells were visualized by a confocal Leica microscope with fluorescent filters for TRICT, FITC and HOECHST respectively. Distribution of the chaperonin is shown by the merge **(D)** of Hsp60 and nuclei staining (Bar=30µM).

2.6 Hsp60 protein expression and localization in NCI-H292 cells: Western Blotting (WB) and Electron Transmission (TEM)-ImmunoGold.

This first set of *in vitro* study results suggests, that the Hsp60 levels were not changed in 16 HBE cells, when exposed to CSE. This could partly be explained because smoke exposure induces oxidative stress which is easily overlooked by the homeostasis maintenance cell systems of

immortalized cells such as 16 HBE or more likely, because the mechanism of immortalization used for the 16-HBE has fallen into genomic portions that regulate the response of these cells to oxidative stress, preventing them to respond properly to the presence of CS.

For this reason, it was investigated whether CSE had a more relevant effect in tumoral cells (NCI-H292, mucoepidermoid carcinoma cells) which are a routine model used in assessment of smoking effects. After testing increasing concentrations of CSE on H292 cells, in order to determine the IC_{50}, using MTT (Fig. 14 A), The Hsp60 levels in H292 cells treated with 2.5, 5 an 10% of CSE for 24 hours, were detected (Fig. 14 B and B1), by western blotting analysis. It was found that Hsp60 levels were increased in dose-dependent way, unlike 16 HBE (10% of CSE was significantly different compared to control, $p<0.05$).

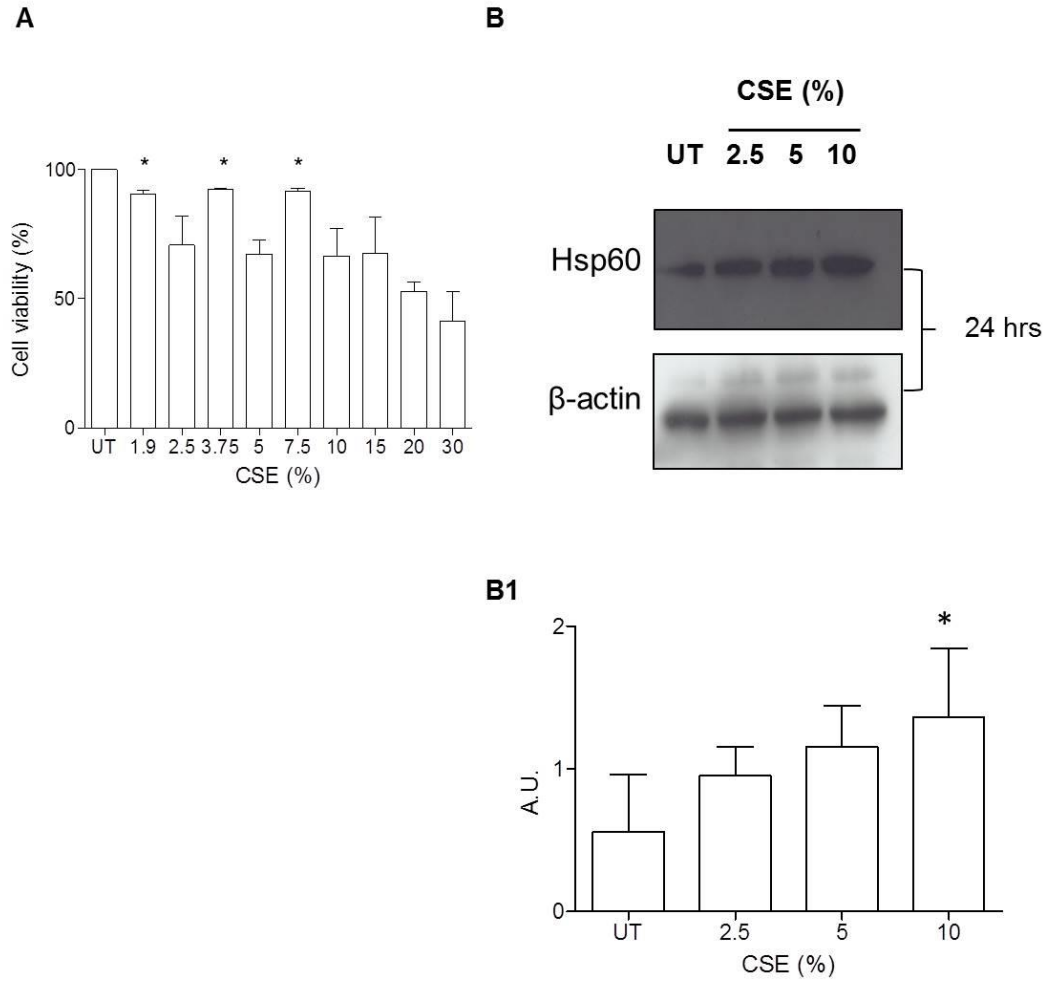

Figure 14.

(A) Graph of MTT assay to determine the percentage of CSE in the treatment of H292 cells. The IC_{50} value after 24 hours was 20% and then, we have chosen sub-lethal doses (2.5, 5 and 10% of CSE). Values represent the mean of three independent experiments ± S.D. (*different from control p <0.001). **(B)** Western blotting of Hsp60 after 24 hours of CSE treatment of H292 cells. In figure **(B1)** representative densitometry of protein bands. Arbitrary units (A.U.) of band intensities were normalized to those of the control in each series of experiments. Hsp60 protein levels were increased significantly after treatment when compared to the untreated cells (10% of CSE was different from control *p <0.05).

Various studies have shown that Hsp60 levels could change in pathological conditions or in inflammatory states [76,123]. It has been demonstrated that Hsp60 can translocate in different cell localizations and come out of the cell, frequently inside extracellular vesicles, such as exosomes. A previous study from Campanella and colleagues [96] proved

the presence of Hsp60 in the plasma membrane of the tumor cells (H292), demonstrated by Transmission Electron Microscopy (TEM)-immunogold. Hsp60 was localized not only in the cytosol but also in plasma membrane as well as close to the plasma membrane, suggesting an active movement of the chaperonin in this area, possibly toward, and also away from the cell (Fig. 15). For these reasons, we investigated a possible mechanism of secretion, through extracellular vesicles, to verify the possible presence of Hsp60 in them (see below).

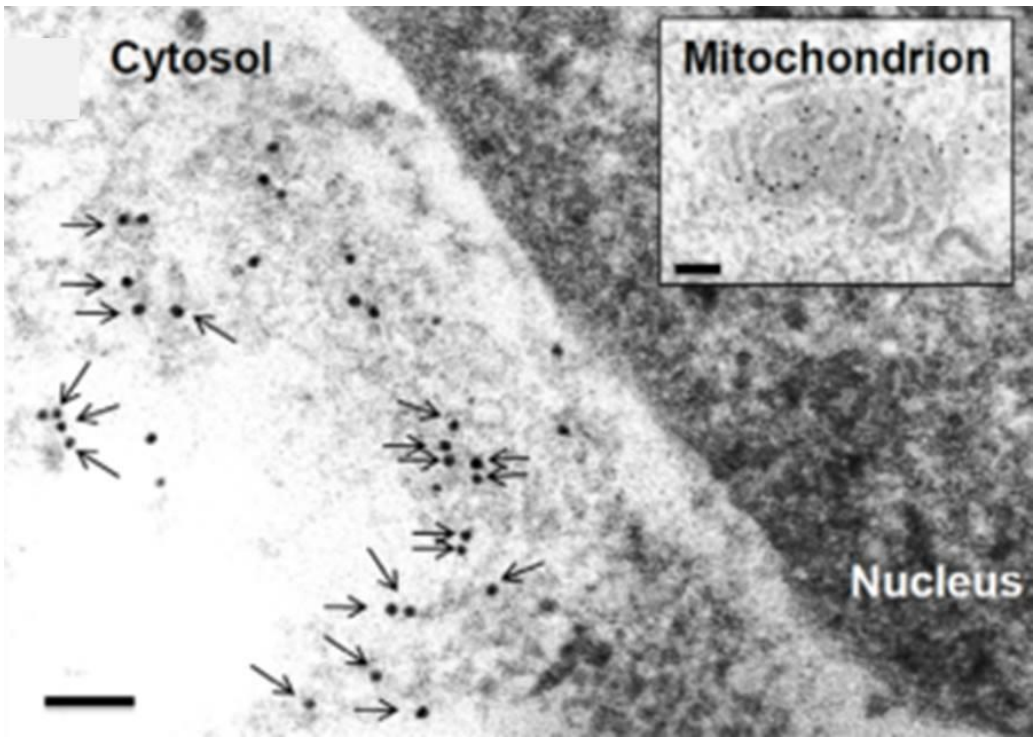

Figure 15.

Modified from Campanella and colleagues, 2012 [96]. Transmission electron microscopy-Immunogold demonstration of Hsp60 (black dots) in H292 cells. Arrows indicate the Hsp60 molecules that are close or onto the cell membrane. The insert shows the typical pattern of Hsp60 in a mitochondrion, which serves as a positive internal control. Bar: 100 nm.

2.7 Exosomes isolated from 16 HBE and H292 cells showed typical characteristics.

Previous observation has shown that Hsp60 is released in the extracellular microenvironment via the exosomes pathway and therefore the experiments below were aimed to investigate whether cigarettes smoke affects the exosomal pathway on tumor cells.

We obtained Extracellular Vesicles (EVs) from 16-HBE and H292 cells, using single step ultracentrifugation. Therefore, we analysed our exosome preparations by TEM, and found that the size and the morphology of the obtained EVs were those of typical exosomes (Fig. 16 A1 and A2; representative TEM images). These results show that exosomal preparation from cell treated with CSE (10%) had more vesicles than preparation from untreated cells. These data are obtained by the “Analyzing particles” of ImageJ software. Our exosomes preparations were analyzed by Nanosight, Nanotracking particle analysis (NTA), that measures the size of each particle and their number, by direct observation of scattered light and the particle motion (Fig. 16 B). We found that our vesicle population consisted $4.05x10^{8}$ vesicles/ml, with size distribution mean of 100 nm (S.D. ±67) (Fig. 16 C).

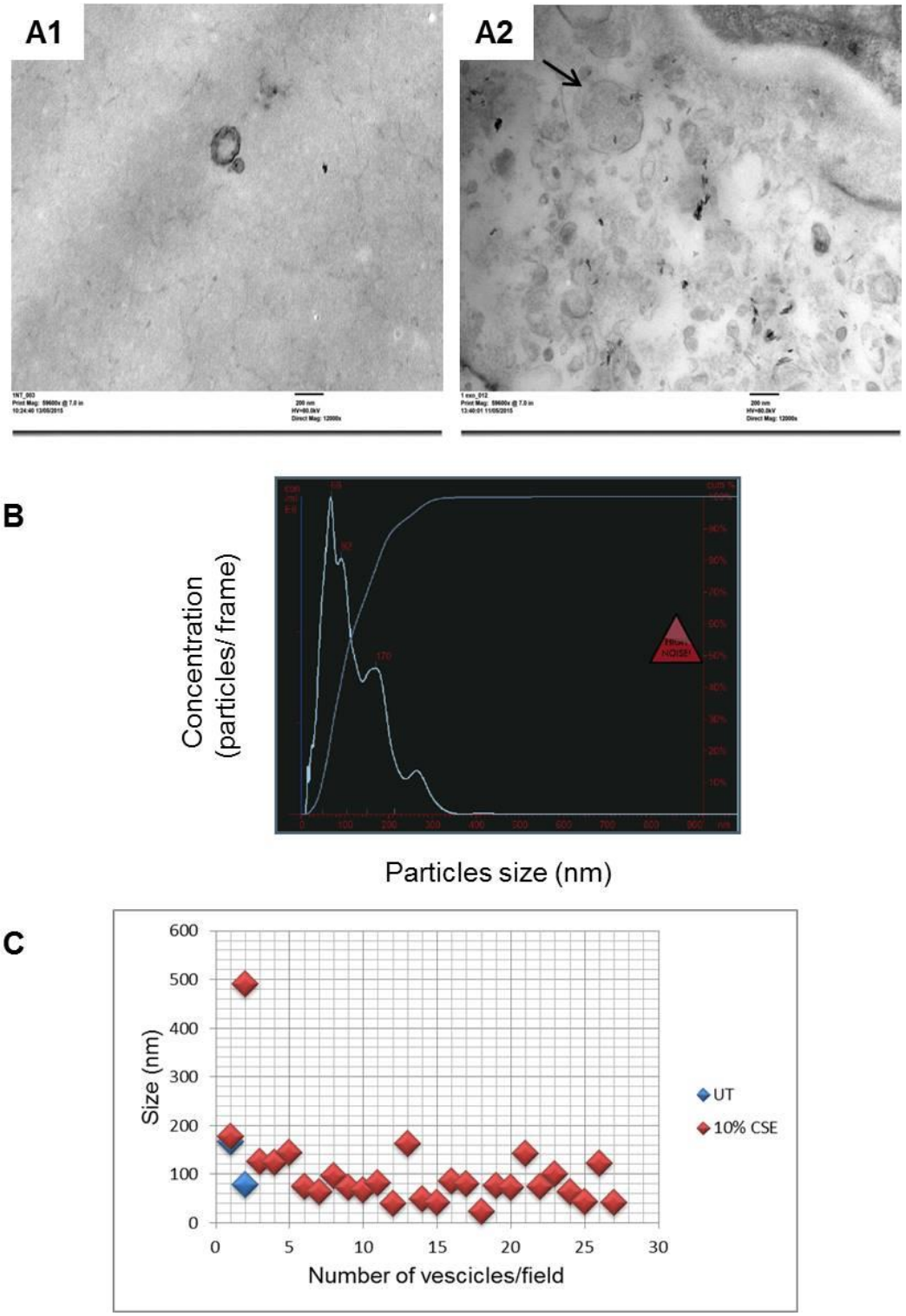

Figure 16.

16 HBE and H292 cells release extracellular vesicles, like exosomes, more concentrated when treated with 10% of CSE than the control. **(A1)** and **(A2)** vesicles compatible with typical exosomes, demonstrated by TEM. An illustrative result for exosomes purified from **(A1)** control H292 cells and **(A2)** H292 cells treated with 10% CSE. (bar=200 nm). The

arrow shows MVE (Multi Vescicular Endosomes) with ongoing inward budding of the limiting membrane. **(B)** Nanotracking particle analysis graph of vesicles number and size. Size vesicles distribution: mean 100 nm±67. Total Concentration: 19.17 particles/frame, corresponding to $4.05x10^8$ particles/ml. **(C)** Graph of number and size distribution of exosomes isolated from untreated cells (blue points) and cells treated with 10% of CSE (red point) and observed by TEM.

2.8 Hsp60 is present in exosomes from H292 cells treated with CSE.

In exosomes from 16-HBE it was not possible to find Hsp60, as expected, considering that it was demonstrated that this protein was not present in membrane of these cells after CSE treatment (Fig. 17 A, upper panel). In basal and conditioned medium, Hsp60 was not detected in exosomes, while, it was detected in the exosomes from H292 cell and a significant increase in Hsp60 levels was observed after CSE treatment (10%) (Fig. 17 A, second panel). Western blotting showed that our exosome preparations expressed typical exosome markers, such as Alix and Hsp70 (Fig. 17 A, middle and bottom panel).

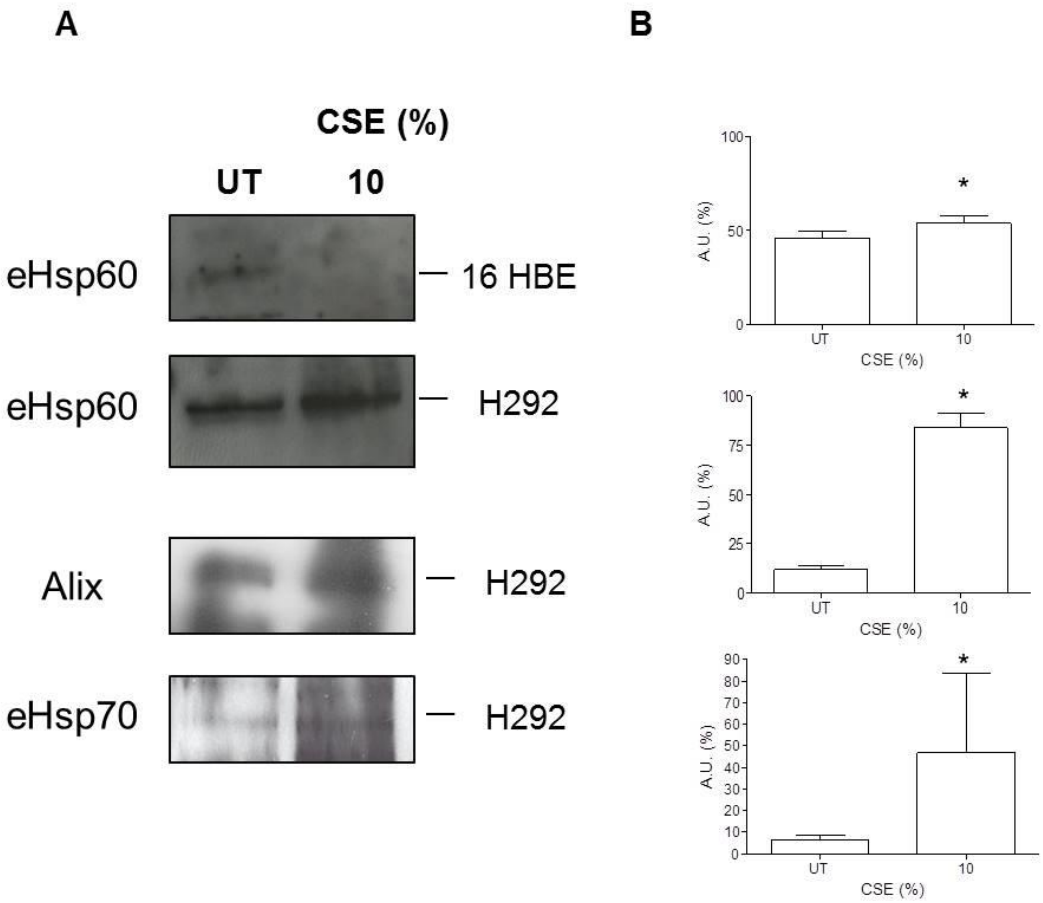

Figure 17.

In **(A)** Representative western blotting of exosomal Hsp60 after 24 hours of CSE treatment of 16 HBE (upper panel) and H292 (second panel). In **(A)** third and fourth panel, respectively Alix and Hsp70 western blots. In **(B)** densitometry of protein bands of Hsp60 obtained from H292 exosomes (10% vs UT * $p<0.05$), for Alix (B, middle panel) and Hsp70 (B, bottom panel).

3. Optimization of a three-dimensional *ex vivo* model mimicking COPD and evaluation of CS exposure effect and inflammatory mechanisms.

3.1 3D outgrowth cultures: growth monitoring and macroscopic effects of CSE.

After the seeding, the bronchial biopsy was routinely observed and photographed in order to monitor the growth and cells morphology (Fig. 18).

During the first days of culture, the cells started to come out of the biopsy (Fig. 18 A and B). Those were mainly fibroblasts, which reconstructed a network. Hereinafter also appeared epithelial cells, which are placed apically to the fibroblasts. After about 10-15 days, the outgrowth recreated the typical morphology of the bronchial epithelium and replaced the Matrigel® with self-produced extracellular matrix (Fig. 18 C). Futhermore, it is possible to see the cilia beating.

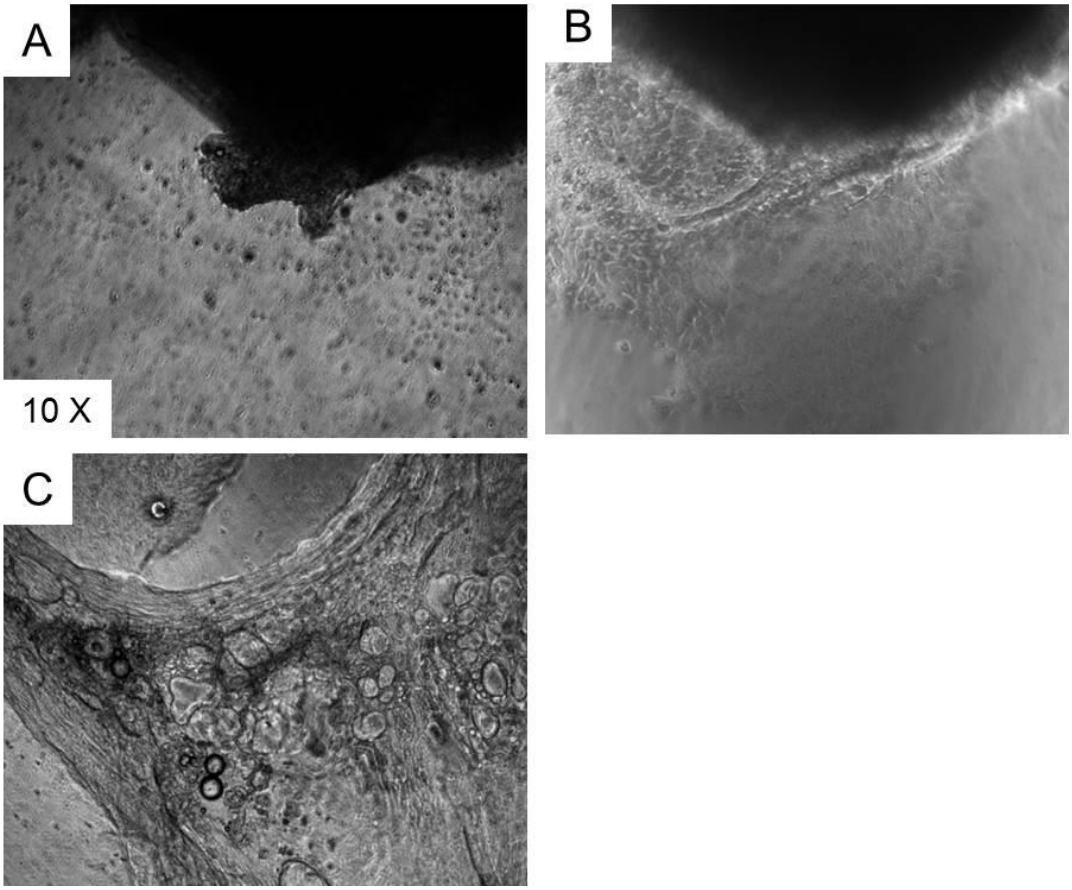

Figure 18.

Bronchial 3D-outgrowth culture: different stages of growing. In **(A)** 2 days, in **(B)** 5 days and in **(C)** 10 days growing after culturing. Phase contrast photos (LEICA DM-IRB).

With the gradual increase in cell growth and expansion, it is been possible to observe an increase of the trans-epithelial resistance (TEER, Trans-epithelial electrical resistance), due to the establishment of the epithelial barrier. TEER was measured by an EVOM meter (Volt meter) (Fig. 19 A). When the outgrowths were treated with 30% CSE, TEER was reduced (Fig. 19 B), due to the influence of smoke extract on the cell junctions and on wall thickness.

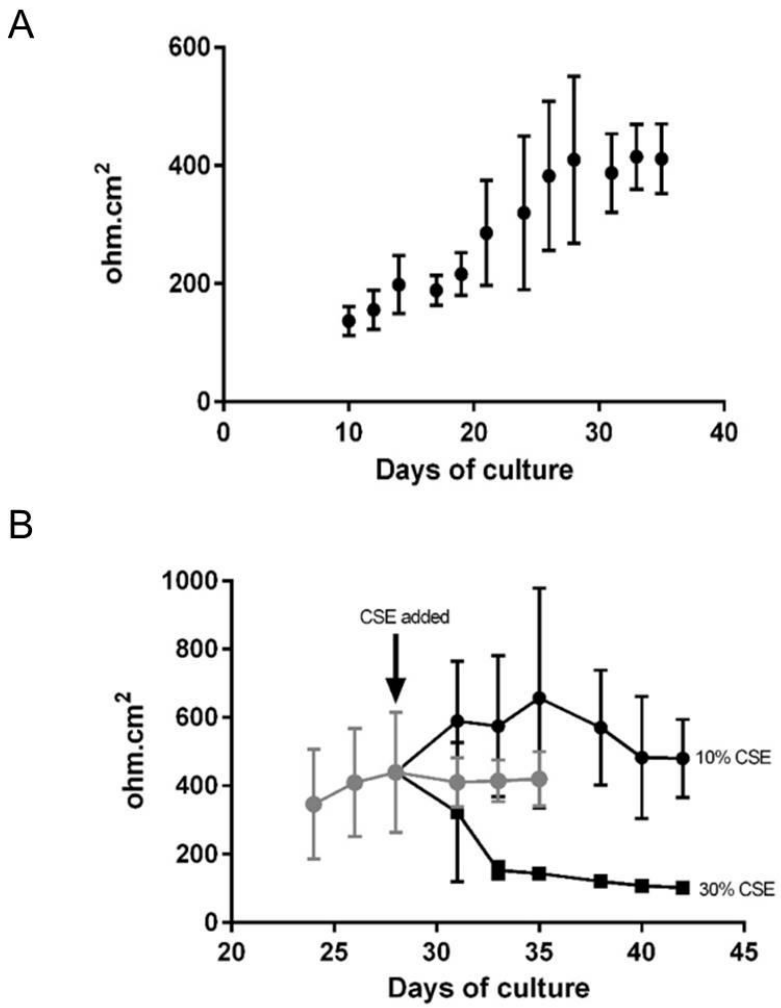

Figure 19.

Trans-epithelial electrical resistance (TEER) was measured every 2 days, from day 10th after the culture placing, to ensure the formation and integrity of tight junctions between cells in the epithelium using an EVOM meter **(A)**. In **(B)** the effect of 10 (●) or 30% (■) CSE on ionic permeability of mature EMTU cultures. After the treatment with 10 and 30% CSE, the EVOM measurement was performed every 2 days, to monitor the effect of CSE in cellular integrity. Grey circles (●) show the electrical resistance of untreated cultures (either pre-CSE exposure or without treatment post 28 days).

Substantial morphological differences were observed in the outgrowths when exposed to CSE (30%) for 21 days, compared with the un-exposed control outgrowths.

CSE reduces the contact between the epithelial cells and fibroblasts, an event that has been described in the literature in the early stages of COPD. This could compromise the normal intercellular communication of the EMTU and could lead to airway wall thickening. In our model it was possible to see a remodelling of EMTU toward metaplasia (Fig. 20 B), as confirmed by the morphology of the epithelial layer that becomes squamous-like (Fig. 20 A and B).

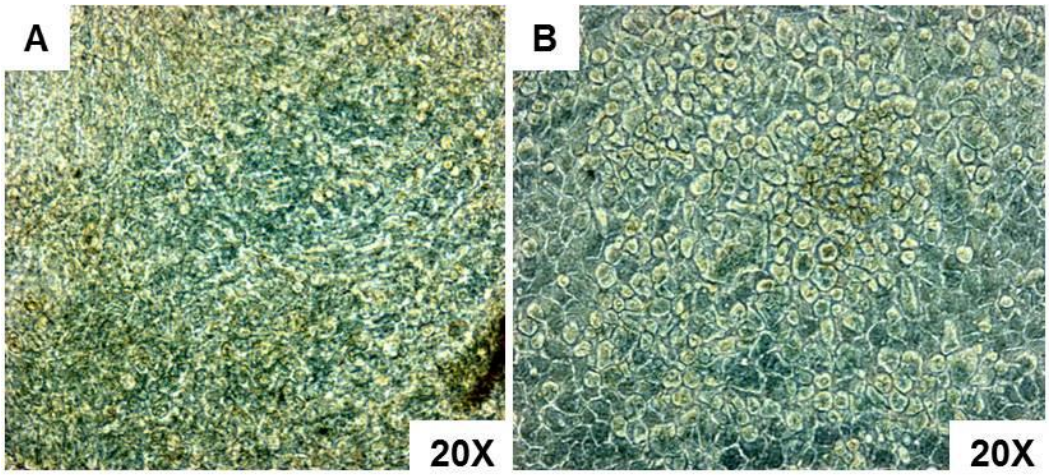

Figure 20.

The phase-contrast microscopy images of 3D outgrowths show the remodelling of morphology of epithelial mesenchymal trophic unit (EMTU) after 21 days of treatment with 30% CSE. **(A)** untreated; **(B)** treated 3D outgrowth.

3.2 Assessment of smoke effect on viability of 3D bronchial outgrowths: in situ apoptosis assay.

To determine the effect of cigarette smoke on DNA fragmentation, outgrowths were exposed to 30% CSE for 7 days and then TUNEL staining was performed (Fig. 21 A). After 7 days of treatment DNA strand breaks significantly increased ($p<0.001$) compared with control (Fig. 21 B).

The percentage of DNA damaged cells increased as a function of CSE concentration.

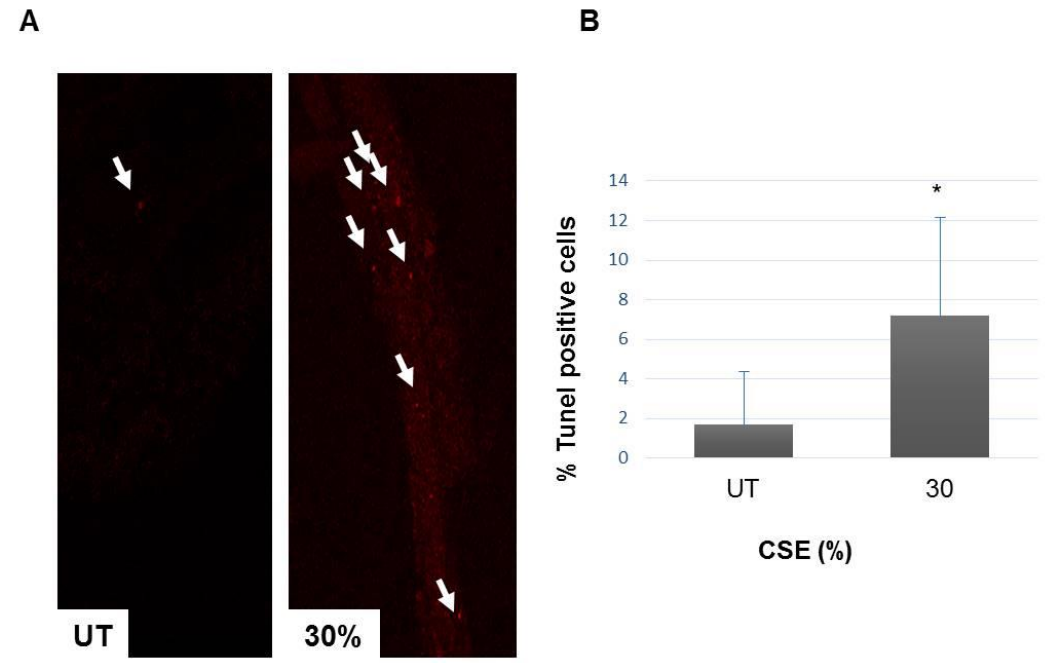

Figure 21.

Apoptosis assay. **(A)** Representative image of TUNEL staining. Percentages of TUNEL positive cells were determined by cell positive counting. **(B)** Data are expressed as means ± SD (* UT vs 30% $p < 0.001$).

3.3 Evaluation of Hsp60 mRNA expression and protein levels of in bronchial 3D outgrowths exposed to CSE.

In an effort to improve our knowledge about Hsp60 mRNA expression in the 3D bronchial culture model, total RNA was extracted from outgrowths and RT-PCR was performed using gene-specific primers. One group of outgrowths was treated for 10 days with CSE (10 and 30%), whereas another group was treated with CSE (10 and 30%) for 10 days and then the medium was replaced with fresh medium for an additional 10 days.

Interestingly, Hsp60 expression levels were markedly elevated after 30% CSE treatment after 10 days, while after 10 days of treatment and 10 days of recovery Hsp60 mRNA was significantly reduced compared to controls (Fig 22 A and B; $p<0.01$). This result suggests that CSE could regulate the

transcriptional levels of this molecular chaperone in the 3D model, differently than the monolayer model.

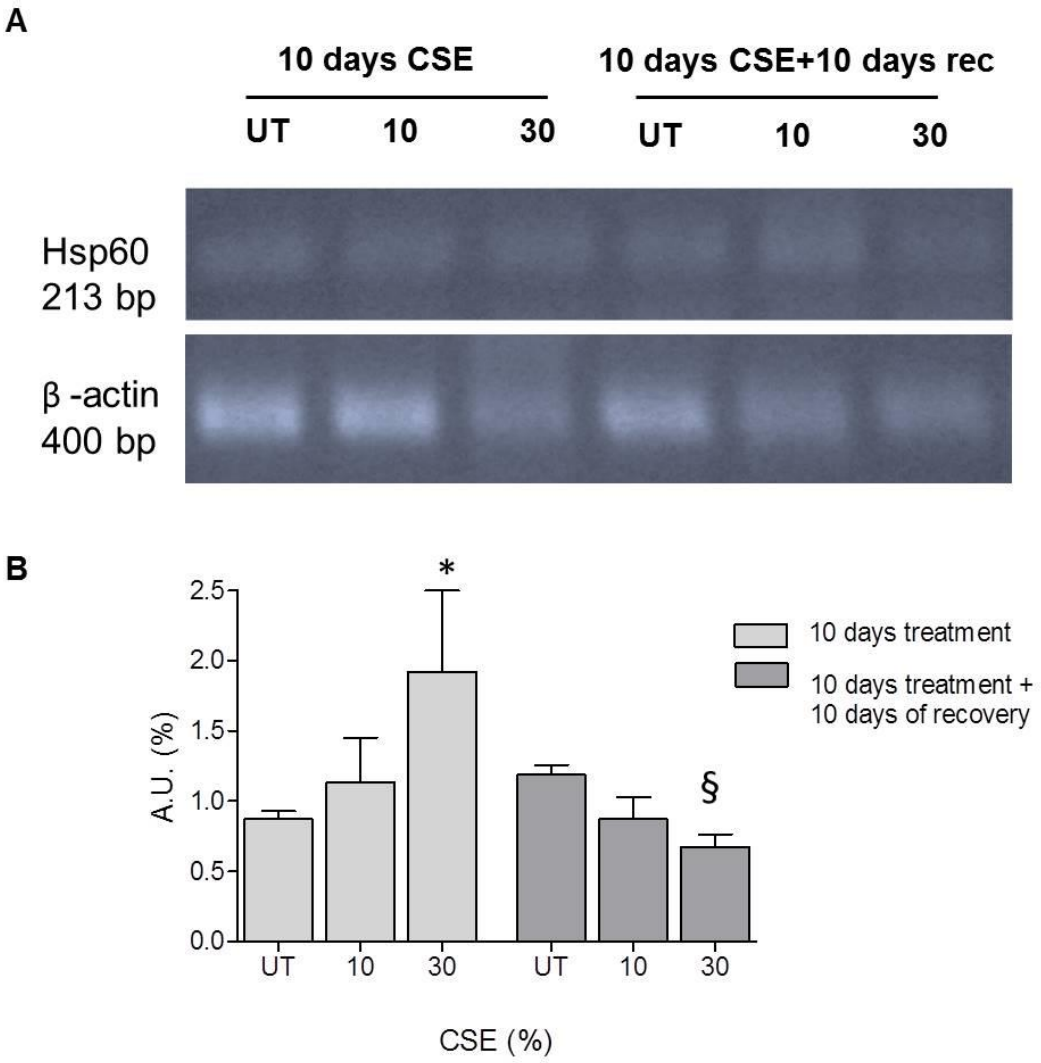

Figure 22.

(A) RT-PCR analysis of Hsp60 mRNA levels and **(B)** densitometry of corresponding bands. Hsp60 mRNA was significantly higher after treatment with 30% CSE when compared with the untreated controls. Values represent the mean of three independent experiments. (*Different than UT $p<0.01$, § different than UT recovery $p<0.05$). β-actin was used as loading control.

In the subsequent experiments we have chosen different time points of treatment, in order to study the real variations in protein levels.

It was found that the results of western blotting analysis Hsp60 protein level (Fig. 23) were comparable with the expression analysis of Hsp60 mRNA. The quantity of Hsp60 was higher after 2 days of treatment than in control samples (Fig. 23 A1, B1) and lower when outgrowth were treated with smoke (10 and 30% of CSE) for 7 and 21 days (Fig. 23 A2, B2 and A3, B3). Also after 21 days of the treatment the Hsp60 mRNA levels were reduced in the treated rather than in the control cells (Fig. 23 C3). These western blotting results are in accordance with the expression analysis results and these difference between expression after 7 and 21 days may be due to the fact that for brief treatment times might lead to an immediate response in which the system increases the levels of this protein, while when the treatment is prolonged the system regains its equilibrium.

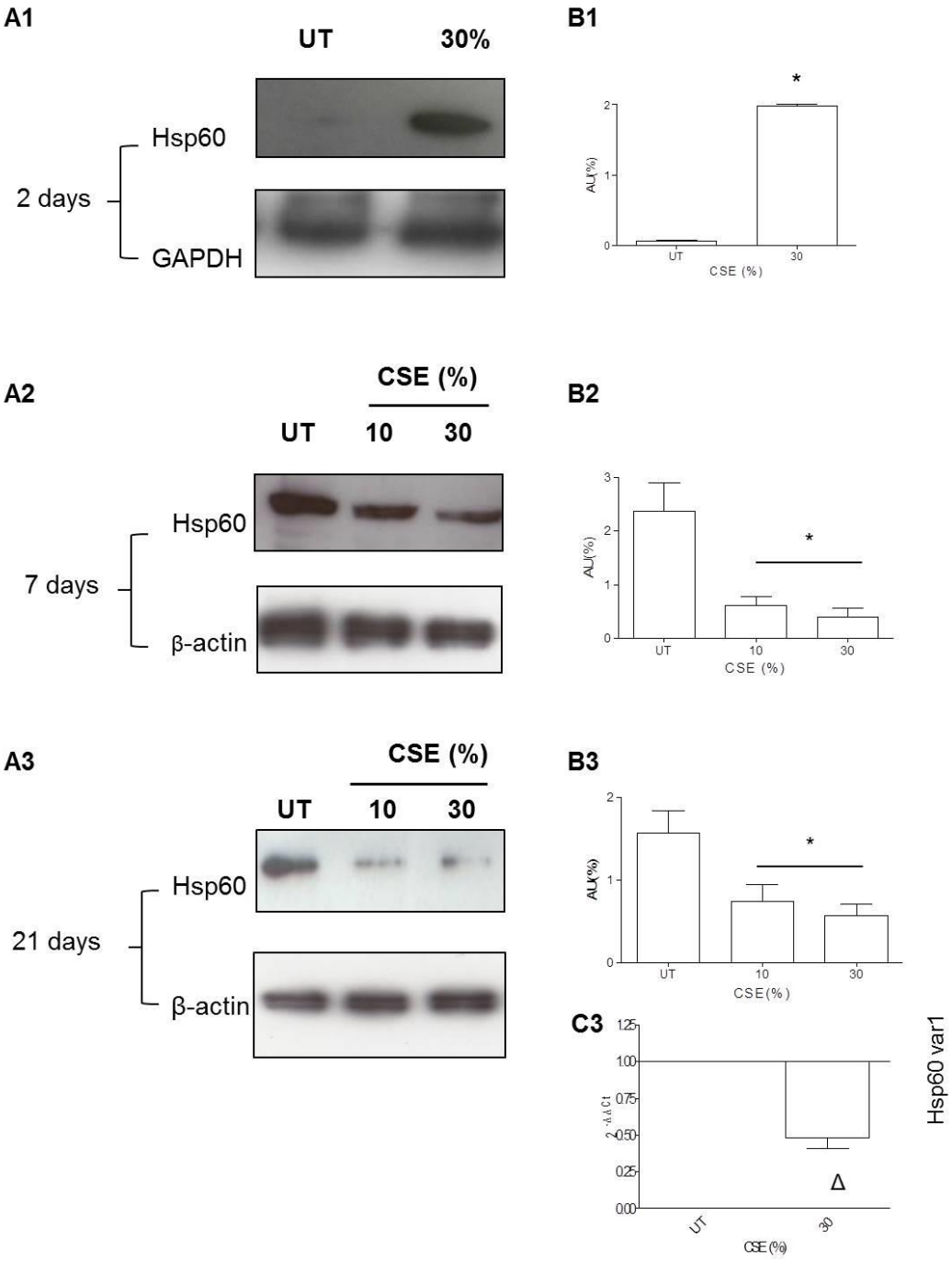

Figure 23.

Western blotting analysis of Hsp60 levels for 2 **(A1)**, 7 **(A2)** and 21 **(A3)** days after the treatment with CSE. In B1, B2 and B3 the corresponding densitometry bands. After 2 days of treatment we observed an increase in Hsp60 protein levels **(A1** and **B1)**. Conversely, after 7 **(A2** and **B2)** and 21 days **(A3** and **B3)** of treatment Hsp60 was reduced in dose dependent mode ($p<0.001$). In **(C3)** Real Time PCR analysis of Hsp60 expression levels after 21 days of treatment with 30% CSE. mRNA levels were considerably reduced (Δ UT vs 30% $p < 0.001$), and confirm the western blotting data.

3.4 Bronchial 3D outgrowths characterization and evaluation of CSE effects: smoke decreases barrier function and Hsp60 levels in epithelium of bronchial 3D outgrowths.

Samples were stained for anti-α-actinin (Fig. 24 A and B, red) to verify the growing and morphology of outgrowth and with Hsp60 (Fig. 24 A and B, green) to study the localization of this protein in 3D bronchial model, considering its decrease after CSE treatment for long time. α-actinin presents typical organization, compatible with his normal localization, along cytoskeleton and near membrane. Hsp60 appears normally cytoplasmic.

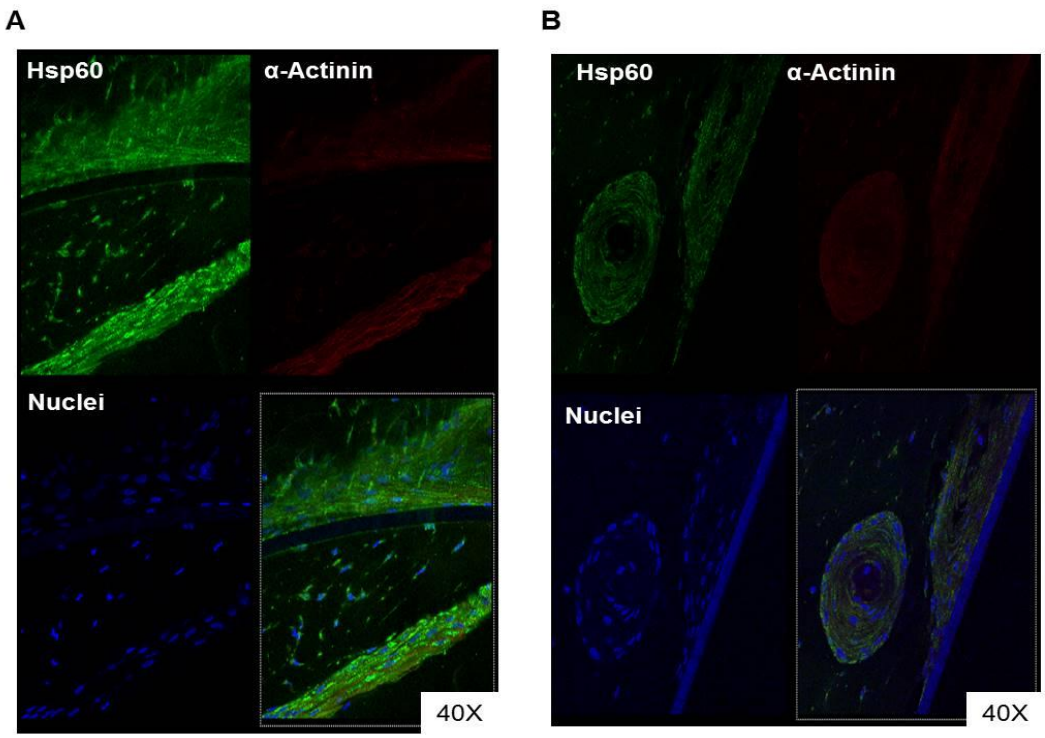

Figure 24.

3D outgrowths were cultured for 44 days, fixed with methanol and triple-stained with TRICT, conjugated with anti-α-actinin antibody, with FICH, conjugated with Hsp60 antibody and with the nuclei probe HOECHST. Cells were analyzed in a Leica laser scanning confocal microscope. In **(A)** and **(B)** different field of an outgrowth cultured for 44 days.

In an effort to elucidate the mechanism by which the trans-epithelial resistance was reduced after treatment with 30% CSE, we investigated the expression and localization of the tight junctions, a component of cell-cell adhesion. Bronchial outgrowths were exposed to 30% of CSE for 21 days and a double immunofluorescence analysis was performed (Figure 25 A and B) in order to evaluate the expression of tight junctions and Hsp60. The overall molecular composition of tight junctions was reduced and modified, appearing discontinuous and fragmented. The immunoreactivity of considered protein was always localized in correspondence of epithelial cells membranes (Figure 25 B). Furthermore, Hsp60 was reduced after treatment, according to western blotting analysis (Figure 25 B).

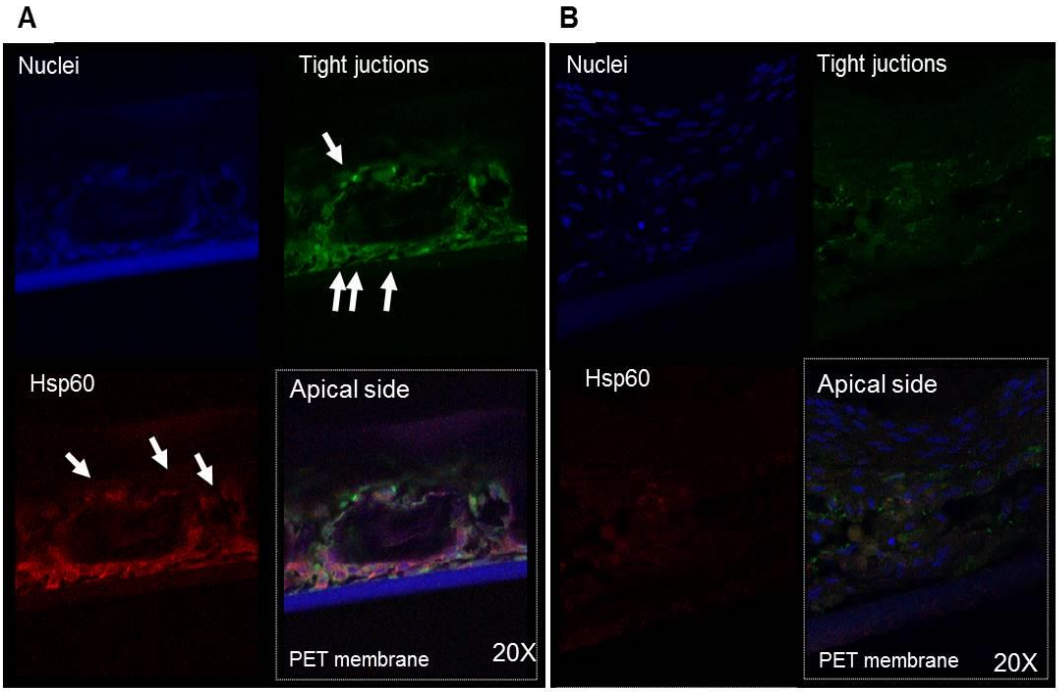

Figure 25.

Double immunofluorescence experiments for tight junction (green) and Hsp60 (red) show a CS-induced disruption of bronchial epithelial tight junctions and a more pronounced reduction of Hsp60 levels **(B)** than in the controls **(A)**.

3.5 Bronchial 3D outgrowths exposed to smoke release exosomes.

In order to understand the localization of Hsp60 after CSE treatment, we evaluated the its eventual secretion in the extracellular environment, by exosomal pathway. Bronchial 3D outgrowths were treated for 7 and 21 days with 30% CSE and the conditioned medium was changed and collected every 2 days. Conditioned media for each group (7 and 21 days) were analysed and compared. From these samples exosomes were obtained and their protein content was quantified in order to assess the exosomal Hsp60 (eHsp60), exosomal Hsp70 (eHsp70) levels and Alix, the latter are well known exosomal markers. We did not find Hsp60 and Alix levels, as it is shown in Figure 26 A (lower panel). On the other hand, we observed an increase in eHsp70 levels in exosomes from 3D outgrowth treated for 21 days when compared to the exosomes controls and exosomes from 3D cultures treated for 7 days. This may be correlated with an increase in dose- and time-dependent exosomes production (Fig. 26 and B). We suspect that this model produces exosomes but probably they are not the main via by which Hsp60 is released.

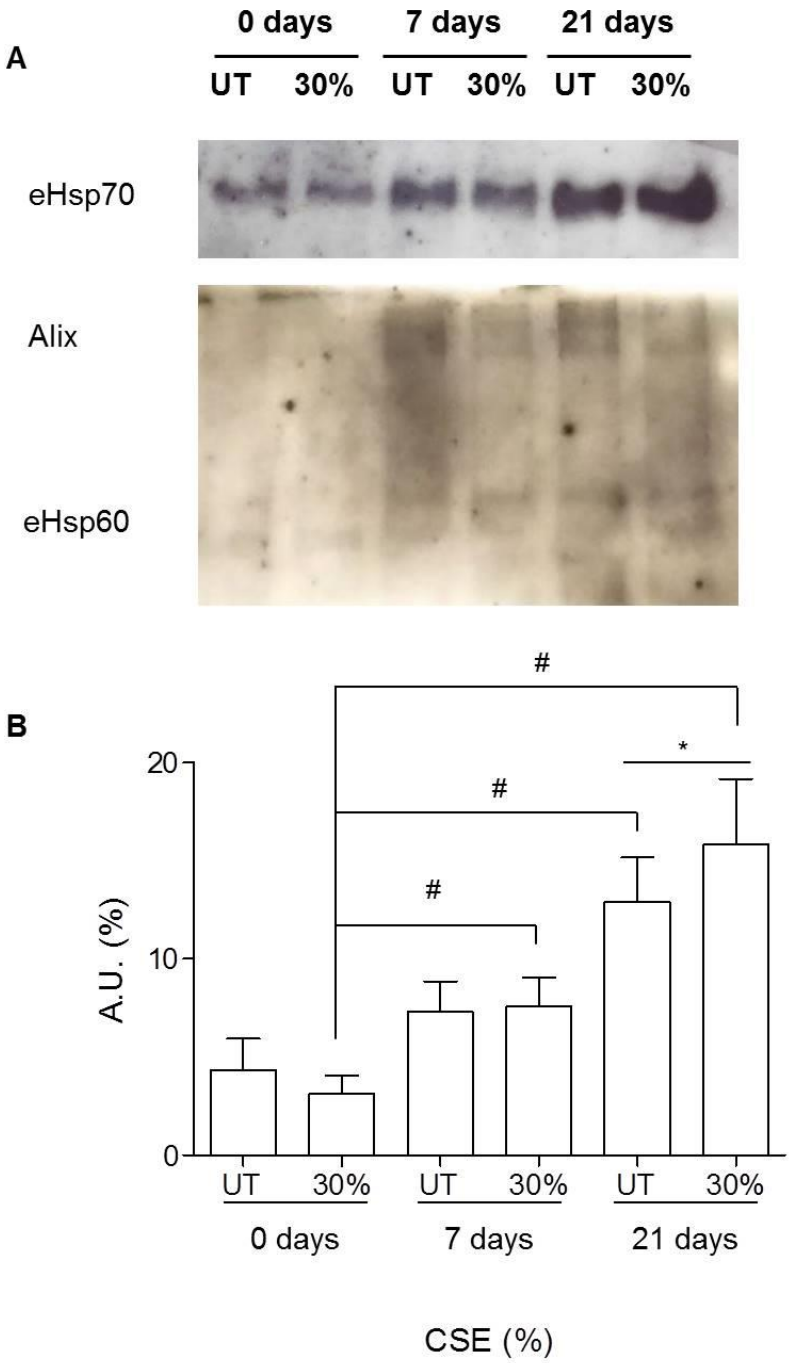

Figure 26.

In **(A)** western blotting analysis of exosomal Hsp70 (upper panel) and exosomal Hsp60 (lower panel) levels after 0, 7 and 21 days of treatment with CSE. In **(B)** the corresponding densitometry bands for eHsp70 levels. eHsp70, an exosomal marker, was present at high levels in exosome preparations from supernatant of bronchial 3D outgrowth treated with 30% CSE for 21 days. Data were analysed by Repeated measure ANOVA test (*p<0.001, UT and 30% after 21 days of treatment vs UT and 30% at 0 days). A difference between UT and 30% CSE treatment after 21 days was statistically

significant (*p<0.05) as well as between 30% 0 days and 30% 7 day and 30% 21 days after the treatment (#p<0.001) .

3.6 Bronchial 3D outgrowths release Hsp60 and cytokines.

To better understand the reason because intracellular levels of Hsp60 were decreased after CSE treatment, the level of this protein was tested in conditioned medium of 3D bronchial outgrowths treated with CSE (30%, after 0, 7, 14 and 21 days), by ELISA assay. We observed a dose- and time-dependent increase in Hsp60 levels (Fig. 28).

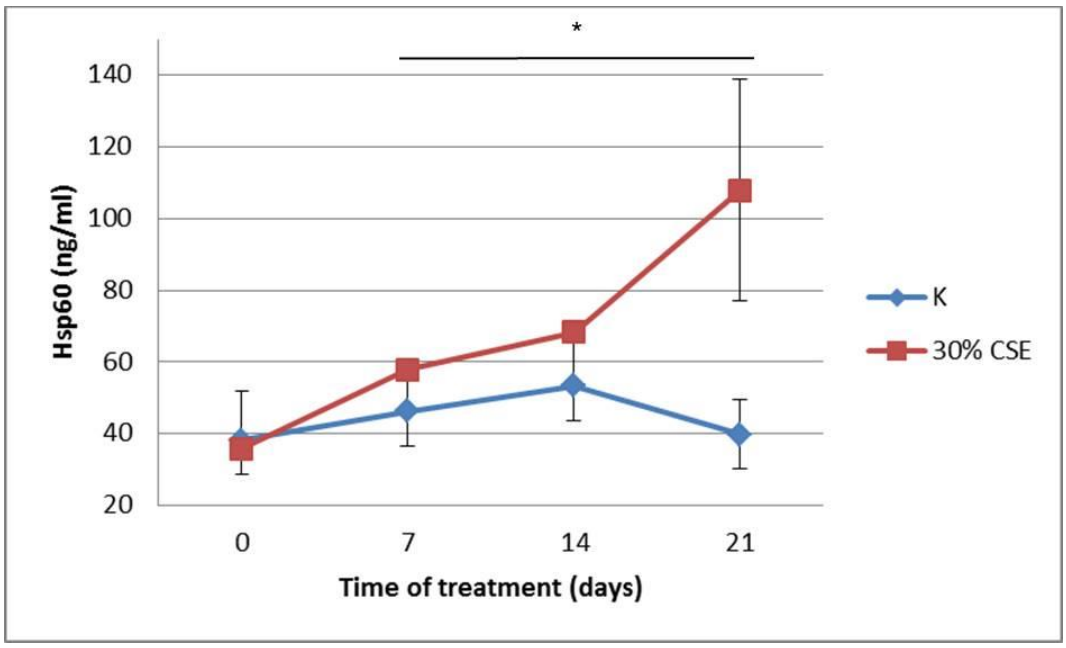

Figure 27.

Effect of CSE treatment on Hsp60 release from 3D bronchial outgrowth. Samples were incubated with 30% CSE for 7, 14 and 21 days to study the release of Hsp60 by sandwich ELISA, in free cell culture supernatants. We found a significant release of Hsp60 in supernatant of outgrowth treated for 21 days, compared with the control (*p<0.001).

In addition, an important goal of this work was to clarify the involvement of Hsp60 in the inflammatory response in COPD. Therefore, the cytokines production from 3D model was verified after exposure to smoke.

Seventeen cytokines have been assessed by Bio-Plex assays (Bio-Plex® MAGPIX™ Multiplex reader), from supernatants collected every two days from 3D outgrowth treated with 30% CSE and grouped into groups: 2, 7, 14 and 21 days after the treatment. A comparison analysis was conducted by repeated measurement ANOVA, between different groups. Among all cytokines tested, the data for 9 cytokines were statistically significant ($p<0.05$).

Supernatant level (pg/ml) of IL1β and IL8 were higher in treated group after 14 and 21 days than in respective control. Conversely, levels of IL4, TNFα, IL12, IL10 and IL13 were lower than in the respective controls ($p<0.05$). However, the differences between treated and control groups for IL2 levels were not significant.

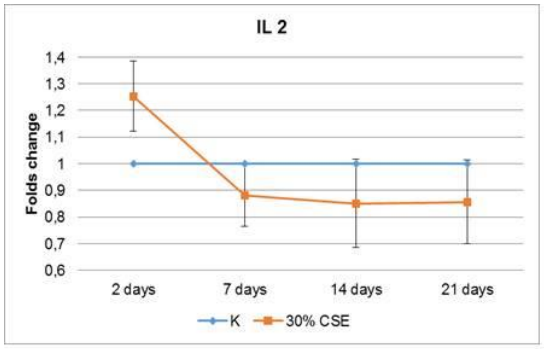

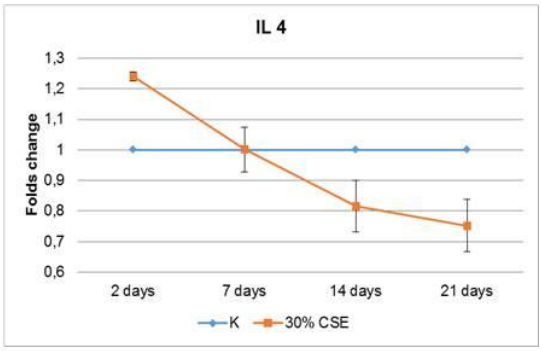

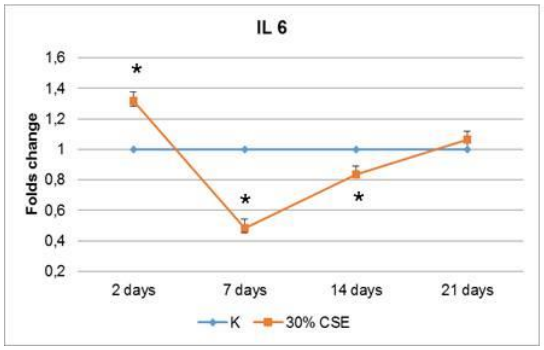

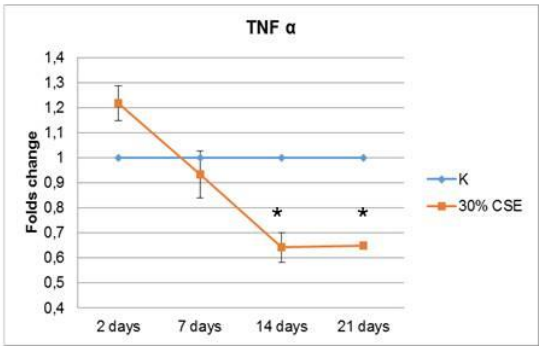

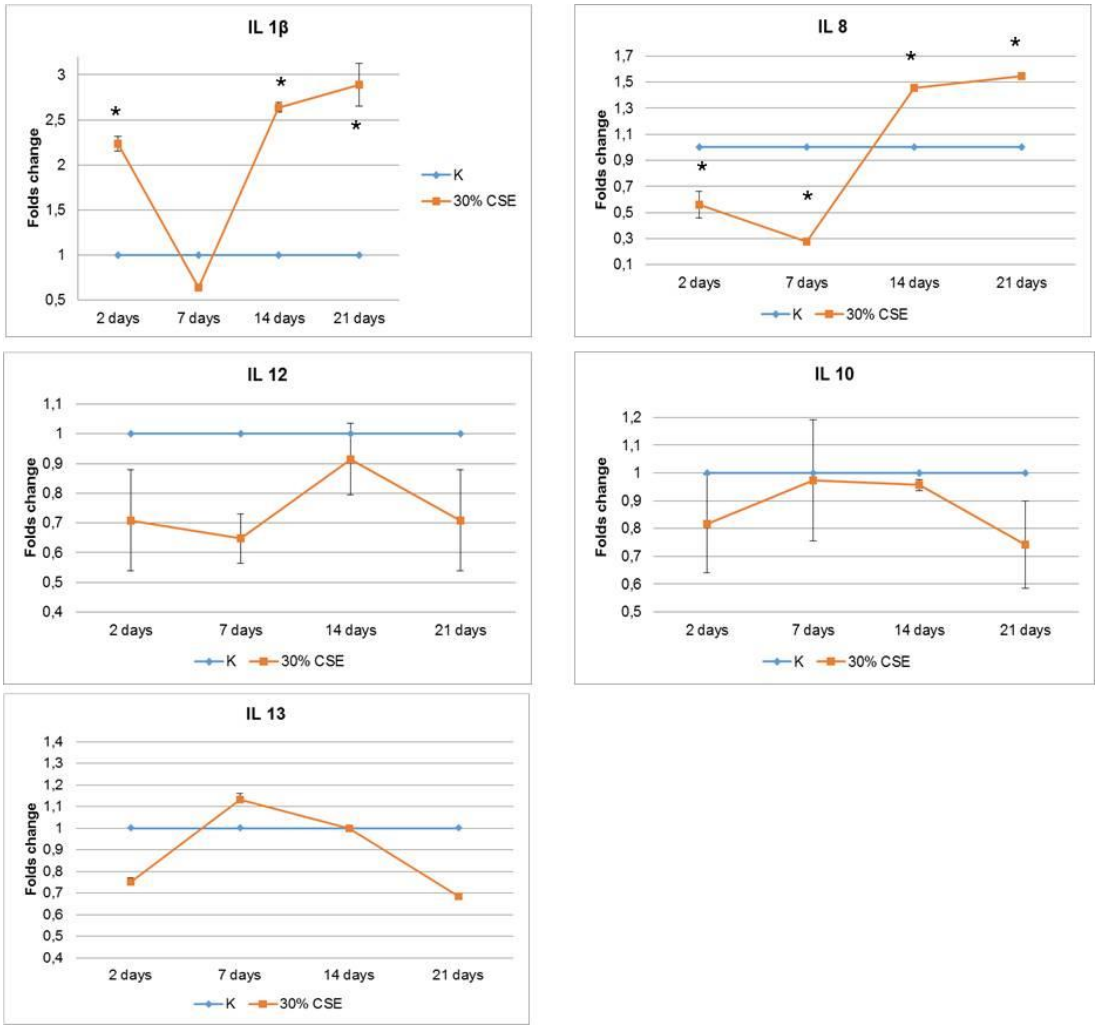

Figure 28.

Conditioned medium levels of IL2 , IL4, IL6, TNFα, IL1β, IL 8, IL 12, IL10 and IL13. Significant differences between treated and control samples are denoted (*p<0.05), as measured by repeated measures ANOVA test. Data are shown as mean ± S.D. (results from three experiments).

In order to find a relationship between Hsp60 release and cytokines levels released in conditioned medium of 3D outgrowth in response to the CSE treatment, a non-parametric correlation analysis was performed. Linear regression curves were developed in GraphPad Prism 6.0 (GraphPad Software Inc., La Jolla, CA, USA). The linear regression curve shows a high degree of positive correlation between Hsp60 and IL8 (r^2 Spearman coefficient=0.508, $p<0.05$) and IL1β (r^2=0.712, $p<0.05$). Otherwise, Hsp60

is negatively correlated with IL2 (r^2=-0.631, p<0.05), IL13 (r^2=-0.685, p<0.05); IL4 (r^2=-0.633, p<0.05), GM-CSF (r^2=-0.926, p<0.05) and IL10 (r^2=-0.589, p<0.05). Other cytokines measured did not correlate with Hsp60 level (Fig. 29).

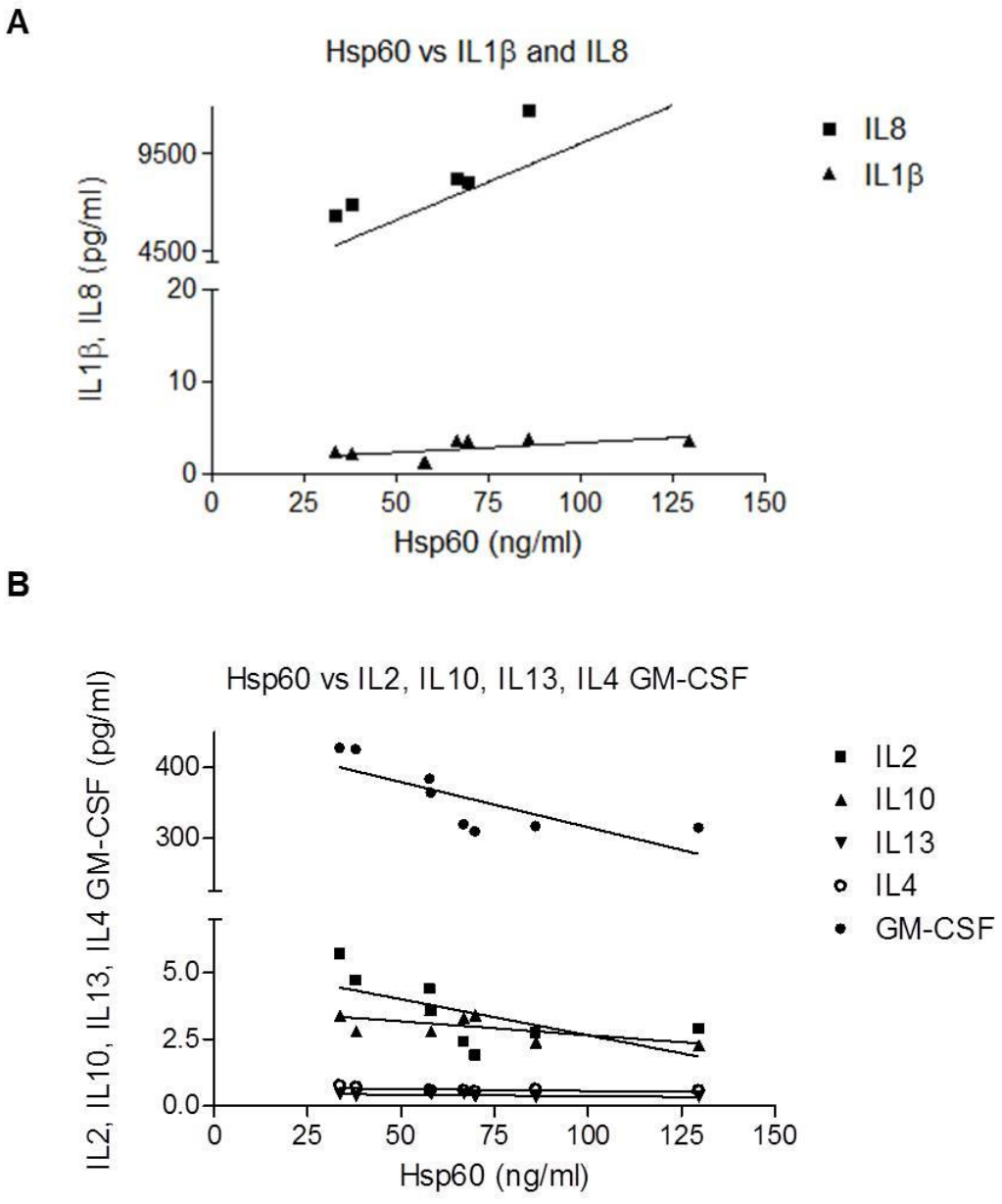

Figure 29.

To test the correlation between the extracellular levels of Hsp60 and any of cytokines measured in bronchial 3D outgrowth, linear regression analysis was performed. Whereas there was a linear positive correlation between Hsp60 levels and those of IL8 and IL1β

(A), negative correlation between Hsp60 levels and IL2, IL13, IL4, GM-CSF and IL10 was found **(B)**.

4. Assessment of circulating levels of Hsp60 in COPD patients and exosomes-PBMC co-cultures.

4.1 Assessment of circulating levels of Hsp60 in COPD patients: ELISA.

Hsp60 levels in plasma of COPD subjects were ranged between 11.857 and 22.571 ng/mL (mean, 17.49 ± 1.194). By contrast, in healthy subjects, Hsp60 was ranged between 7.571 and 18.143 ng/mL (mean, 12.73 ± SD 0.8736). The difference between Hsp60 levels in COPD patients versus healthy subjects was significant ($p<0.05$), as shown in Figure 30.

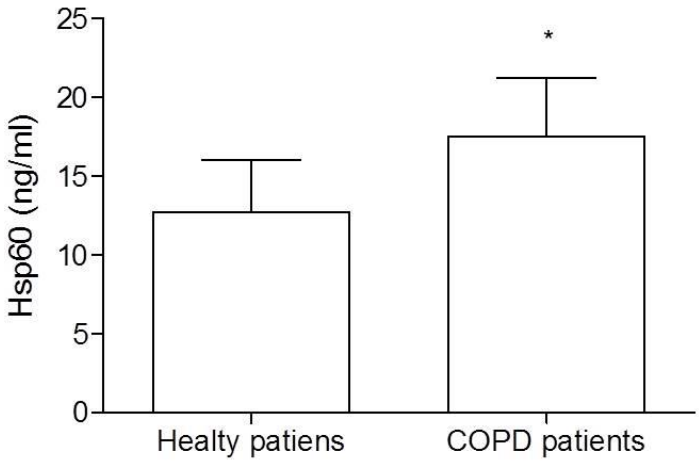

Figure 30.

Hsp60 plasma levels measured by ELISA in COPD patients vs healthy donors. Statistical analysis were performed by t-test (*$p<0.05$).

4.2 Establishing of exosomes-(PBMC) peripheral blood mononuclear cells co-cultures.

The cross-talk in our model of EMTU exposed to smoke and immune system cells via the exosomes was mimicked using a co-culture model. In

this co-culture model the effects of exosomes released from both CSE-treated and untreated bronchial 3D outgrowth, and free Hsp60, on activation of immune system, based on cytokines releasing was assessed. The PBMC cells isolated from COPD patients, were treated for 24 hours with exosomes isolated from untreated and treated (30% CSE) conditioned medium of outgrowths. Also, 10 µg/ml of recombinant Hsp60 were used to treat PBMC cells. The levels of 17 cytokines produced by these cells and released in the conditioned medium, were assessed using Bio-Plex Pro Assay (Table 8).

Cytokine	Groups of treatment			
	Ctrl	**Exosome 21 days Ctrl**	**Exosome 21 days 30% CSE**	**Recombinant Hsp60**
IL 17A	0.0[a] ±0.0[b] (0.0-0.0)[c]	26.82 ±5.090 (22.57-31.08)	21.66 ±6.105 (15.25-28.07)	21.12 ±2.816 (18.76-23.47)
IL 1β	2.008 ±1.768 (0.7434-3.273)	87.26 ±22.12 (64.05-110.5)*	42.27 ±3.620 (38.47-46.07)* #	49.85 ±26.06 (28.06-71.63)* #
IL 2	1.0 ±0.0 (1.0-1.0)	18.99 ±6.332 (13.69-24.28)	20.36 ±6.607 (14.83-25.88)	15.36 ±2.331 (12.91-17.80)
IL 4	1.000 ±0.0 (1.0-1.0)	10.02 ±2.752 (5.644-14.40)	9.374 ±3.167 (5.442-13.31)	7.845 ±1.834 (4.926-10.76)
IL 5	OOR<	OOR<	OOR<	OOR<
IL 6	36.37 ±13.20 (15.37-57.37)	1015 ±461.0 (281.6-1749)	861.5 ±452.3 (141.9-1581)	764.2 ±252.5 (362.5-1166)
IL 7	11.93 ±1.581 (10.61-13.25)	9.643 ±1.196 (8.643-10.64)§	9.417 ±1.849 (7.48-11.36)§	16.06 ±2.795 (14.06-18.06)*
IL 8	131.7 ±35.29 (102.2-161.2)	3342 ±786.6 (2685-4000)* §	3526 ±765.1 (2723-4328)* §	1759 ±160.4 (1504-2015)*
Il 10	3.680 ±0.8974 (3.038-4.322)	76.99 ±19.41 (60.76-93.21)*§	65.41 ±19.75 (48.90-81.91)*	51.69 ±8.196 (43.09-60.29)*
IL 12	2.394 ±0.5250 (1.742-3.046)	26.33 ±4.074 (19.84-32.81)	24.17 ±4.569 (16.90-31.44)	19.06 ±2.432 (15.19-22.93)
IL 13	OOR <	OOR <	OOR <	OOR <
G-CSF	0.0 ±0.0 (0.0-0.0)	43.16 ±17.78 (21.08-65.23)	34.93 ±23.78 (5.398-64.45)	40.20 ±32.17 (0.2488-80.15)
GM-CSF	OOR <	OOR <	OOR <	OOR <

INF γ	0.0 ±0.0 (0.0-0.0)	161.3 ±49.46 (99.86-222.7)	178.9 ±31.35 (101.1-256.8)	122.1 ±20.93 (70.09-174.1)
MCP-1	36.41 ±12.96 (25.58-47.24)	466.3 ±272.4 (238.6-694.0)	417.9 ±180.6 (266.9-568.9)	365.9 ±213.6 (213.1-518.8)
MIP-1β	234.5 ±132.9 (69.43-399.5)	16442 ±0.0 (69.43-399.5)	5562 ±0.0 (69.43-399.5)	3417 ±0.0 (69.43-399.5)
TNF α	2.286 ±1.288 (1.364-3.208)	55.11 ±11.20 (45.74-64.47)*	40.06 ±5.406 (34.39-45.73)* #	35.19 ±5.524 (29.40-40.99)* #

Table 8.

Cytokines levels measured by Multiplex Assay. Values are expressed in pg/ml. ([a] mean; [b] S.D. (standard deviation); [c] 95% C.I. (confidence interval) of mean. OOR = Out of Range; OOR> = Out of Range Above; OOR< = Out of Range Below. *p<0.05 vs Ctrl; #p <0.05 vs Exo 21 days Ctrl; §p <0.05 vs rHSP60). Statistical analyses and differences were tested for significance using one-way ANOVA.

The PBMC cells from COPD patients released greater levels of IL 6, IL 7, IL 8 and MIP-1β, then IL 17A, IL2, IL 4, IL 5, IL 10, IL 12, IL 13, C-CSF, GM-CSF, INF γ, MCP-1 and TNF α. All cytokines were higher expressed in conditioned medium of treated PBMC cells than in the respective controls.

The cytokines distribution, presented in Table 8, shows a significant variation between the different groups (Conditioned medium from untreated PBMC, conditioned medium from treated PBMC with 3D outgrowth 21 days Ctrl, conditioned medium from treated PBMC with 3D outgrowth 21 days 30% CSE and conditioned medium from PBMC treated with human recombinant Hsp60), in the pro-inflammatory IL 1β, IL 7, IL 8, TNF-α and the anti-inflammatory IL 10 levels.

As summarized in Figure 31 the secretion of IL 1β, TNF-α and IL 10 was more induced by exosome 21 days ctrl, than exosome 21 days 30% CSE. The secretion of IL 7 was more induced when PBMC cells were stimulated with the human recombinant Hsp60 and, conversely, IL 8 was more expressed by PBMC cells treated with both exosome 21 days ctrl and 21 days 30% CSE.

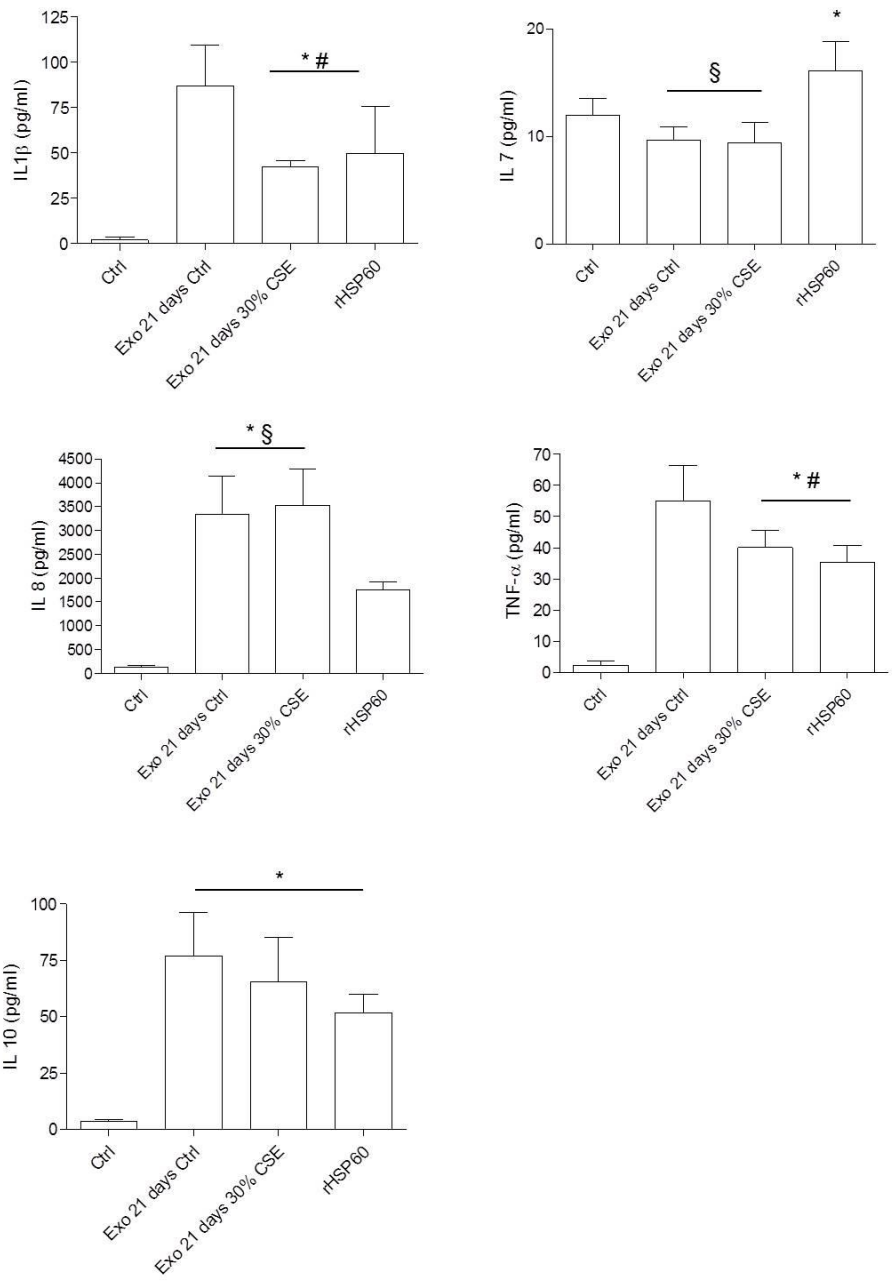

Figure 31.

Cytokines release was measured by BioPlex Pro Assay. Monocytes from COPD patients released greater levels of IL 6, IL 7, IL 8 and MIP-1β, then the others tested, relative to controls. (*p<0.05 vs Ctrl; $^{\#}$p <0.05 vs Exo 21 days Ctrl; §p <0.05 vs rHSP60). A significant variation between the different groups in IL 1β, IL 7, IL 8, TNF-α and IL 10 was observed.

In addition, the positive correlation was observed between Hsp60 free in plasma of COPD plasma, tested by ELISA, and cytokines levels released from monocytes exposed to human recombinant Hsp60. Also in this case,

the linear regression curves were developed by GraphPad Prism 6.0 statistical program. The linear regression curve shows a high degree of positive correlation between Hsp60 and IL1β (r^2 =0.8, p <0.05) and IL 7 (r^2=0.7, p <0.05). Any other correlation between cytokines assessed and Hsp60 levels have not been found.

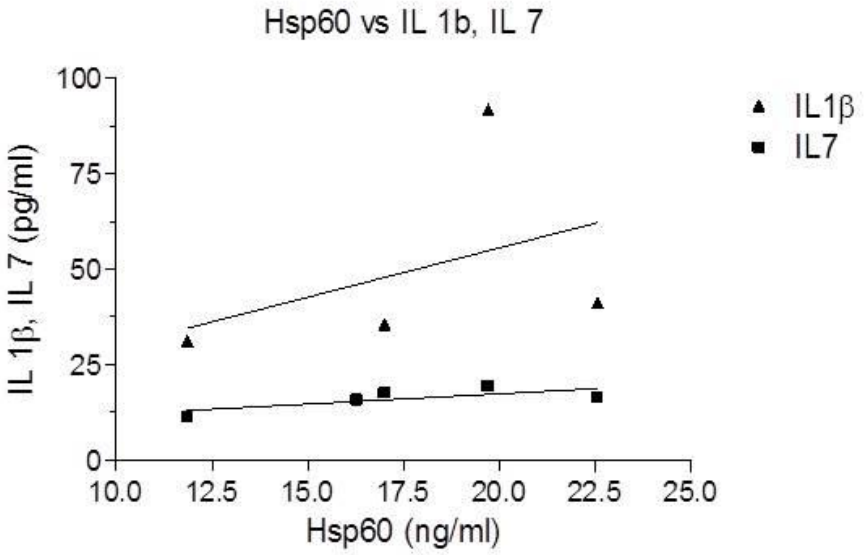

Figure 32.

To test the correlation between the levels of Hsp60 in plasma of COPD patients and those of cytokines released by PBMC cells stimulated with the human recombinant Hsp60, linear regression analysis was performed. A linear positive correlation between Hsp60 levels and those of IL 1β and IL 7 was found. The Spearman coefficient (r^2) was 0.8 for IL 1β (p <0.05) and 0.7 for IL 7 (p <0.05).

Discussion

The main risk factor of COPD, a very debilitating immune-mediated disease, is cigarette smoke [10]. The main pathological hallmarks of COPD are inflammation of the peripheral and central airways with small airways and vascular remodelling as well as the emphysema, mucus overproduction and chronic bronchitis that allow to the destruction of the lung parenchyma.

The prolonged exposure to CS causes numerous effects on the respiratory mucosa, at the molecular level and then on the cell function. Smoke evokes the inflammatory response by activation of epithelial cells, fibroblasts, macrophages, dendritic cells and T-cells, inducing the immunomodulatory response and cytokines [124–126], interleukins and chemoattractant production. Smoke exposure alters mitochondrial structure and function [127], activates mitogens [128] and its role in the extracellular matrix remodelling by lung fibroblast [129] and in the reprogramming of apical junction architecture in epithelial cells [24], has been proved. Increasing evidence shows a predominant role of Hsps in smoke response and in COPD pathogenesis [69,71,72].

It has been established that Hsps are released in the extracellular environment, by several cell types and that they have powerful effects. Previous studies have indicated a crucial role of Hsp60 in modulating immunity and inflammation [130]. Frequently, in response to stress, Hsp-peptide complexes are released from dead or dying cells and they bind to the receptors present on antigen-presenting cells, determining antigen cross-presentation, an important mechanism of the immune system [130]. Nevertheless, certain cells can actively secrete Hsps under a number of pathological conditions, implicating the immunity, such as arthritis [131], multiple sclerosis [132], diabetes [133] and COPD [70,71]. Particularly, Hsp60, is released in response to stress and is correlated with the number of neutrophils present in the bronchial mucosa of patients with stable COPD, suggesting that this chaperonin plays a role in controlling neutrophil functions and bronchial inflammation in these patients [65].

Based on these considerations, the aim of this thesis was to find a further correlation between the chronic inflammation in COPD and Hsp60, which acts as a cytokine perpetuating inflammation.

To achieve this goal, we have considered three possible models to study: 1) *in vivo* model, using bronchial specimens obtained from smokers and non-smokers, to evaluate the differences in Hsp60 levels and localization; 2) in the *in vitro* model we have induced the oxidative stress, a hallmark of COPD mucosa, by smoke, in order to determine whether Hsp60 was up-regulated or down-regulated and if it was, consequently, secreted in extracellular space; 3) ultimately, the *ex vivo*, an organotypic model, was established, where we were able to recapitulate the organization and the interaction of cells in EMTU, in order to study the smoking-induced stress and verify its effects in the *in vivo*-like system. Moreover, we have reproduced the cross talk between bronchial mucosa and immune system, highlighting the key role of the extracellular Hsp60, which is strictly involved in chronic immune system activation.

In preliminary data of this work, represented by our *in vivo* model, we not found significant differences in Hsp60 levels between non-smokers and smokers. Conversely, in a previous work, in which biopsies of COPD patients were used, the Hsp60 levels were higher in severe/very severe COPD compared to control smokers with normal lung function [65].

A proteomic analysis of rats lung exposed to smoke shows that Hsp60 is one of the most altered proteins, together with proteins that regulate apoptosis, stress response, cell structure, and inflammation [134]. The function of these proteins ensures the homeostasis maintaining, although when they are overexpressed, are strictly associated to cell transformation [134].

The results obtained demonstrate the dissimilar modulation of Hsp60 in our different models. Particularly, 16-HBE cells did not show significant variations in Hsp60 levels and localization. These data were consistent with those obtained in our *in vivo* model. On the other hand, such result are not in accordance with previous data where the exposure of 16-HBE

cells to oxidant and pro-inflammatory stress, H_2O_2-induced, caused the upregulation of Hsp60 and the release of this chaperonin in the extracellular medium [65]. This discrepancy could be due to the different stimulus used, which could activate different pathways, involved in response to stress. We used different doses of CSE for different time-points and probably immortalized cells were able to overcome the stress induced by CSE, activating other pathways. Moreover, the complexity of CS, which is a mixture of components, induces a complex of biological responses, involving an enormous number of signalling pathways. Furthermore, we hypothesize that the mechanism of immortalization has influenced the Hsp60 function in these cells.

Conversely, in mucoepidermoid cancer cell line (H292), we showed an increase of Hsp60 levels and this protein was exported outside of the cell, in response to sub-lethal doses of CSE. Furthermore, it has already been demonstrated that Hsp60 increased in cancerous tissue and is liberated in circulation [97,135]. Hsp60 is present mostly in the cytoplasm and extracellular sites of cancer cells rather than normal cells [136–138], and moreover, this protein is present in the plasma membrane, where it could serve as a ligand for immune system cells [139,140]. The relation between smoking, COPD, and lung carcinogenesis is still an open field of investigation; in fact, each inhaled insults could cause the metaplasia and thus cell transformation and cancer [141].

Here, the possible pathway involved in Hsp60 secretion has been investigated focusing in on exosomes secretion. Hsp60 is physiologically secreted in the extracellular space by a mechanism which is independent of cell death, as a consequence of cell-cell communication or depending on the pathological condition. The results obtained in a previous work of our laboratory, it has been demonstrated that Hsp60 can reach the cell membrane and is released by exosomes in tumor cells (H292) but not by normal cells (16-HBE) [81]. The data obtained from the *in vitro* model of this thesis are in accordance with these previous results while the new finding is that Hsp60 was actively secreted also after CSE exposure. Therefore,

following the stress induced by smoke, Hsp60 is overexpressed and released into the extracellular environment where it can acts as a danger signal inducing stress or damage of the cells or it can promote the immunological escape of cancerous or pre-cancerous cells [142,143].

It has been reported that Hsp60 has a key role in immune-modulation, since activates human monocytes and macrophages to synthesize pro-inflammatory cytokines (such as TNFα, IL-12, IL-15) and nitric oxide, also synergizing with IFN-γ in inducing cytokine synthesis [144,145]. This effect is mediated by binding to Toll-Like Receptor (TLR) 2 and 4, which induce the NFkB-dependent signalling pathway leading to cytokine secretion.

Based on the data obtained using the *in vivo* and *in vitro* models, we studied the effect of CSE on the morphology of our *ex vivo* model, mimicking COPD, focusing on Hsp60 levels and its release after smoke exposure. The *in vitro* models, currently used, are a monolayer epithelial cell culture and often are not useful to reproduce the events occurring *in vivo,* resembling only partially the human bronchial epithelium. 3D models, instead, have a high degree of similarity with human lung tissue. The bronchial 3D outgrowths, in particular, have a high potential to reproduce the real morphology and functions of EMTU, allowing the study of the cellular responses in a setting that resemble *in vivo* environments. This is a suitable model to investigate the oxidant effects induced by CS and drugs and therapeutic molecules finding as well.

In this study, the smoke effects on human bronchial mucosa were evaluated after mid- to long-term exposures to CSE, in order to highlight the response to the chemical constituents of CSE that relate to oxidative stress. CSE induces a variety of macroscopic morphological changes, as it has previously been characterized [146,147]. The bronchial mucosa undergoes epithelial-mesenchymal transition (EMT) in which cells lose cell polarity, and the columnar epithelium become squamous; loss of the ciliated cells and a thickening of the basement membrane is observed. These modifications are typical in the remodelling of bronchial mucosa in COPD. Moreover, downregulation of cell adhesion proteins, specifically

the tight junctions, has been also observed allowing migratory and invasiveness capabilities. These events has been seen in our *ex vivo* model, by direct observation (phase contrast microscopy monitoring), TEER measurement and immunofluorescence for ZO-1 protein (tight junctions) [120,148,149]. Indeed, our model was able to reproduce most likely the tissue changes typical of the mucosa in COPD.

In the present work, it has also been confirmed that CSE induces apoptosis in the bronchial mucosa, although a previous work, in monolayer *in vitro* model, has showed that smoke-induced cell dead could be mediated by the Apoptosis Induced Factor (AIF) [150].

Interestingly, when bronchial 3D outgrowths were treated with low doses of CSE, the TEER appeared to be higher than in the untreated cells. Probably, low doses of CSE induce activation of growth and survival factors, described previously in fibroblast, which could be responsible for increased cell proliferation and fibrosis in COPD mucosa [151]. Moreover, it has been shown that CSE activates NFkB, which could regulate the cell survival following smoke-induced DNA damage [152].

In the literature, there are several studies about the relation between Hsps and smoke [153] in particular it has been reported the role of Hsp70 [71,154,155], while few studies take in account the involvement of Hsp60 [156]. At the best of our knowledge, this is the first study which analyses the effect of smoke on Hsp60 expression in an organotypic model. The data, obtained in our 3D model suggest that the increased levels of Hsp60 after the acute treatments with CSE might represent a cytoprotection effect. It is well established that Hsp60 overexpression in various cell lines protects from the oxidative injury, suppressing mitochondrial membrane permeability and inhibiting apoptotic and necrotic cell death [157]. However, after a chronic stimulation (7 and 21 days) of the 3D outgrowths, we observed a decrease of Hsp60 gene and protein levels. Probably, the modulation of Hsp60 expression is related to cell transformation and carcinogenesis that could occur in this model as described previously in bronchial biopsies from COPD and lung cancer patients [141].

In response to CSE treatment, the bronchial 3D outgrowths secrete Hsp60 in the extracellular environment probably without using the exosomal pathway, since Hsp60 was not detected in the exosomes preparation. We demonstrated that the levels of extracellular Hsp60 were higher in a dose- and time-dependent mode, suggesting an extracellular signalling role of this chaperonin. Hsp60 might play a role as immune modulator, as demonstrated previously due to its capacity to interact with both the innate and adaptive immune system [158, 159].

To further elucidate the extracellular functions of Hsp60, we have investigated if there was a correlation between the levels of Hsp60 and the levels of cytokines, released by the 3D outgrowths exposed to smoke. We found a significant correlation between Hsp60 levels and IL 8 and -1β, while Hsp60 negatively correlated with IL 2, -10, -13, -4 and GM-CSF. It is interesting to note that Holz and colleagues, demonstrated that after airways inflammation IL 1β, -6 and -8 were significantly increased [160]. Additionally, the cytokine IL-8 was significantly increased only in bronchial epithelium of patients with severe/very severe COPD compared with control healthy smokers [161]. Bronchial cells exposed to smoke secrete high levels of IL 8, as demonstrated by Moon and colleagues [162]. Taken together these observations and our findings, we can assert that Hsp60 expression could be correlated with the inflammatory state of COPD since it has been already demonstrated that the levels of this protein has been related to the number of inflammatory cells in the mucosa of COPD patients [65].

In order to find out if our data can be translated *in vivo*, we have analysed the levels of Hsp60 in the plasma of COPD patients, compared with those of healthy donors. As expected, the circulating levels of Hsp60, in COPD patients, were higher than in controls confirming the results obtained ex vivo. Hence, Hsp60 could be used as biomarker to monitor COPD pathogenesis and the inflammatory response involved in this disease.

An increasing number of scientific papers demonstrates the function of molecular chaperones as an extracellular signal [57], and in particular of

Hsp60 [96,143,163,164] even if the significance of the cell–cell signalling through the Hsps is still under debate [158,159].

In our model, Hsp60 appears to be secreted in conventional mode, independent from exosomal pathway. For this reason, we decided to mimic Hsp60 capability to interact and activate human monocytes using a commercial recombinant Hsp60 (rHsp60) and exosome released from 3D outgrowth exposed to smoke. The cytokine levels in the conditioned medium of the monocytes co-cultures were higher when treated with rHsp60 compared to exosomes treatment confirming monocytes activation and the hypothesis that Hsp60 could be considered as a cytokine-like molecule. We found that after rHsp60 stimulation IL 1β and IL 7 levels were higher compared to the controls and there was a positive correlation between IL 1β and IL 7 levels with Hsp60 levels in plasma of COPD patients. These two cytokines are chemotactic and growth factors which stimulate cell proliferation and differentiation of macrophages and lymphocytes, respectively. Taken together these data strengthen our hypothesis and only few studies considered Hsps as monocyte cytokine inducers because the difficulties founded in the experimental methods and statistical analyses [165,166]. The extracellular behaviour and the effect of Hsp60 on the target cells could depend of the stimulation of a number of signalling pathways involving cytokines gene transcription and could give molecular response difficult to understand.

Final remarks.

To summarise the data obtained and described in this thesis, we have found that Hsp60 levels did not show significant differences between smokers and non-smokers, in the *in vivo* study. In the *in vitro* model, we observed that Hsp60 is subjected to variation in levels and distribution, in H292 cancer cell line but not in normal cells, demonstrating the correlation between smoke and lung cancer. This relation was also established in the *ex vivo* model, in which a CS-induced remodelling characteristic of the epithelial-mesenchymal transition occurred. We showed that our *ex vivo* model is useful to reproduce the morphological and functional changes in

bronchial mucosa exposed to smoke. Indeed, we observed, for long-time exposure to smoke, an intracellular reduction and, contemporary, an extracellular increase in Hsp60 levels, suggesting that Hsp60 might be released from the smoke-stressed human mucosa into the circulatory torrent. Here, this chaperonin could be able to act as a chemokine at distant site triggering the activation of the immune system and perpetuating the inflammatory response in the bronchial mucosa. This was demonstrated by the correlation between Hsp60 with the cytokines IL 1β and IL 8 released from 3D outgrowths exposed to CSE and by the correlation between Hsp60 with the cytokines IL 1β and IL 7 released from PBMC stimulated with Hsp60.

Taken together these observations and results suggested that Hsp60 represents a new biomarkers for diagnostic and prognostic purposes in COPD management as well as in other inflammatory chronic disease.

The prospective for new therapies, together with a deeper analysis of molecular events and the possible modulation of Hsp60 activation and releasing pathways, needs to be further studied.

References

1. Drake, R. L. *Gray’s Atlas of Anatomy*. (Elsevier Health Sciences, 2008). at <https://books.google.com/books?id=LZZ5AAAAQBAJ&pgis=1>
2. Reynolds, S. D. & Malkinson, A. M. Clara cell: progenitor for the bronchiolar epithelium. *Int. J. Biochem. Cell Biol.* **42,** 1–4 (2010).
3. Kaminsky, D. *Netter Collection of Medical Illustrations: Respiratory System*. (Elsevier Health Sciences, 2011). at <https://books.google.com/books?id=5ntXQpPwesYC&pgis=1>
4. Wheater’s Functional Histology, 5E, eBooks from Elsevier UK. at <http://elsevierelibrary.co.uk/product/wheater>
5. *Upper and Lower Respiratory Disease*. (CRC Press, 2003). at <https://books.google.com/books?id=lTHMBQAAQBAJ&pgis=1>
6. Elsevier: Concise Histology Gartner & Hiatt. at <http://www.elsevier.ca/ISBN/9780702031144/Concise-Histology>
7. Pauwels, R. A., Buist, A. S., Calverley, P. M., Jenkins, C. R. & Hurd, S. S. Global strategy for the diagnosis, management, and prevention of chronic obstructive pulmonary disease. NHLBI/WHO Global Initiative for Chronic Obstructive Lung Disease (GOLD) Workshop summary. *Am. J. Respir. Crit. Care Med.* **163,** 1256–76 (2001).
8. Rernnad, S. I. & Vestbo, J. COPD: the dangerous underestimate of 15%. *Lancet* **367,** 1216–1219 (2006).
9. Macnee, W. Pathogenesis of chronic obstructive pulmonary disease. *Clin. Chest Med.* **28,** 479–513, v (2007).
10. Stevens, G. Global Health Risks: Mortality and burden of disease attributable to selected major risks. *Bull. World Health Organ.* **87,** 646–646 (2009).
11. Di Stefano, a *et al.* Cellular and molecular mechanisms in chronic obstructive pulmonary disease: an overview. *Clin. Exp. Allergy* **34,** 1156–67 (2004).
12. Xu, X., Weiss, S. T., Rijcken, B. & Schouten, J. P. Smoking, changes in smoking habits, and rate of decline in FEV1: new insight into gender differences. *Eur. Respir. J.* **7,** 1056–61 (1994).
13. Rovina, N., Koutsoukou, A. & Koulouris, N. G. Inflammation and immune response in COPD: where do we stand? *Mediators Inflamm.* **2013,** 413735 (2013).
14. Evans, M. J., Van Winkle, L. S., Fanucchi, M. V. & Plopper, C. G. The attenuated fibroblast sheath of the respiratory tract epithelial-mesenchymal trophic unit. *Am. J. Respir. Cell Mol. Biol.* **21,** 655–657 (1999).
15. Gizycki, M. J., Adelroth, E., Rogers, A. V, O’Byrne, P. M. & Jeffery, P. K. Myofibroblast involvement in the allergen-induced late response in mild atopic asthma. *Am. J. Respir. Cell Mol. Biol.* **16,** 664–73 (1997).
16. Wang, H. *et al.* Effect of cigarette smoke on fibroblast-mediated gel contraction is dependent on cell density. *Am. J. Physiol. Lung Cell. Mol. Physiol.* **284,** L205–13 (2003).
17. Carnevali, S. *et al.* Cigarette smoke extract induces oxidative stress and apoptosis in human lung fibroblasts. *Am. J. Physiol. Lung Cell. Mol. Physiol.* **284,** L955–63 (2003).
18. Ojo, O. *et al.* Pathological changes in the COPD lung mesenchyme - Novel

lessons learned from in??vitro and in??vivo studies. *Pulm. Pharmacol. Ther.* **29,** 121–128 (2014).

19. Puchelle, E., Zahm, J.-M., Tournier, J.-M. & Coraux, C. Airway Epithelial Repair, Regeneration, and Remodeling after Injury in Chronic Obstructive Pulmonary Disease. *Proceedings of the American Thoracic Society* (2012). at <http://www.atsjournals.org/doi/abs/10.1513/pats.200605-126SF?journalCode=pats#.VT9YUyHtmko>

20. CHEN, Y., CHEN, P., HANAOKA, M., DROMA, Y. & KUBO, K. Enhanced levels of prostaglandin E 2 and matrix metalloproteinase-2 correlate with the severity of airflow limitation in stable COPD. *Respirology* **13,** ???–??? (2008).

21. Haq, I. *et al.* Association of MMP-2 polymorphisms with severe and very severe COPD: a case control study of MMPs-1, 9 and 12 in a European population. *BMC Med. Genet.* **11,** 7 (2010).

22. Barnes, P. J. & Adcock, I. M. Chronic obstructive pulmonary disease and lung cancer: a lethal association. *Am. J. Respir. Crit. Care Med.* **184,** 866–7 (2011).

23. Milara, J., Peiró, T., Serrano, A. & Cortijo, J. Epithelial to mesenchymal transition is increased in patients with COPD and induced by cigarette smoke. *Thorax* **68,** 410–20 (2013).

24. Shaykhiev, R. *et al.* Cigarette smoking reprograms apical junctional complex molecular architecture in the human airway epithelium in vivo. *Cell. Mol. Life Sci.* **68,** 877–92 (2011).

25. Qu, P. *et al.* Stat3 downstream genes serve as biomarkers in human lung carcinomas and chronic obstructive pulmonary disease. *Lung Cancer* **63,** 341–347 (2009).

26. Malhotra, D. *et al.* Expression of concern: Decline in NRF2-regulated antioxidants in chronic obstructive pulmonary disease lungs due to loss of its positive regulator, DJ-1. *Am. J. Respir. Crit. Care Med.* **178,** 592–604 (2008).

27. Laucho-Contreras, M. E., Taylor, K. L., Mahadeva, R., Boukedes, S. S. & Owen, C. A. Automated measurement of pulmonary emphysema and small airway remodeling in cigarette smoke-exposed mice. *J. Vis. Exp.* 52236 (2015). doi:10.3791/52236

28. Groneberg, D. a & Chung, K. F. Models of chronic obstructive pulmonary disease. *Respir. Res.* **5,** 18 (2004).

29. Churg, A., Cosio, M. & Wright, J. L. Mechanisms of cigarette smoke-induced COPD: insights from animal models. *Am. J. Physiol. Lung Cell. Mol. Physiol.* **294,** L612–31 (2008).

30. March, T. H. *et al.* Cigarette smoke exposure produces more evidence of emphysema in B6C3F1 mice than in F344 rats. *Toxicol. Sci.* **51,** 289–99 (1999).

31. Dhami, R. *et al.* Acute Cigarette Smoke–Induced Connective Tissue Breakdown Is Mediated by Neutrophils and Prevented by α 1-Antitrypsin. *Am. J. Respir. Cell Mol. Biol.* **22,** 244–252 (2000).

32. Zhang, S., Smartt, H., Holgate, S. T. & Roche, W. R. Growth factors secreted by bronchial epithelial cells control myofibroblast proliferation: an in vitro co-culture model of airway remodeling in asthma. *Lab. Invest.* **79,** 395–405 (1999).

33. Lee, J., Cuddihy, M. J. & Kotov, N. A. Three-dimensional cell culture matrices: state of the art. *Tissue Eng. Part B. Rev.* **14,** 61–86 (2008).

34. Hong, K. U., Reynolds, S. D., Watkins, S., Fuchs, E. & Stripp, B. R. Basal cells are a multipotent progenitor capable of renewing the bronchial epithelium. *Am. J.*

Pathol. **164,** 577–88 (2004).

35. Antoni, D., Burckel, H., Josset, E. & Noel, G. Three-Dimensional Cell Culture: A Breakthrough in Vivo. *Int. J. Mol. Sci.* **16,** 5517–5527 (2015).

36. Vaughan, M. B., Ramirez, R. D., Wright, W. E., Minna, J. D. & Shay, J. W. A three-dimensional model of differentiation of immortalized human bronchial epithelial cells. *Differentiation.* **74,** 141–8 (2006).

37. Mio, T. *et al.* Cigarette smoke induces interleukin-8 release from human bronchial epithelial cells. *Am. J. Respir. Crit. Care Med.* **155,** 1770–6 (1997).

38. Lucantoni, G. *et al.* The red blood cell as a biosensor for monitoring oxidative imbalance in chronic obstructive pulmonary disease: an ex vivo and in vitro study. *Antioxid. Redox Signal.* **8,** 1171–82

39. Lee, Y. C. & Rannels, D. E. Regulation of extracellular matrix synthesis by TNF-alpha and TGF-beta1 in type II cells exposed to coal dust. *Am. J. Physiol.* **275,** L637–44 (1998).

40. Nakajoh, M. *et al.* Retinoic acid inhibits elastase-induced injury in human lung epithelial cell lines. *Am. J. Respir. Cell Mol. Biol.* **28,** 296–304 (2003).

41. Hoffmann, D., Djordjevic, M. V & Hoffmann, I. The changing cigarette. *Prev. Med. (Baltim).* **26,** 427–34

42. Krimmer, D. I. & Oliver, B. G. G. What can in vitro models of COPD tell us? *Pulm. Pharmacol. Ther.* **24,** 471–477 (2011).

43. Kode, A., Yang, S.-R. & Rahman, I. Differential effects of cigarette smoke on oxidative stress and proinflammatory cytokine release in primary human airway epithelial cells and in a variety of transformed alveolar epithelial cells. *Respir. Res.* **7,** 132 (2006).

44. Li, C.-J., Ning, W., Matthay, M. A., Feghali-Bostwick, C. A. & Choi, A. M. K. MAPK pathway mediates EGR-1-HSP70-dependent cigarette smoke-induced chemokine production. *Am. J. Physiol. Lung Cell. Mol. Physiol.* **292,** L1297–303 (2007).

45. Wu, H. *et al.* Interleukin-33/ST2 signaling promotes production of interleukin-6 and interleukin-8 in systemic inflammation in cigarette smoke-induced chronic obstructive pulmonary disease mice. *Biochem. Biophys. Res. Commun.* **450,** 110–6 (2014).

46. Heijink, I. H. *et al.* Role of aberrant WNT signalling in the airway epithelial response to cigarette smoke in chronic obstructive pulmonary disease. *Thorax* **68,** 709–16 (2013).

47. Guo, L. *et al.* WNT/β-catenin signaling regulates cigarette smoke-induced airway inflammation via the PPARδ/p38 pathway. *Lab. Invest.* (2015). doi:10.1038/labinvest.2015.101

48. Macario, A. J. L. & Conway de Macario, E. Molecular chaperones: multiple functions, pathologies, and potential applications. *Front. Biosci.* **12,** 2588–600 (2007).

49. Macario, A. J. L. & Conway de Macario, E. Sick chaperones, cellular stress, and disease. *N. Engl. J. Med.* **353,** 1489–501 (2005).

50. Voellmy, R. Transduction of the stress signal and mechanisms of transcriptional regulation of heat shock/stress protein gene expression in higher eukaryotes. *Crit. Rev. Eukaryot. Gene Expr.* **4,** 357–401 (1994).

51. Walsh, D. *et al.* The role of heat shock proteins in mammalian differentiation and development. *Environ. Med.* **43,** 79–87 (1999).

52. Murshid, A., Gong, J. & Calderwood, S. K. The role of heat shock proteins in antigen cross presentation. *Front. Immunol.* **3,** 63 (2012).

53. Prohászka, Z. & Füst, G. Immunological aspects of heat-shock proteins-the optimum stress of life. *Mol. Immunol.* **41,** 29–44 (2004).

54. Czarnecka, a M., Campanella, C., Zummo, G. & Cappello, F. Mitochondrial chaperones in cancer: from molecular biology to clinical diagnostics. *Cancer Biol Ther* **5,** 714–720 (2006).

55. Macario, A. J. L., Cappello, F., Zummo, G. & Conway de Macario, E. Chaperonopathies of senescence and the scrambling of interactions between the chaperoning and the immune systems. *Ann. N. Y. Acad. Sci.* **1197,** 85–93 (2010).

56. Garrido, C., Gurbuxani, S., Ravagnan, L. & Kroemer, G. Heat shock proteins: endogenous modulators of apoptotic cell death. *Biochem. Biophys. Res. Commun.* **286,** 433–42 (2001).

57. Calderwood, S. K., Mambula, S. S. & Gray, P. J. Extracellular heat shock proteins in cell signaling and immunity. *Ann. N. Y. Acad. Sci.* **1113,** 28–39 (2007).

58. Kampinga, H. H. *et al.* Guidelines for the nomenclature of the human heat shock proteins. *Cell Stress Chaperones* **14,** 105–11 (2009).

59. Search | HUGO Gene Nomenclature Committee. at <http://www.genenames.org/cgi-bin/search?search_type=all&search=Heat+shock+protein&submit=Submit>

60. Rappa, F. *et al.* HSP-molecular chaperones in cancer biogenesis and tumor therapy: an overview. *Anticancer Res.* **32,** 5139–50 (2012).

61. RAPPA, F. *et al.* HSP-Molecular Chaperones in Cancer Biogenesis and Tumor Therapy: An Overview. *Anticancer Res* **32,** 5139–5150 (2012).

62. Asea, A. *et al.* Novel signal transduction pathway utilized by extracellular HSP70: role of toll-like receptor (TLR) 2 and TLR4. *J. Biol. Chem.* **277,** 15028–34 (2002).

63. Becker, T., Hartl, F.-U. & Wieland, F. CD40, an extracellular receptor for binding and uptake of Hsp70-peptide complexes. *J. Cell Biol.* **158,** 1277–85 (2002).

64. Ogden, C. A. *et al.* C1q and mannose binding lectin engagement of cell surface calreticulin and CD91 initiates macropinocytosis and uptake of apoptotic cells. *J. Exp. Med.* **194,** 781–95 (2001).

65. Cappello, F. *et al.* Convergent sets of data from in vivo and in vitro methods point to an active role of Hsp60 in chronic obstructive pulmonary disease pathogenesis. *PLoS One* **6,** e28200 (2011).

66. Li, Z., Menoret, A. & Srivastava, P. Roles of heat-shock proteins in antigen presentation and cross-presentation. *Curr. Opin. Immunol.* **14,** 45–51 (2002).

67. Somersan, S. *et al.* Primary tumor tissue lysates are enriched in heat shock proteins and induce the maturation of human dendritic cells. *J. Immunol.* **167,** 4844–52 (2001).

68. Panjwani, N. N., Popova, L. & Srivastava, P. K. Heat shock proteins gp96 and hsp70 activate the release of nitric oxide by APCs. *J. Immunol.* **168,** 2997–3003 (2002).

69. Cherneva, R. V. *et al.* The role of small heat-shock protein αB-crystalline (HspB5) in COPD pathogenesis. *Int. J. COPD* **7,** 633–640 (2012).

70. van Noort, J. M. *et al.* Activation of an immune-regulatory macrophage response and inhibition of lung inflammation in a mouse model of COPD using heat-shock protein alpha B-crystallin-loaded PLGA microparticles. *Biomaterials* **34,** 831–40

(2013).

71. Dong, J. *et al.* Increased expression of heat shock protein 70 in chronic obstructive pulmonary disease. *Int. Immunopharmacol.* **17,** 885–93 (2013).

72. Hu, R. *et al.* Heat shock protein 27 and cyclophilin A associate with the pathogenesis of COPD. *Respirology* **16,** 983–993 (2011).

73. Usefulness of the hsp60 gene for the identification and classification of Gram-negative anaerobic rods. - PubMed - NCBI. at <http://www.ncbi.nlm.nih.gov/pubmed/20671088>

74. Campanella, C. *et al.* A comparative analysis of the products of GROEL-1 gene from Chlamydia trachomatis serovar D and the HSP60 var1 transcript from Homo sapiens suggests a possible autoimmune response. *Int. J. Immunogenet.* **36,** 73–8 (2009).

75. Pace, A. *et al.* Hsp60, a novel target for antitumor therapy: structure-function features and prospective drugs design. *Curr. Pharm. Des.* **19,** 2757–64 (2013).

76. Cappello, F. *et al.* Hsp60 chaperonopathies and chaperonotherapy: targets and agents. *Expert Opin. Ther. Targets* **18,** 185–208 (2014).

77. Cappello, F. *et al.* Hsp60 and human aging: Les liaisons dangereuses. *Front. Biosci. (Landmark Ed.* **18,** 626–37 (2013).

78. Flohé, S. B. *et al.* Human heat shock protein 60 induces maturation of dendritic cells versus a Th1-promoting phenotype. *J. Immunol.* **170,** 2340–8 (2003).

79. Ausiello, C. M. *et al.* 60-kDa heat shock protein of Chlamydia pneumoniae promotes a T helper type 1 immune response through IL-12/IL-23 production in monocyte-derived dendritic cells. *Microbes Infect.* **8,** 714–720 (2006).

80. Tomasello, G. *et al.* Changes in immunohistochemical levels and subcellular localization after therapy and correlation and colocalization with CD68 suggest a pathogenetic role of Hsp60 in ulcerative colitis. *Appl. Immunohistochem. Mol. Morphol.* **19,** 552–61 (2011).

81. Merendino, A. M. *et al.* Hsp60 is actively secreted by human tumor cells. *PLoS One* **5,** e9247 (2010).

82. Raposo, G. & Stoorvogel, W. Extracellular vesicles: Exosomes, microvesicles, and friends. *J. Cell Biol.* **200,** 373–383 (2013).

83. Lopez-Verrilli, M. a. & Court, F. a. Exosomes: Mediators of communication in eukaryotes. *Biol. Res.* **46,** 5–11 (2013).

84. Pan, B. T., Blostein, R. & Johnstone, R. M. Loss of the transferrin receptor during the maturation of sheep reticulocytes in vitro. An immunological approach. *Biochem. J.* **210,** 37–47 (1983).

85. Vlassov, A. V., Magdaleno, S., Setterquist, R. & Conrad, R. Exosomes: Current knowledge of their composition, biological functions, and diagnostic and therapeutic potentials. *Biochim. Biophys. Acta - Gen. Subj.* **1820,** 940–948 (2012).

86. Van Niel, G., Porto-Carreiro, I., Simoes, S. & Raposo, G. Exosomes: A common pathway for a specialized function. *J. Biochem.* **140,** 13–21 (2006).

87. Colombo, M. *et al.* Analysis of ESCRT functions in exosome biogenesis, composition and secretion highlights the heterogeneity of extracellular vesicles. *J. Cell Sci.* **126,** 5553–65 (2013).

88. Möbius, W. *et al.* Immunoelectron microscopic localization of cholesterol using biotinylated and non-cytolytic perfringolysin O. *J. Histochem. Cytochem.* **50,** 43–55 (2002).

89. Trajkovic, K. *et al.* Ceramide triggers budding of exosome vesicles into multivesicular endosomes. *Science* **319,** 1244–7 (2008).

90. Ratajczak, J. *et al.* Embryonic stem cell-derived microvesicles reprogram hematopoietic progenitors: evidence for horizontal transfer of mRNA and protein delivery. *Leukemia* **20,** 847–56 (2006).

91. Kosaka, N. *et al.* Secretory mechanisms and intercellular transfer of microRNAs in living cells. *J. Biol. Chem.* **285,** 17442–52 (2010).

92. Fernández-Messina, L., Gutiérrez-Vázquez, C., Rivas-García, E., Sánchez-Madrid, F. & de la Fuente, H. Immunomodulatory role of microRNAs transferred by extracellular vesicles. *Biol. Cell* **107,** 61–77 (2015).

93. Qu, Y., Franchi, L., Nunez, G. & Dubyak, G. R. Nonclassical IL-1 beta secretion stimulated by P2X7 receptors is dependent on inflammasome activation and correlated with exosome release in murine macrophages. *J. Immunol.* **179,** 1913–25 (2007).

94. Phoonsawat, W., Aoki-Yoshida, A., Tsuruta, T. & Sonoyama, K. Adiponectin is partially associated with exosomes in mouse serum. *Biochem. Biophys. Res. Commun.* **448,** 261–6 (2014).

95. Chen, L., Chen, R., Kemper, S., Charrier, A. & Brigstock, D. R. Suppression of fibrogenic signaling in hepatic stellate cells by Twist1-dependent microRNA-214 expression: Role of exosomes in horizontal transfer of Twist1. *Am. J. Physiol. Gastrointest. Liver Physiol.* ajpgi.00140.2015 (2015). doi:10.1152/ajpgi.00140.2015

96. Campanella, C. *et al.* The odyssey of Hsp60 from tumor cells to other destinations includes plasma membrane-associated stages and Golgi and exosomal protein-trafficking modalities. *PLoS One* **7,** e42008 (2012).

97. Campanella, C. *et al.* Heat shock protein 60 levels in tissue and circulating exosomes in human large bowel cancer before and after ablative surgery. *Cancer* (2015). doi:10.1002/cncr.29499

98. Waldenstrom, A. & Ronquist, G. Role of Exosomes in Myocardial Remodeling. *Circ. Res.* **114,** 315–324 (2014).

99. Ostrowski, M. *et al.* Rab27a and Rab27b control different steps of the exosome secretion pathway. *Nat. Cell Biol.* **12,** 19–30; sup pp 1–13 (2010).

100. Xie, Y. *et al.* Dendritic cells recruit T cell exosomes via exosomal LFA-1 leading to inhibition of CD8+ CTL responses through downregulation of peptide/MHC class I and Fas ligand-mediated cytotoxicity. *J. Immunol.* **185,** 5268–78 (2010).

101. van Niel, G. *et al.* The tetraspanin CD63 regulates ESCRT-independent and -dependent endosomal sorting during melanogenesis. *Dev. Cell* **21,** 708–21 (2011).

102. Rana, S., Yue, S., Stadel, D. & Zöller, M. Toward tailored exosomes: the exosomal tetraspanin web contributes to target cell selection. *Int. J. Biochem. Cell Biol.* **44,** 1574–84 (2012).

103. Schorey, J. S. & Bhatnagar, S. Exosome function: from tumor immunology to pathogen biology. *Traffic* **9,** 871–81 (2008).

104. Choi, D.-S. *et al.* Proteomic analysis of microvesicles derived from human colorectal cancer cells. *J. Proteome Res.* **6,** 4646–55 (2007).

105. Muralidharan-Chari, V., Clancy, J. W., Sedgwick, A. & D’Souza-Schorey, C. Microvesicles: mediators of extracellular communication during cancer progression. *J. Cell Sci.* **123,** 1603–11 (2010).

106. Lancaster, G. I. & Febbraio, M. a. Exosome-dependent trafficking of HSP70: A novel secretory pathway for cellular stress proteins. *J. Biol. Chem.* **280,** 23349–23355 (2005).

107. Klöhn, P.-C., Castro-Seoane, R. & Collinge, J. Exosome release from infected dendritic cells: a clue for a fast spread of prions in the periphery? *J. Infect.* **67,** 359–68 (2013).

108. Ogorevc, E., Kralj-Iglic, V. & Veranic, P. The role of extracellular vesicles in phenotypic cancer transformation. *Radiol. Oncol.* **47,** 197–205 (2013).

109. Yamada, T., Shigemura, H., Ishiguro, N. & Inoshima, Y. Cell Infectivity in relation to bovine leukemia virus gp51 and p24 in bovine milk exosomes. *PLoS One* **8,** e77359 (2013).

110. Tasaki, M. *et al.* Transmission of circulating cell-free AA amyloid oligomers in exosomes vectors via a prion-like mechanism. *Biochem. Biophys. Res. Commun.* **400,** 559–62 (2010).

111. Campanella, C. *et al.* Exosomal Heat Shock Proteins as New Players in Tumour Cell-to-cell Communication. *J. Circ. Biomarkers* 1 (2014). doi:10.5772/58721

112. Royal, J. *et al.* Hsp10 nuclear localization and changes in lung cells response to cigarette smoke suggest novel roles for this chaperonin.

113. Cozens, A. L. *et al.* CFTR expression and chloride secretion in polarized immortal human bronchial epithelial cells. *Am. J. Respir. Cell Mol. Biol.* **10,** 38–47 (1994).

114. Carp, H. & Janoff, A. Possible mechanisms of emphysema in smokers. In vitro suppression of serum elastase-inhibitory capacity by fresh cigarette smoke and its prevention by antioxidants. *Am. Rev. Respir. Dis.* **118,** 617–21 (1978).

115. Campanella, C. *et al.* Upon oxidative stress, the antiapoptotic Hsp60/procaspase-3 complex persists in mucoepidermoid carcinoma cells. *Eur. J. Histochem.* **52,** 221–8 (2008).

116. Rappa, F. *et al.* Comparative analysis of hsp10 and hsp90 expression in healthy mucosa and adenocarcinoma of the large bowel. *Anticancer Res.* **34,** 4153–9 (2014).

117. Campanella, C. *et al.* The histone deacetylase inhibitor SAHA induces HSP60 nitration and its extracellular release by exosomal vesicles in human lung-derived carcinoma cells. (2015).

118. Marino Gammazza, A. *et al.* Elevated blood Hsp60, its structural similarities and cross-reactivity with thyroid molecules, and its presence on the plasma membrane of oncocytes point to the chaperonin as an immunopathogenic factor in Hashimoto’s thyroiditis. *Cell Stress Chaperones* **19,** 343–53 (2014).

119. Marcilla, A. *et al.* Extracellular Vesicles from Parasitic Helminths Contain Specific Excretory/Secretory Proteins and Are Internalized in Intestinal Host Cells. *PLoS One* **7,** e45974 (2012).

120. Schamberger, A. C., Staab-Weijnitz, C. a., Mise-Racek, N. & Eickelberg, O. Cigarette smoke alters primary human bronchial epithelial cell differentiation at the air-liquid interface. *Sci. Rep.* **5,** 8163 (2015).

121. Di Felice, V. *et al.* Silk fibroin scaffolds enhance cell commitment of adult rat cardiac progenitor cells. *J. Tissue Eng. Regen. Med.* n/a–n/a (2013). doi:10.1002/term.1739

122. Lee, J.-K. *et al.* Exosomes derived from mesenchymal stem cells suppress angiogenesis by down-regulating VEGF expression in breast cancer cells. *PLoS One* **8,** e84256 (2013).

123. Deniset, J. F. & Pierce, G. N. Heat Shock Proteins: Mediators of Atherosclerotic Development. *Curr. Drug Targets* **16,** 816–26 (2015).

124. Vassallo, R., Kroening, P. R., Parambil, J. & Kita, H. Nicotine and oxidative cigarette smoke constituents induce immune-modulatory and pro-inflammatory dendritic cell responses. *Mol. Immunol.* **45,** 3321–3329 (2008).

125. Yang, S.-R. *et al.* Cigarette smoke induces proinflammatory cytokine release by activation of NF-kappaB and posttranslational modifications of histone deacetylase in macrophages. *Am. J. Physiol. Lung Cell. Mol. Physiol.* **291,** L46–57 (2006).

126. Glader, P. *et al.* Cigarette smoke extract modulates respiratory defence mechanisms through effects on T-cells and airway epithelial cells. *Respir. Med.* **100,** 818–827 (2006).

127. Hoffmann, R. F., Zarrintan, S., Brandenburg, S. M., Kol, A. & Bruin, H. G. De. Prolonged cigarette smoke exposure alters mitochondrial structure and function in airway epithelial cells Prolonged cigarette smoke exposure alters mitochondrial structure and function in airway epithelial cells. *Respir. Res.* **14,** 1 (2013).

128. Vallese, D. *et al.* Phospho-p38 MAPK Expression in COPD Patients and Asthmatics and in Challenged Bronchial Epithelium. *Respiration* **89,** 329–342 (2015).

129. La Rocca, G. *et al.* Cigarette smoke exposure inhibits extracellular MMP-2 (gelatinase A) activity in human lung fibroblasts. *Respir. Res.* **8,** 23 (2007).

130. Noessner, E. *et al.* Tumor-derived heat shock protein 70 peptide complexes are cross-presented by human dendritic cells. *J. Immunol.* **169,** 5424–32 (2002).

131. De Graeff-Meeder, E. R. *et al.* Recognition of human 60 kD heat shock protein by mononuclear cells from patients with juvenile chronic arthritis. *Lancet (London, England)* **337,** 1368–72 (1991).

132. Stinissen, P. *et al.* Increased frequency of gamma delta T cells in cerebrospinal fluid and peripheral blood of patients with multiple sclerosis. Reactivity, cytotoxicity, and T cell receptor V gene rearrangements. *J. Immunol.* **154,** 4883–94 (1995).

133. Tun, R. Y. *et al.* Antibodies to heat shock protein 65 kD in type 1 diabetes mellitus. *Diabet. Med.* **11,** 66–70

134. Carter, C. A., Misra, M. & Pelech, S. Proteomic analyses of lung lysates from short-term exposure of Fischer 344 rats to cigarette smoke. *J. Proteome Res.* **10,** 3720–31 (2011).

135. Cappello, F. *et al.* The expression of HSP60 and HSP10 in large bowel carcinomas with lymph node metastase. *BMC Cancer* **5,** 139 (2005).

136. Soltys, B. J. & Gupta, R. S. Immunoelectron microscopic localization of the 60-kDa heat shock chaperonin protein (Hsp60) in mammalian cells. *Exp. Cell Res.* **222,** 16–27 (1996).

137. Soltys, B. J. & Gupta, R. S. Mitochondrial proteins at unexpected cellular locations: export of proteins from mitochondria from an evolutionary perspective. *Int. Rev. Cytol.* **194,** 133–96 (2000).

138. Ikawa, S. & Weinberg, R. A. An interaction between p21ras and heat shock protein hsp60, a chaperonin. *Proc. Natl. Acad. Sci. U. S. A.* **89,** 2012–6 (1992).

139. Soltys, B. J. & Gupta, R. S. Cell surface localization of the 60 kDa heat shock chaperonin protein (hsp60) in mammalian cells. *Cell Biol. Int.* **21,** 315–20 (1997).

140. Barazi, H. O., Zhou, L., Templeton, N. S., Krutzsch, H. C. & Roberts, D. D.

Identification of heat shock protein 60 as a molecular mediator of alpha 3 beta 1 integrin activation. *Cancer Res.* **62,** 1541–8 (2002).

141. Cappello, F. *et al.* Hsp60 and Hsp10 down-regulation predicts bronchial epithelial carcinogenesis in smokers with chronic obstructive pulmonary disease. *Cancer* **107,** 2417–24 (2006).

142. Nakamura, H. & Minegishi, H. HSP60 as a drug target. *Curr. Pharm. Des.* **19,** 441–51 (2013).

143. Cappello, F., Angileri, F., de Macario, E. C. & Macario, A. J. L. Chaperonopathies and chaperonotherapy. Hsp60 as therapeutic target in cancer: potential benefits and risks. *Curr. Pharm. Des.* **19,** 452–7 (2013).

144. Chen, W., Syldath, U., Bellmann, K., Burkart, V. & Kolb, H. Human 60-kDa heat-shock protein: a danger signal to the innate immune system. *J. Immunol.* **162,** 3212–9 (1999).

145. Osterloh, A. *et al.* Heat shock protein 60 (HSP60) stimulates neutrophil effector functions. *J. Leukoc. Biol.* **86,** 423–34 (2009).

146. Liang, Z. *et al.* ERK5 negatively regulates tobacco smoke-induced pulmonary epithelial-mesenchymal transition. *Oncotarget* **6,** 19605–18 (2015).

147. Zhao, Y. *et al.* NF-κB-mediated inflammation leading to EMT via miR-200c is involved in cell transformation induced by cigarette smoke extract. *Toxicol. Sci.* **135,** 265–76 (2013).

148. Gualerzi, A., Sciarabba, M., Tartaglia, G., Sforza, C. & Donetti, E. Acute effects of cigarette smoke on three-dimensional cultures of normal human oral mucosa. *Inhal. Toxicol.* **24,** 382–389 (2012).

149. Schamberger, A. C. *et al.* Cigarette smoke-induced disruption of bronchial epithelial tight junctions is prevented by transforming growth factor-β. *Am. J. Respir. Cell Mol. Biol.* **50,** 1040–52 (2014).

150. Bucchieri, F. *et al.* Cigarette Smoke Causes Caspase-Independent Apoptosis of Bronchial Epithelial Cells from Asthmatic Donors. *PLoS One* **10,** e0120510 (2015).

151. Wong, L. S. *et al.* Effects of ‘second-hand’ smoke on structure and function of fibroblasts, cells that are critical for tissue repair and remodeling. *BMC Cell Biol.* **5,** 13 (2004).

152. Liu, X. *et al.* NF-kappaB mediates the survival of human bronchial epithelial cells exposed to cigarette smoke extract. *Respir. Res.* **9,** 66 (2008).

153. Vayssier, M., Favatier, F., Pinot, F., Bachelet, M. & Polla, B. S. Tobacco smoke induces coordinate activation of HSF and inhibition of NFkappaB in human monocytes: effects on TNFalpha release. *Biochem. Biophys. Res. Commun.* **252,** 249–56 (1998).

154. Zhang, L. *et al.* Resveratrol exerts an anti-apoptotic effect on human bronchial epithelial cells undergoing cigarette smoke exposure. *Mol. Med. Rep.* **11,** 1752–8 (2015).

155. de Vries, M. *et al.* Pim1 kinase protects airway epithelial cells from cigarette smoke-induced damage and airway inflammation. *Am. J. Physiol. Lung Cell. Mol. Physiol.* **307,** L240–51 (2014).

156. Kreutmayer, S. B. *et al.* Dynamics of heat shock protein 60 in endothelial cells exposed to cigarette smoke extract. *J. Mol. Cell. Cardiol.* **51,** 777–80 (2011).

157. He, L. & Lemasters, J. J. Heat shock suppresses the permeability transition in rat liver mitochondria. *J. Biol. Chem.* **278,** 16755–60 (2003).

158. Quintana, F. J. & Cohen, I. R. The HSP60 immune system network. *Trends Immunol.* **32,** 89–95 (2011).

159. Pockley, A. G., Muthana, M. & Calderwood, S. K. The dual immunoregulatory roles of stress proteins. *Trends Biochem. Sci.* **33,** 71–9 (2008).

160. Holz, O. *et al.* Efficacy and safety of inhaled calcium lactate PUR118 in the ozone challenge model--a clinical trial. *BMC Pharmacol. Toxicol.* **16,** 21 (2015).

161. Vaitkus, M. *et al.* Reactive oxygen species in peripheral blood and sputum neutrophils during bacterial and nonbacterial acute exacerbation of chronic obstructive pulmonary disease. *Inflammation* **36,** 1485–93 (2013).

162. Moon, H.-G. *et al.* CCN1 secretion and cleavage regulate the lung epithelial cell functions after cigarette smoke. *Am. J. Physiol. Lung Cell. Mol. Physiol.* **307,** L326–37 (2014).

163. Hayoun, D. *et al.* HSP60 is transported through the secretory pathway of 3-MCA-induced fibrosarcoma tumour cells and undergoes N-glycosylation. *FEBS J.* **279,** 2083–95 (2012).

164. Tian, T. *et al.* Dynamics of exosome internalization and trafficking. *J. Cell. Physiol.* **228,** 1487–1495 (2013).

165. Kaiser, F., Steptoe, A., Thompson, S. & Henderson, B. Monocyte cytokine synthesis in response to extracellular cell stress proteins suggests these proteins exhibit network behaviour. *Cell Stress Chaperones* **19,** 135–44 (2014).

166. Tonello, L. *et al.* Data mining-based statistical analysis of biological data uncovers hidden significance: clustering Hashimoto’s thyroiditis patients based on the response of their PBMC with IL-2 and IFN-γ secretion to stimulation with Hsp60. *Cell Stress Chaperones* **20,** 391–5 (2015).